Study of the $e^+e^- \to \pi^+\pi^-\psi(2S)$ reaction at $\sqrt{s} > 4.6$ GeV and search for the charged $Z_c(4430)$ exotic state

DocDB: https://docbes3.ihep.ac.cn/cgi-bin/DocDB/ShowDocument?docid=1520

Marco Scodeggio

mscodegg@fe.infn.it

BESIII Analyses @Ferrara

27th June 2025

Preamble

What and Why

The **$e^+e^- \to \pi^+\pi^-\psi(2S)$** reaction offers the possibility to probe the ***XYZ* sector**,
via the investigation of 2 exotic states

The **Y(4660)** via the $e^+e^- \to [\pi^+\pi^-/f_0(980)]\psi(2S)$

Y(4660), **observed by BaBar**[1], **BELLE**[2], and **BESIII**[3] hypothesised to be a **baryonium**[4], a **molecule**[5], or a **tetraquark**[6]

Study of the exotic $Z_c(4430)$ state through the
$e^+e^- \to \pi^\pm Z_c(4430) \to \pi^+\pi^-\psi(2S)$

Z^+_c(4430) was **observed** and studied in the *B*-decays in the $\pi\psi(2S)$ invariant mass **by BELLE**[7] (and **by LHCb**[8])

Motivation

In Refs. [9, 10], the $Z_c(3900)^\pm$ state is seen both in $\pi\psi(2S)$ and $\pi J/\psi$, and in relation with the Y(4260) resonance

Ref. [10] finds $R = \sigma(\pi^\pm Z_c(3900)^\mp \to \pi^+\pi^- J/\psi)/\sigma(\pi^+\pi^- J/\psi) \sim 22\%$,
neglecting the the J/ψ to $\psi(2S)$ PHSP change,
~100 events are expected around Y (4660)

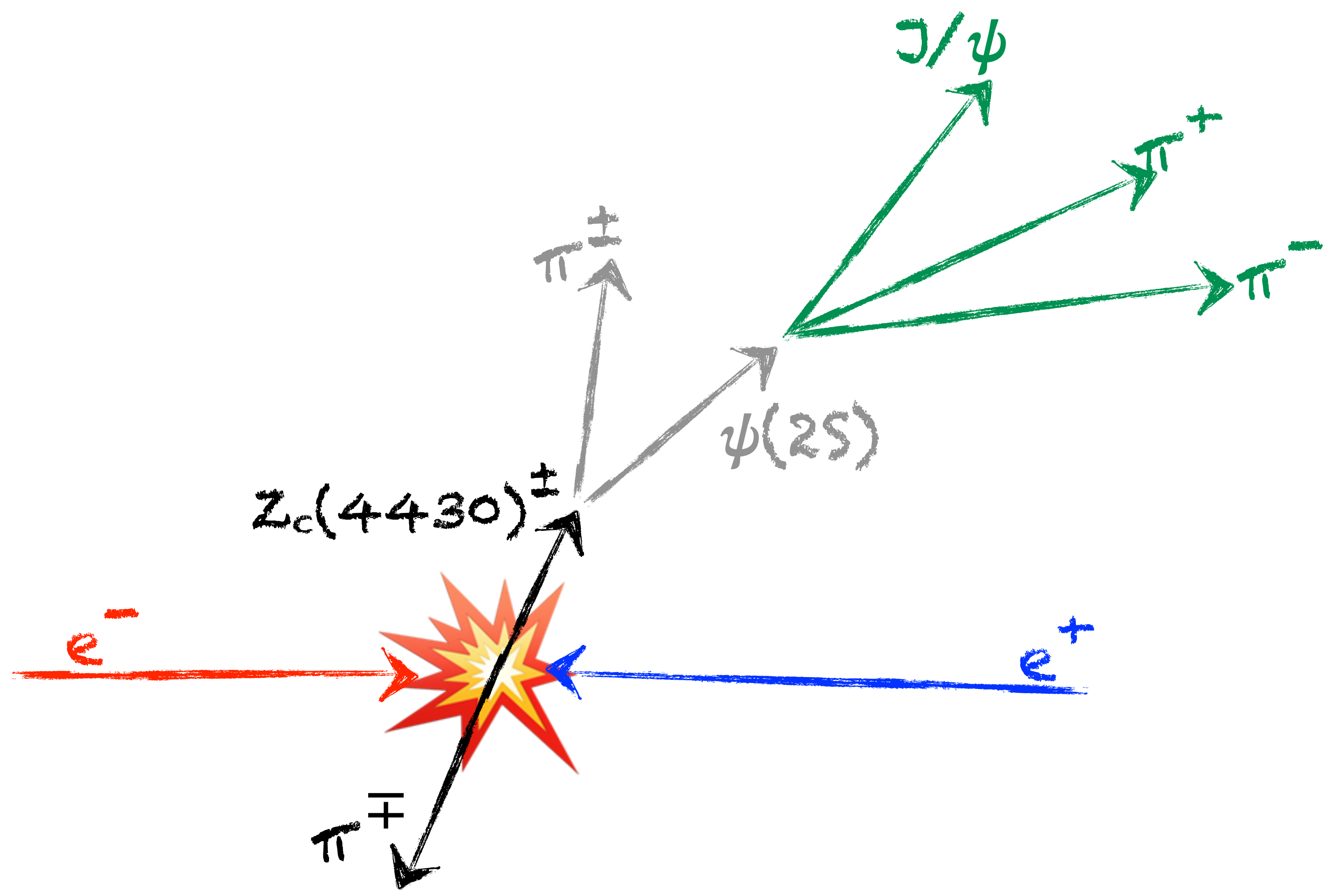

[1] Phys. Rev. D **89**, 111103
[2] Phys. Rev. D **91**, 112007
[3] Phys. Rev. D **104**, 052012
[4] J. Phys. G **35**, 075008 (2008)
[5] Phys. Lett. B **665**, 26-29
[6] Phys. Rev. D **89**, 114010
[7] Phys. Rev. D **88**, 074026
[8] Phys. Rev. Lett. **112**, 222002
[9] Phys. Rev. D **96**, 032004
[10] Phys. Rev. Lett **110**, 252001

Preamble

What and Why

The **$e^+e^- \to \pi^+\pi^-\psi(2S)$** reaction offers the possibility to probe the ***XYZ* sector**,
via the investigation of 2 exotic states

The **Y(4660)** via the $e^+e^- \to [\pi^+\pi^-/f_0(980)]\psi(2S)$

Y(4660), **observed by BaBar**[1], **BELLE**[2], and **BESIII**[3] hypothesised to be a **baryonium**[4], a **molecule**[5], or a **tetraquark**[6]

Study of the exotic $Z_c(4430)$ state through the $e^+e^- \to \pi^\pm Z_c(4430) \to \pi^+\pi^-\psi(2S)$

$Z^+_c(4430)$ was **observed** and studied in the *B*-decays in the $\pi\psi(2S)$ invariant mass **by BELLE**[7] (and **by LHCb**[8])

How

The study will make use of the 12 datasets @$\sqrt{s}$ > 4.6 GeV

No $Z_c(4430)$ **signal** was observed in the **mono-energetic datasets**[11], so the main idea is to merge all the data @$\sqrt{s}$ > 4.6 GeV to use the whole statistics

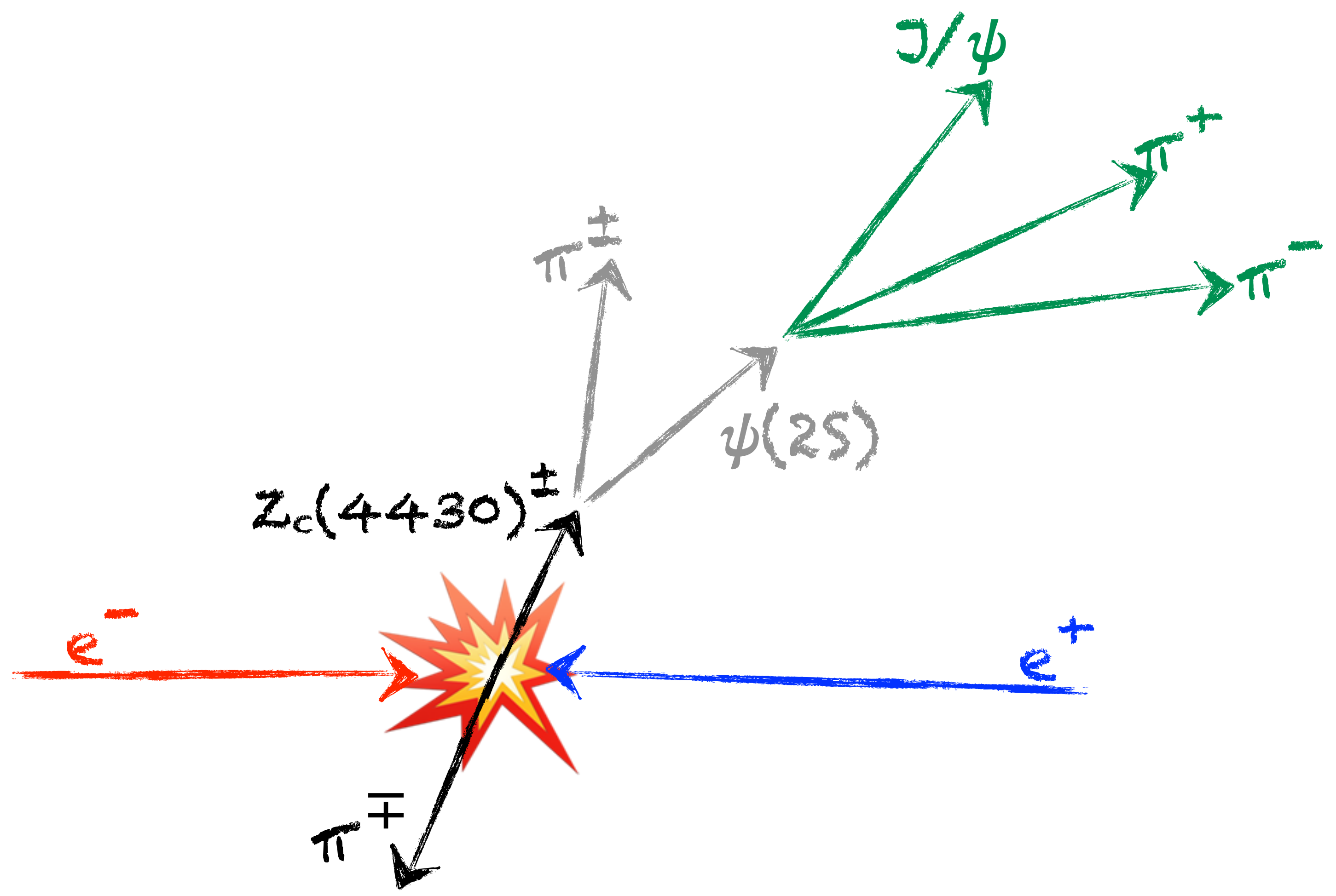

[1] Phys. Rev. D **89**, 111103
[2] Phys. Rev. D **91**, 112007
[3] Phys. Rev. D **104**, 052012
[4] J. Phys. G **35**, 075008 (2008)
[5] Phys. Lett. B **665**, 26-29
[6] Phys. Rev. D **89**, 114010
[7] Phys. Rev. D **88**, 074026
[8] Phys. Rev. Lett. **112**, 222002
[9] Phys. Rev. D **96**, 032004
[10] Phys. Rev. Lett **110**, 252001
[11] Phys. Rev. D **104**, 052012

Preamble

Datasets

Dataset	E_{CoM} (MeV)	$\mathcal{L}$ (pb^{-1})	Boss Version
4610	$4611.86 \pm 0.12 \pm 0.30$	$103.65 \pm 0.05 \pm 0.55$	7.0.6
4620	$4628.00 \pm 0.06 \pm 0.32$	$521.53 \pm 0.11 \pm 2.76$	
4640	$4640.91 \pm 0.06 \pm 0.38$	$551.65 \pm 0.12 \pm 2.92$	
4660	$4661.24 \pm 0.06 \pm 0.29$	$529.43 \pm 0.12 \pm 2.81$	
4680	$4681.92 \pm 0.08 \pm 0.29$	$1667.39 \pm 0.21 \pm 8.84$	
4700	$4698.82 \pm 0.10 \pm 0.36$	$535.54 \pm 0.12 \pm 2.84$	
4740	$4739.70 \pm 0.20 \pm 0.30$	$163.87 \pm 0.07 \pm 0.87$	7.0.7
4750	$4750.05 \pm 0.12 \pm 0.29$	$366.55 \pm 0.10 \pm 1.94$	
4780	$4780.54 \pm 0.12 \pm 0.30$	$511.47 \pm 0.12 \pm 2.71$	
4840	$4843.07 \pm 0.20 \pm 0.31$	$525.16 \pm 0.12 \pm 2.78$	
4914	$4918.02 \pm 0.34 \pm 0.34$	$207.82 \pm 0.08 \pm 1.10$	
4946	$4950.93 \pm 0.36 \pm 0.38$	$159.28 \pm 0.07 \pm 0.84$	

How

The study will make use of the 12 datasets @$\sqrt{s}$ > 4.6 GeV

No $Z_c(4430)$ **signal** was observed in the **mono-energetic datasets**[11], so the main idea is to merge all the data @$\sqrt{s}$ > 4.6 GeV to use the whole statistics

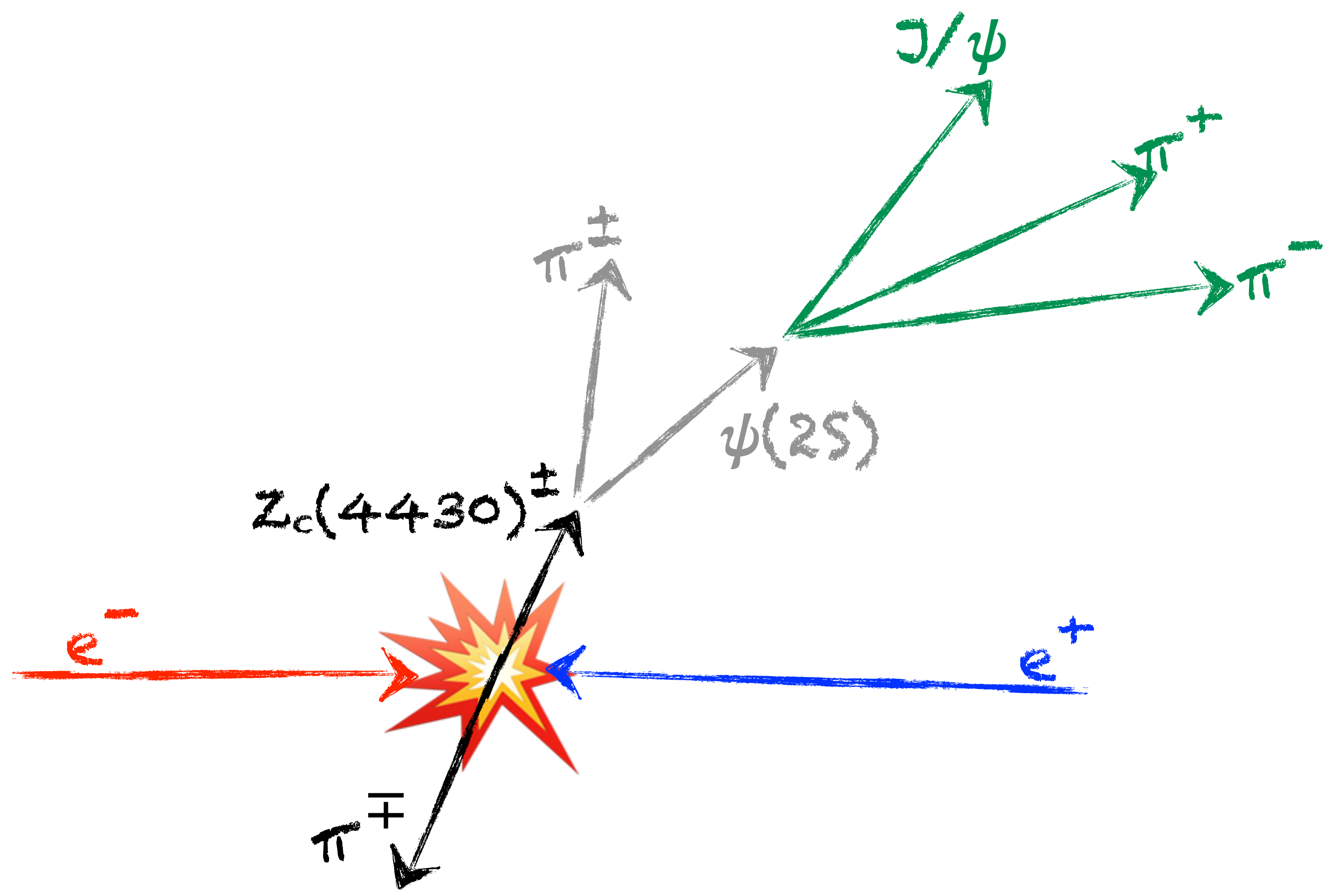

[1] Phys. Rev. D **89**, 111103
[2] Phys. Rev. D **91**, 112007
[3] Phys. Rev. D **104**, 052012
[4] J. Phys. G **35**, 075008 (2008)
[5] Phys. Lett. B **665**, 26-29
[6] Phys. Rev. D **89**, 114010
[7] Phys. Rev. D **88**, 074026
[8] Phys. Rev. Lett. **112**, 222002
[9] Phys. Rev. D **96**, 032004
[10] Phys. Rev. Lett **110**, 252001
[11] Phys. Rev. D **104**, 052012

Preamble

DEC Cards

$e^+e^- \to \pi^\pm Z_c(4430)$

```
noPhotos
Particle vpho 4.6819 0

Decay vpho
  0.5000 dummy10_1 pi- PHSP;
  0.5000 anti-dummy10_1 pi+ PHSP;
Enddecay

Decay dummy10_1
  1.0000 pi+ psi(2S) PHSP;
Enddecay

Decay anti-dummy10_1
  1.0000 pi- psi(2S) PHSP;
Enddecay

Decay psi(2S)
  1.0000 pi+ pi- J/psi PHSP;
Enddecay

Decay J/psi
  0.5000 e+ e- PHSP;
  0.5000 mu+ mu- PHSP;
Enddecay

End
```

$Z_c(4430)$

$M_{Zc} = 4478^{+15}_{-18}$ MeV

$\sigma_{Zc} = 181 \pm 31$ MeV

Signal MC samples

300k events

$e^+e^- \to \pi^+\pi^-\psi(2S)$

```
Particle vpho 4.6819 0.0
Decay vpho
  1.0000 ConExc -2 100443 211 -211;
Enddecay

Decay vhdr
  1.0000 psi(2S) pi+ pi- VVPIPI;
Enddecay

Decay psi(2S)
1.000 J/psi pi+ pi- JPIPI;
Enddecay

Decay J/psi
  0.5000 e+ e- PHOTOS VLL;
  0.5000 mu+ mu- PHOTOS VLL;
Enddecay

End
```

Preamble

DEC Cards

$e^+e^- \to f_0(980)\psi(2S)$

```
Particle vpho 4.6819 0.0
Decay vpho
  1.0000 ConExc -2 100443 9010221;
Enddecay

Decay vhdr
  1.0000 psi(2S) f_0 PHSP;
Enddecay

Decay psi(2S)
1.000 J/psi pi+ pi- JPIPI;
Enddecay

Decay f_0
  1.0000 pi+ pi- PHSP;
Enddecay

Decay J/psi
  0.5000 e+ e- PHOTOS VLL;
  0.5000 mu+ mu- PHOTOS VLL;
Enddecay

End
```

Signal MC samples
300k events

$e^+e^- \to \pi^+\pi^-\psi(2S)$

```
Particle vpho 4.6819 0.0
Decay vpho
  1.0000 ConExc -2 100443 211 -211;
Enddecay

Decay vhdr
  1.0000 psi(2S) pi+ pi- VVPIPI;
Enddecay

Decay psi(2S)
1.000 J/psi pi+ pi- JPIPI;
Enddecay

Decay J/psi
  0.5000 e+ e- PHOTOS VLL;
  0.5000 mu+ mu- PHOTOS VLL;
Enddecay

End
```

Signal MC Studies

Signal MC sample
300k events

Event Selection

Goodness Cuts

Vertex: $R_{xy} < 1cm$ & $R_z < 10$ cm

Polar angle: $|\cos\theta| < 0.93$

Channel ID

charged tracks > 4

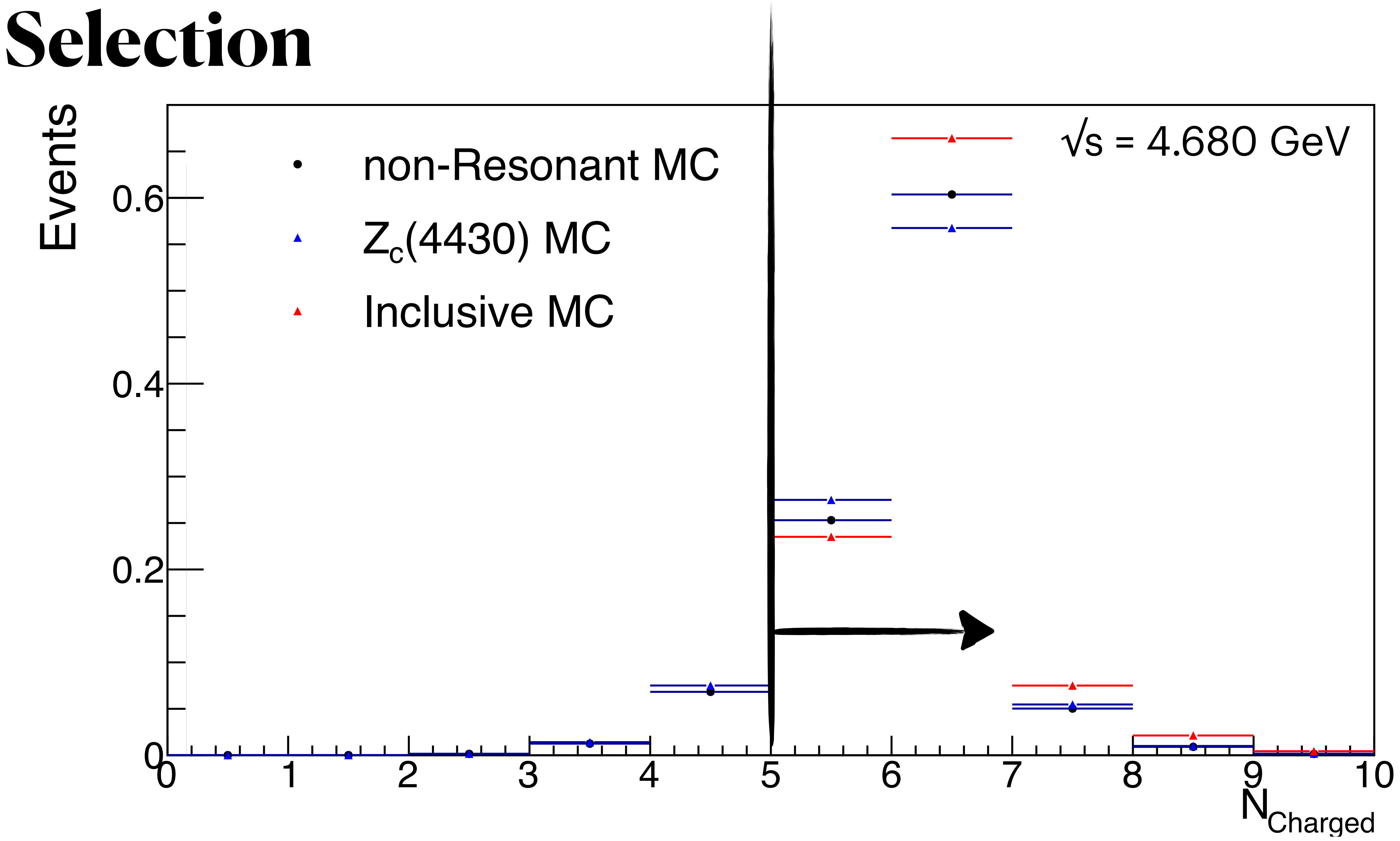

Signal MC Studies

Signal MC sample
300k events

Event Selection

Goodness Cuts

Vertex: $R_{xy} < 1\text{cm}$ & $R_z < 10$ cm

Polar angle: $|\cos\theta| < 0.93$

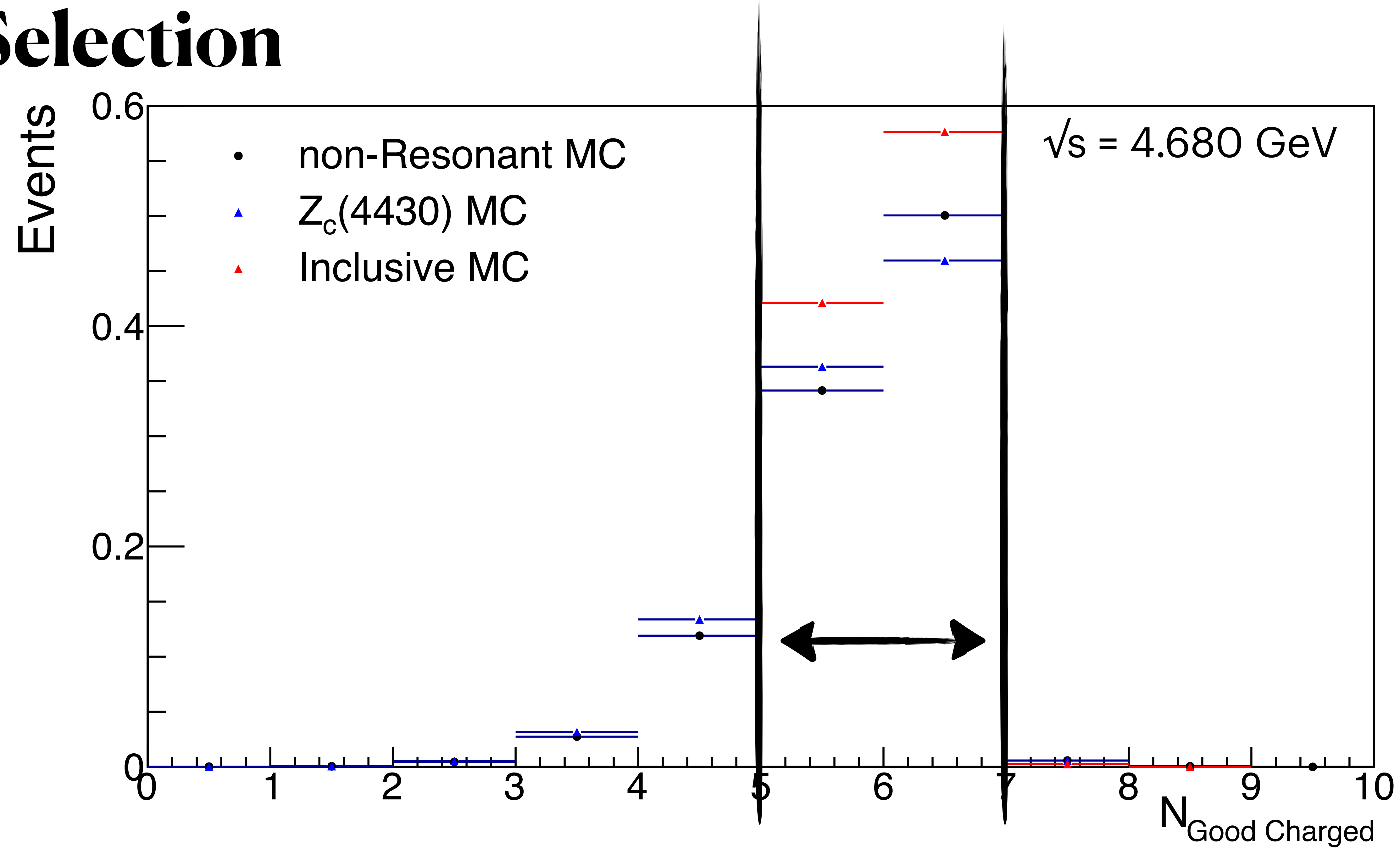

Channel ID

charged tracks > 4

2 good charged topologies

$2\ell\,3\pi$

$2\ell\,4\pi$

Signal MC Studies

Signal MC sample
300k events

Goodness Cuts

Vertex: R_{xy} < 1cm & R_z < 10 cm

Polar angle: |cos θ| < 0.93

Channel ID

charged tracks > 4

Leptons	Pions
p_T > 1 GeV	p_T < 0.85 GeV
E/p (e) > 0.7	
E/p (μ) < 0.6	

E/p Selection

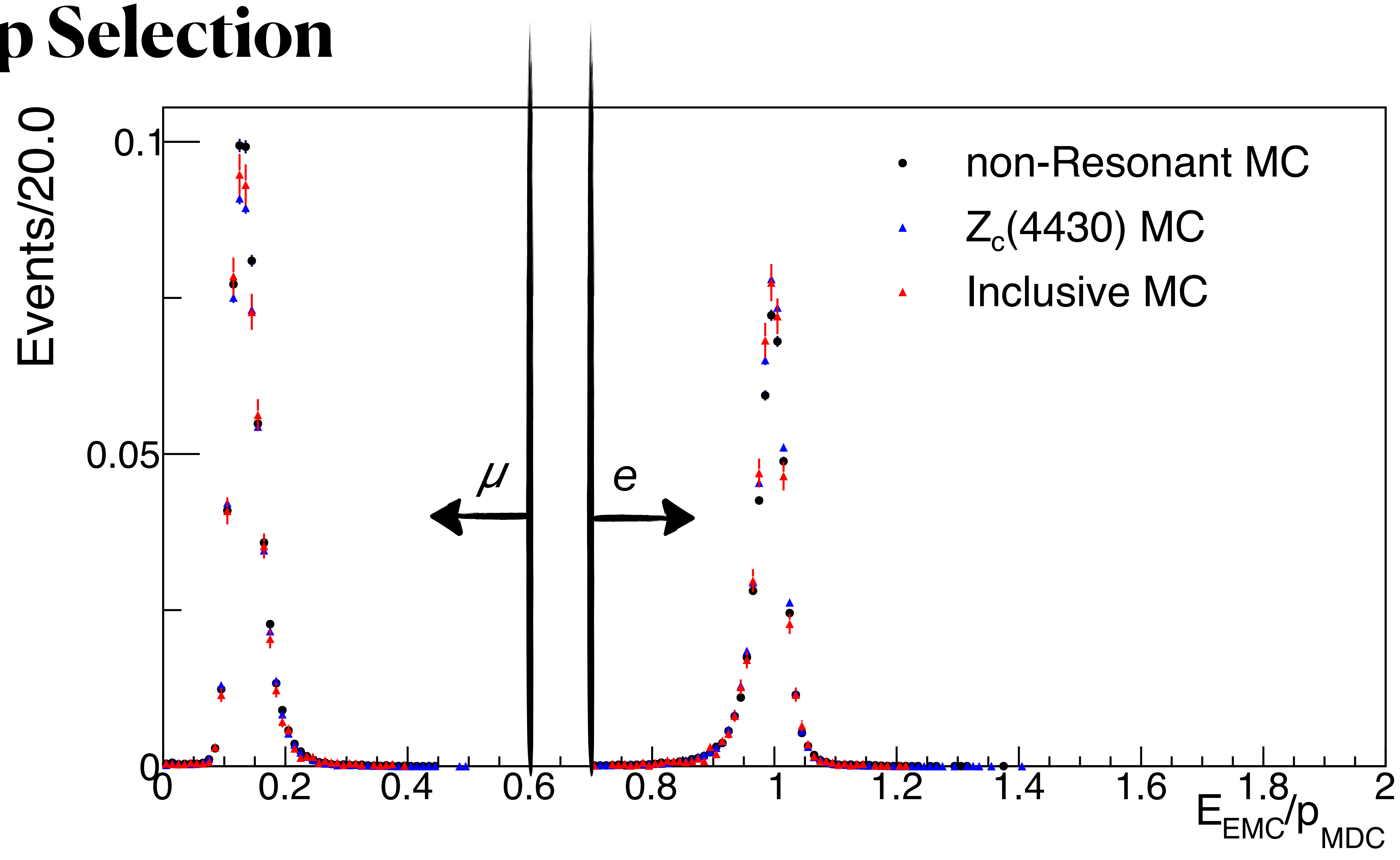

2 good charged topologies

$2\ell\,3\pi$

$2\ell\,4\pi$

Event Selection

Signal MC sample
300k events

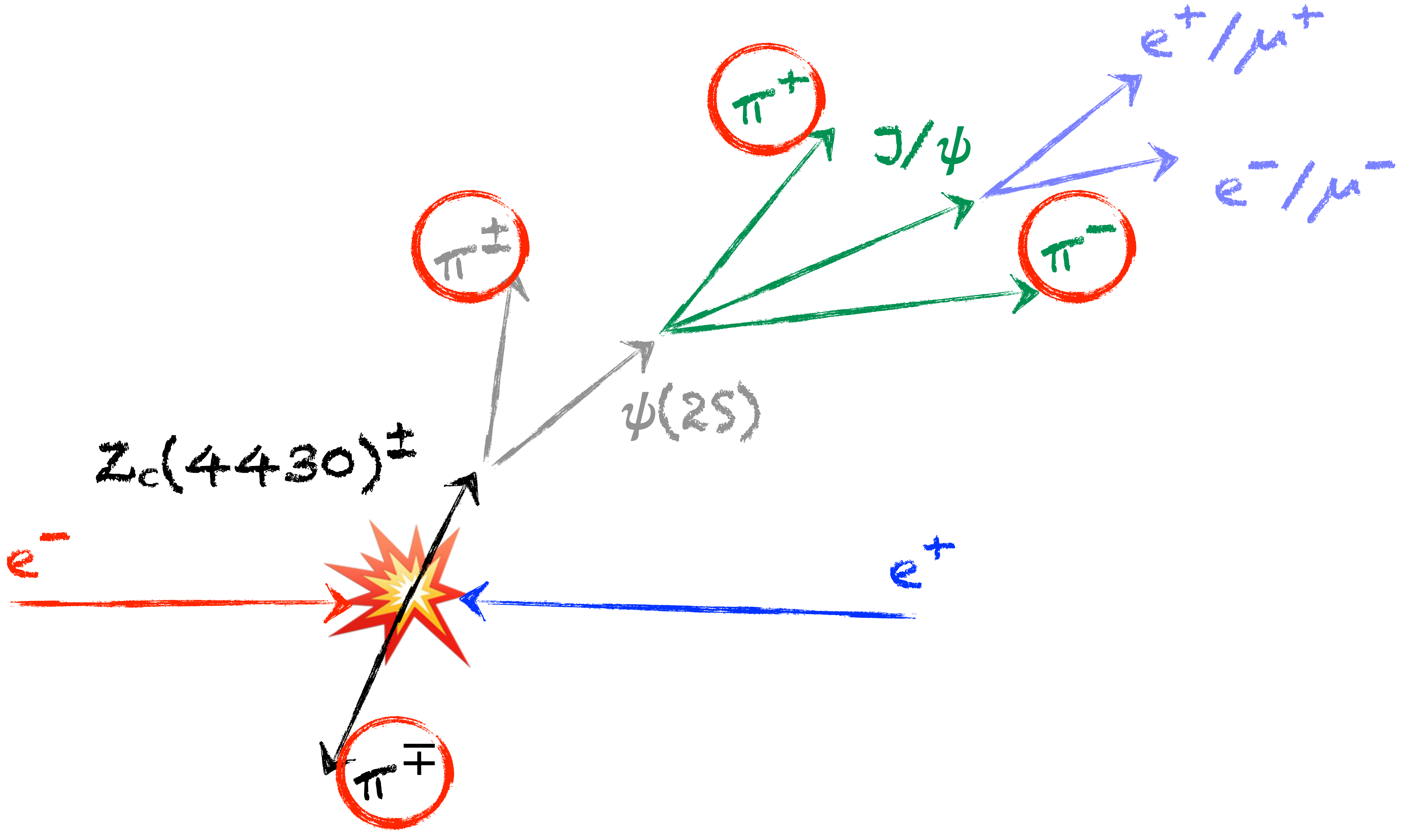

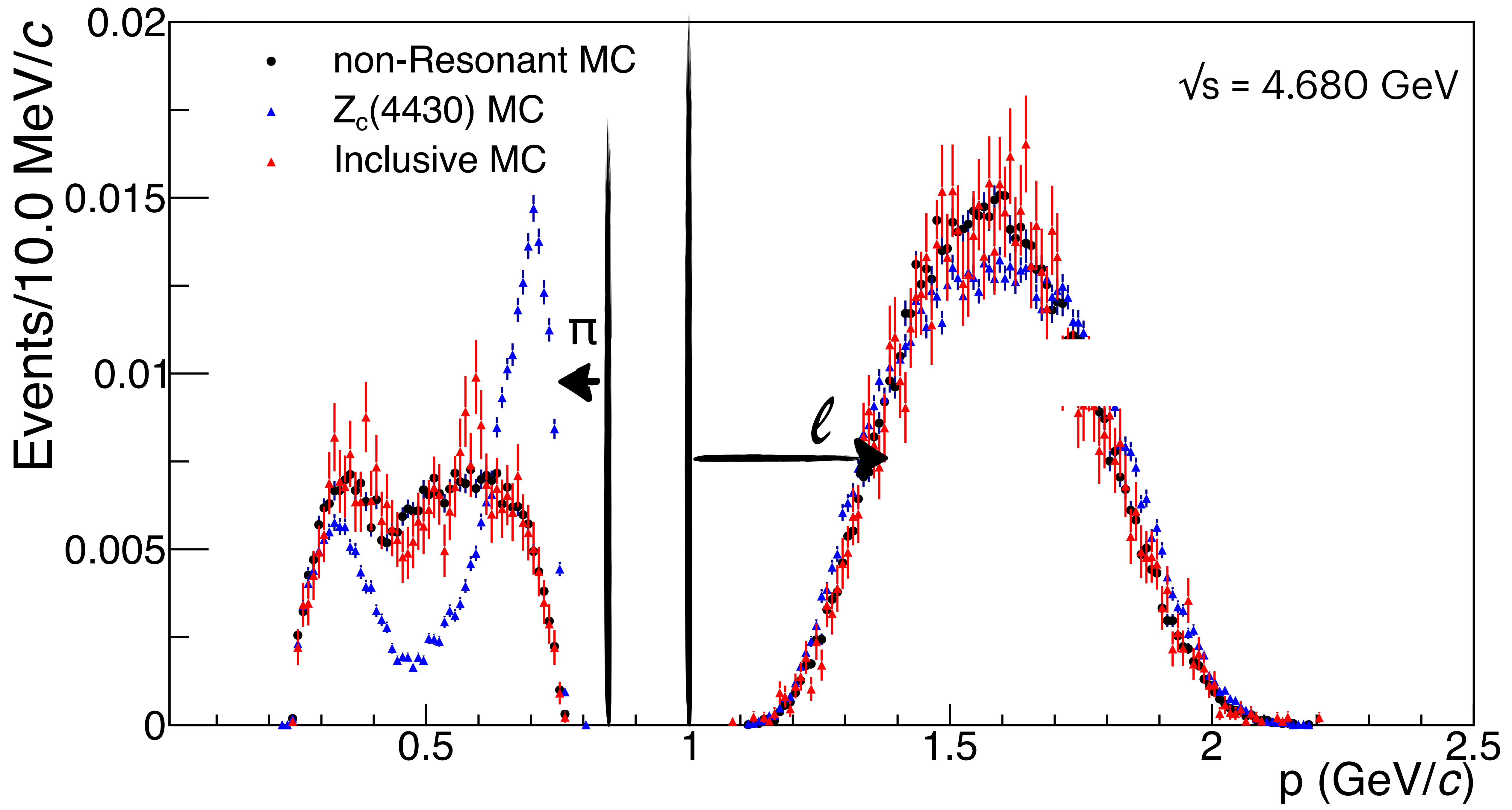

2 good charged topologies
$2\ell 4\pi$
$2\ell 3\pi$

Channel ID

Pions	Leptons
p < 0.85 GeV	p > 1.00 GeV
	E/p (e) > 0.7
	E/p (μ) < 0.6

Event Selection

Signal MC sample
300k events

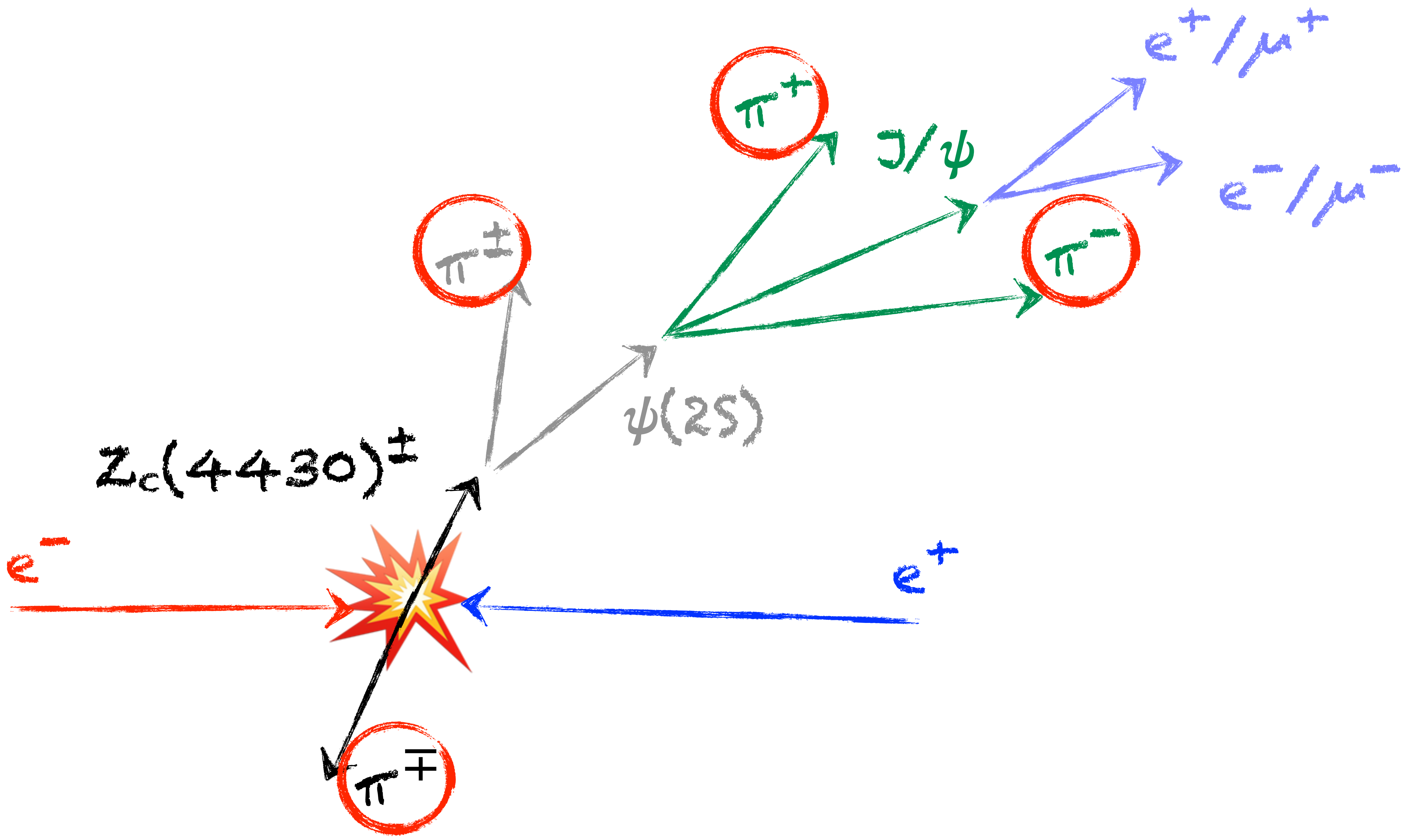

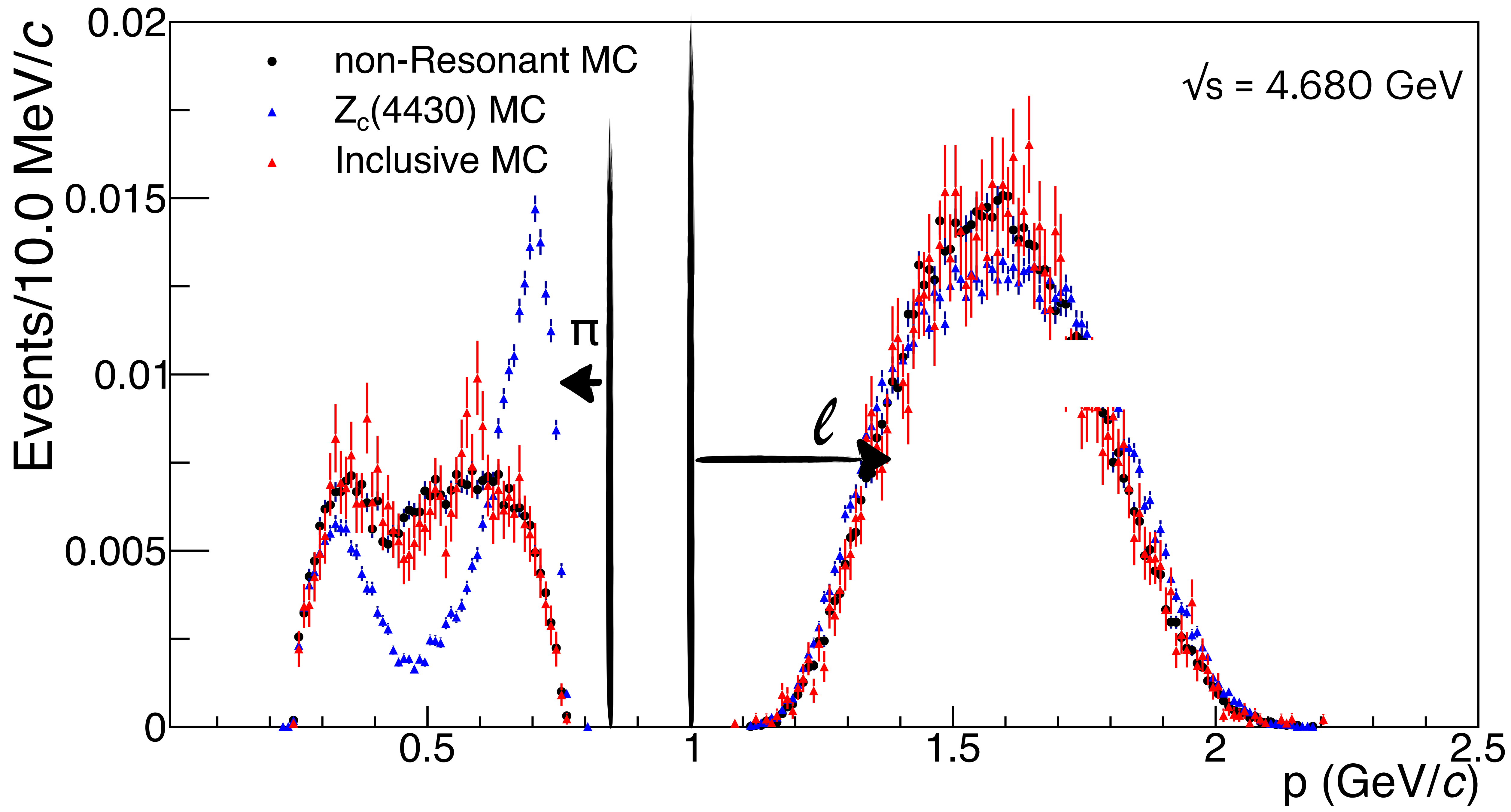

2 good charged topologies

$2\ell 4\pi$

$2\ell 3\pi$

Channel ID

Pions	Leptons
p < 0.85 GeV	p > 1.00 GeV
	E/p (e) > 0.7
	E/p (μ) < 0.6

Optimisation

$$\frac{\epsilon}{a/2 + \sqrt{B}}$$

Event Selection

Charged Particles Momentum Optimisation

Punzi FoM optimisation
∀ √s and using only MC datasets

√s	p_{ch} [GeV/*c*]	√s	p_{ch} [GeV/*c*]
4.612	0.71	**4.740**	0.81
4.626	0.73	**4.750**	0.82
4.640	0.74	**4.780**	0.85
4.660	0.75	**4.840**	0.86
4.680	0.77	**4.914**	0.96
4.700	0.79	**4.946**	0.97

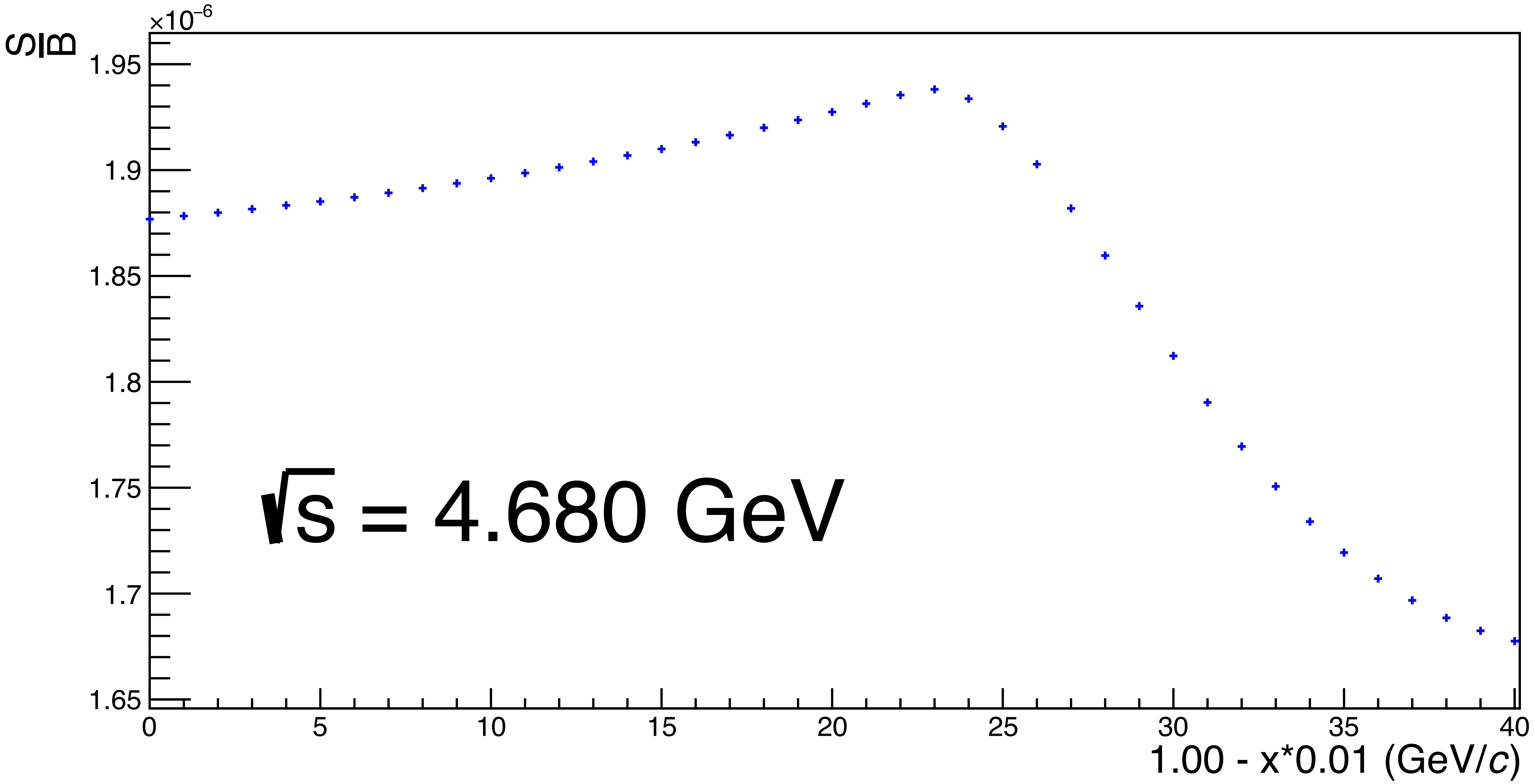

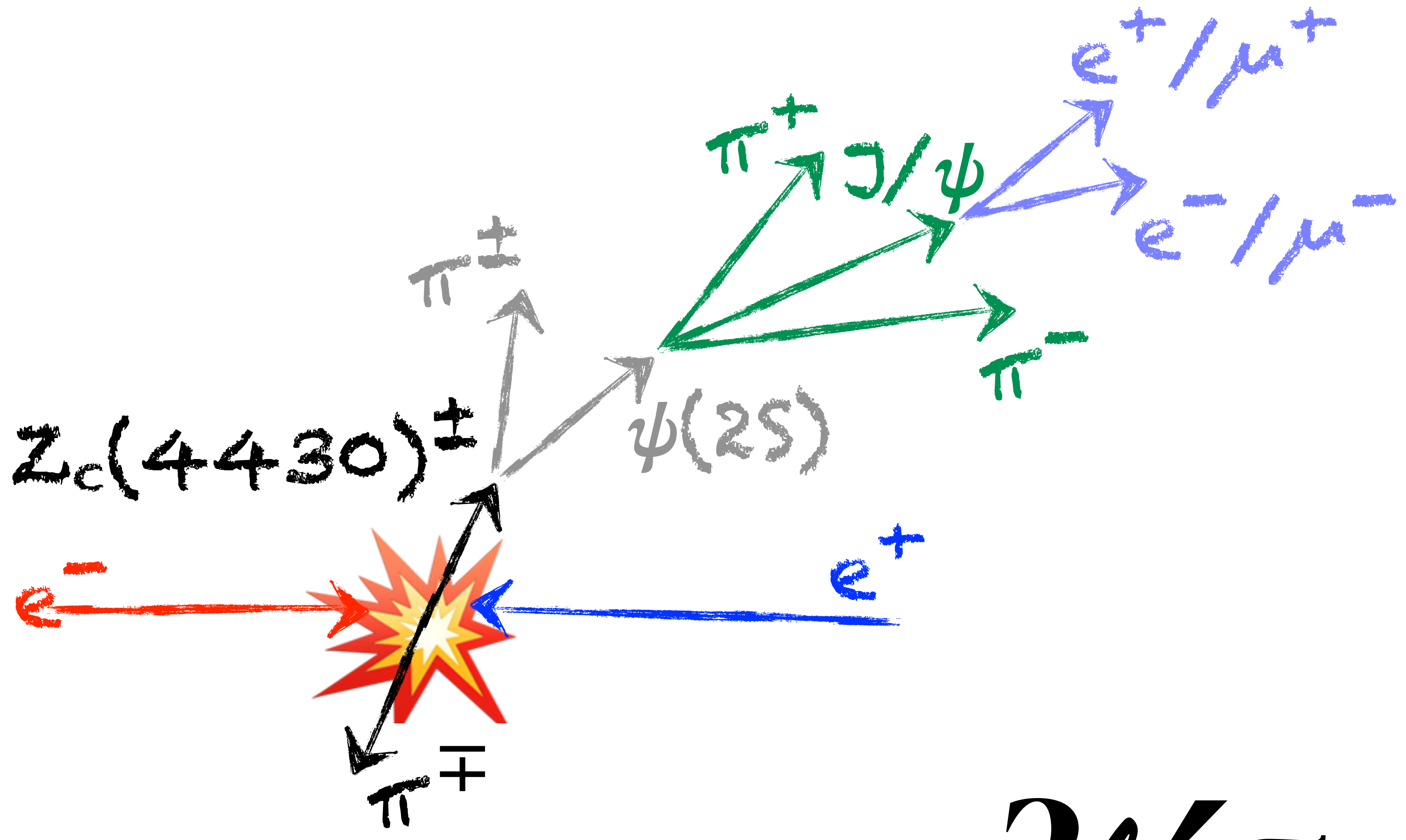

Event Selection

Topology-dependent Kinematic Fits

$2\ell 4\pi$

6-constraint (6C) kinematic fit

1C on the $M_{J/\psi}$
1C on the $M_{\psi(2S)}$
4C on the $p_{Tot} = (\sqrt{s}*\sin(0.011), 0, 0, M_{\sqrt{s}})$

The ππ couples are selected via the best χ^2

$2\ell 3\pi$

2-constraint (2C) kinematic fit

1C on the $M_{J/\psi}$
1C on the $M_{\psi(2S)}$
$[p_{Tot} = (\sqrt{s}*\sin(0.011), 0, 0, M_{\sqrt{s}})]$

ππ and $\pi\pi_{Miss}$* couples are selected via the best χ^2

*π_{Miss} either from prompt production or from ψ(2S) decay, but not from $Z_c(4430)$ by asking $p(\pi_{Miss}) < 0.50$ GeV

Event Selection

Signal Windows Definition

Signal MC sample
300k Events

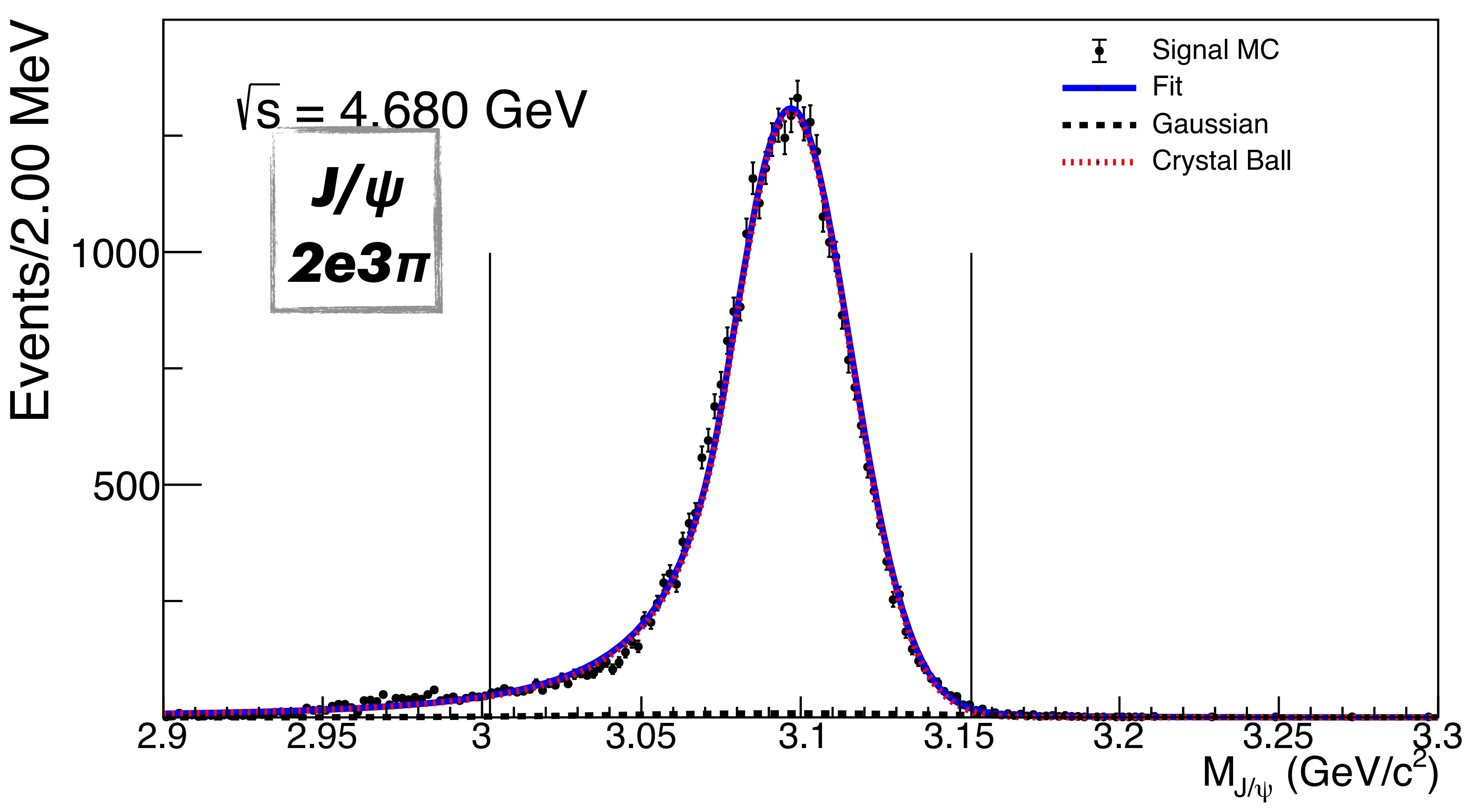

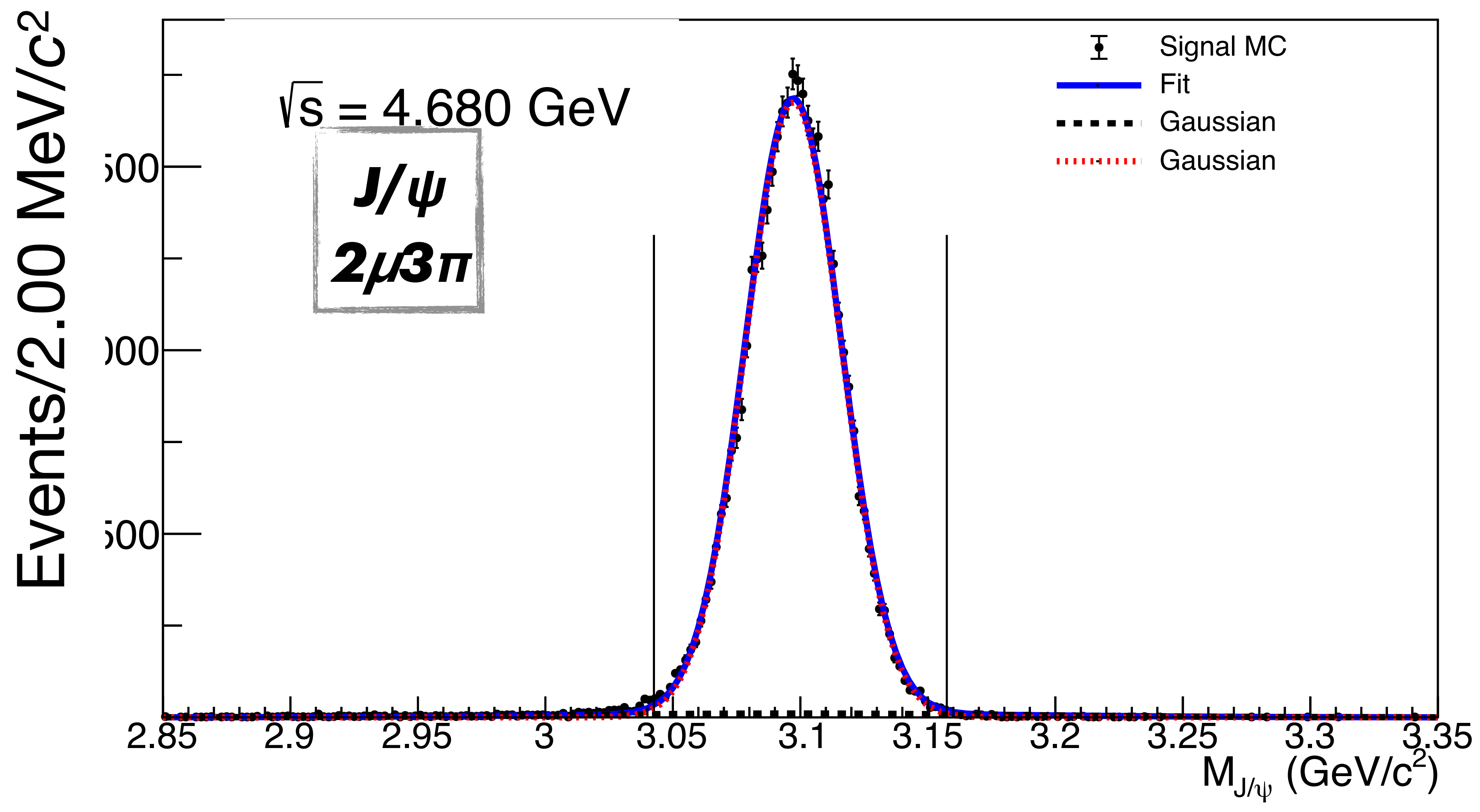

Selection performed on both the topologies on M(J/ψ) and M(ψ(2S))

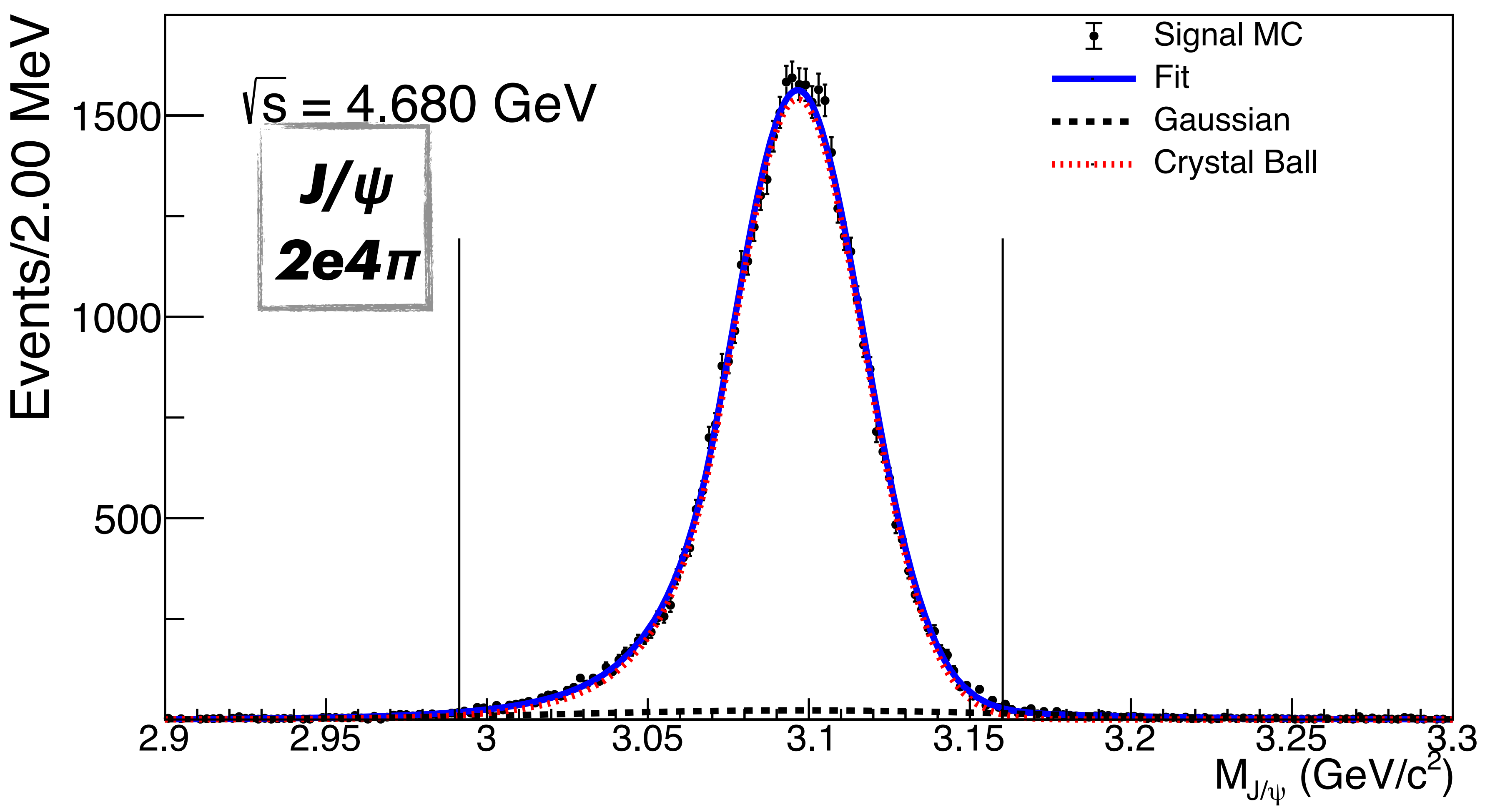

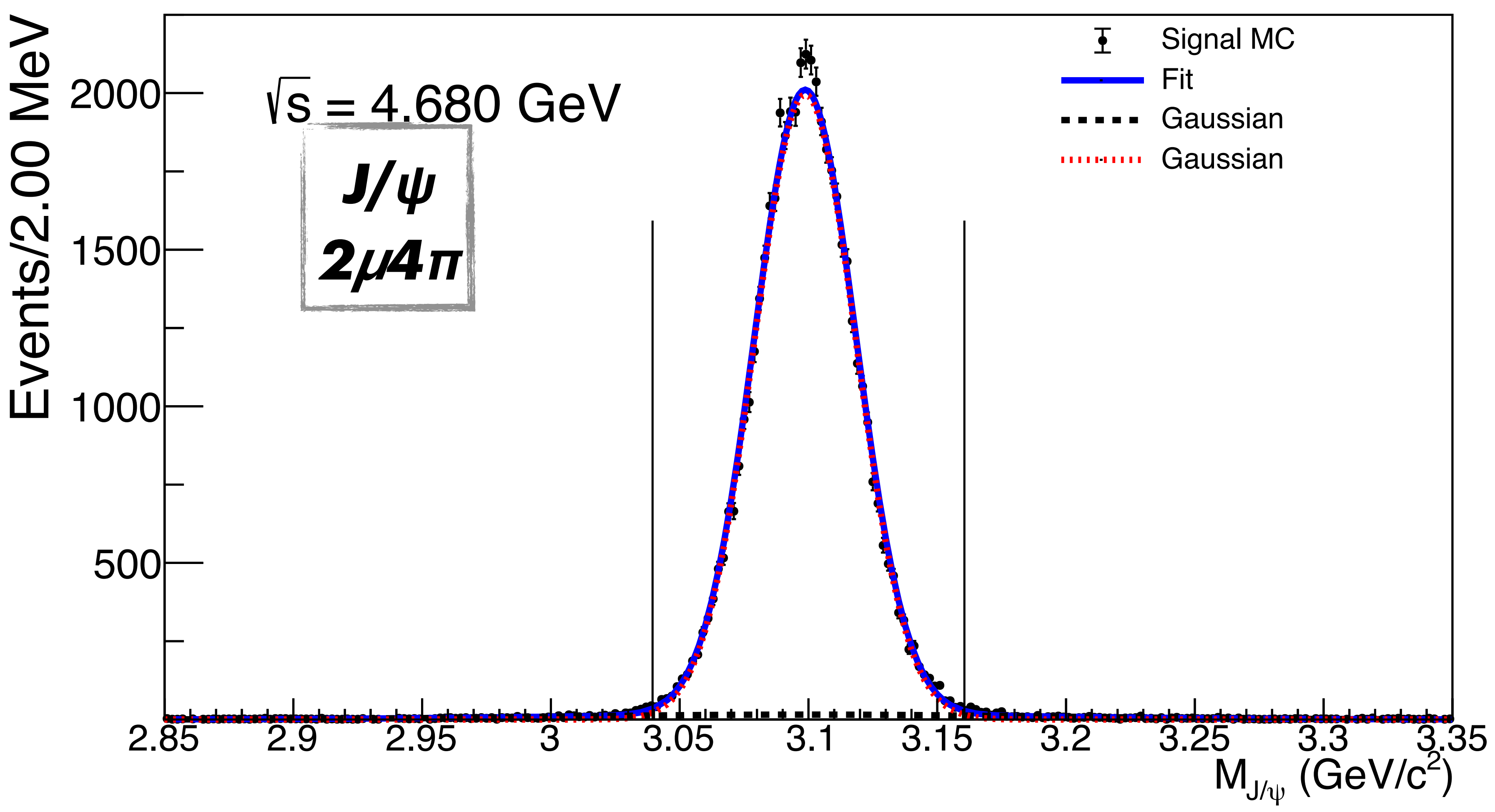

σ of the distributions are in the [19, 25] MeV/c^2 range

Event Selection

Signal Windows Definition

Signal MC sample
300k Events

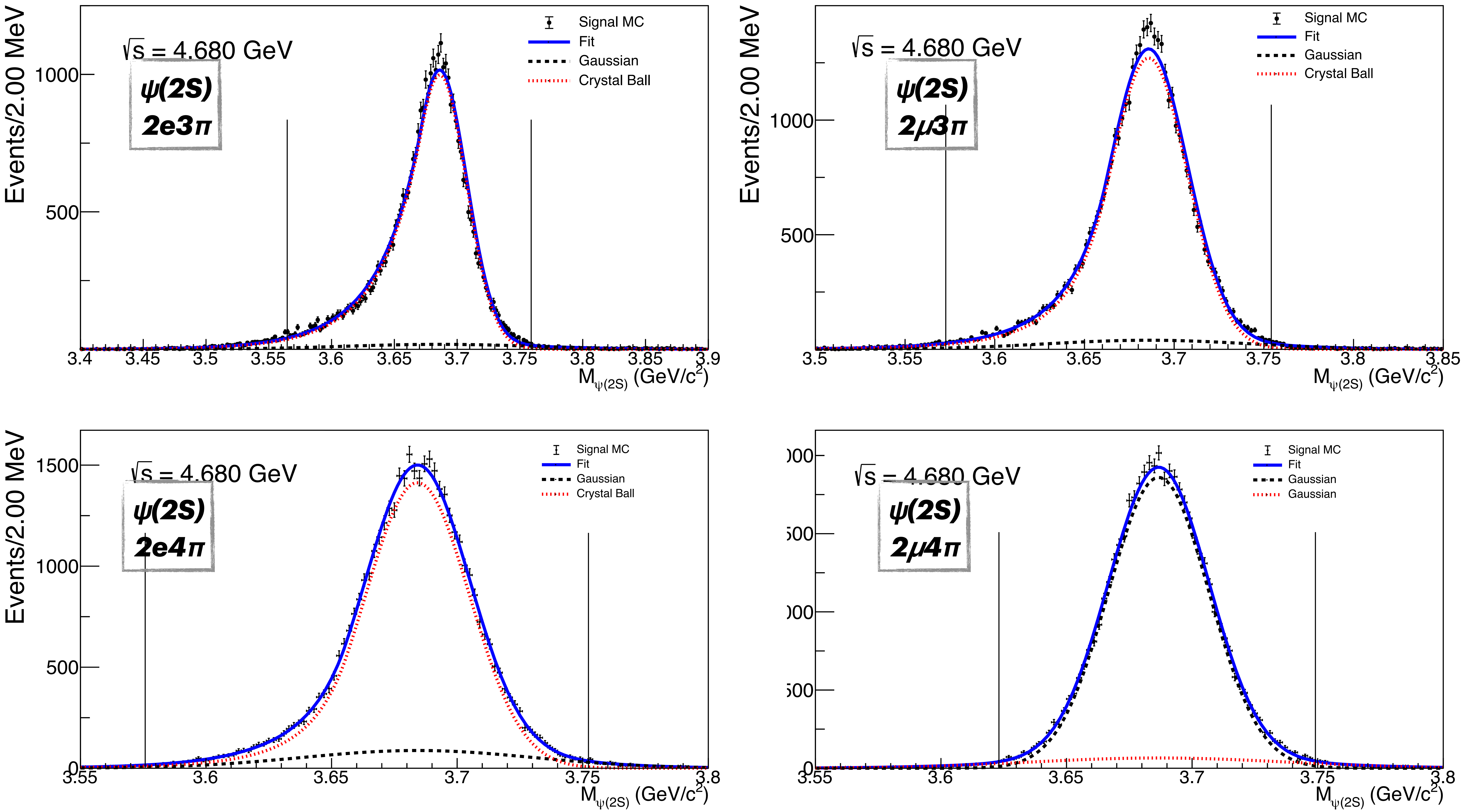

Selection performed on both the topologies on M(J/ψ) and M(ψ(2S))

σ of the distributions are in the [19, 25] MeV/c^2 range

Event Selection

Signal Windows Definition

Signal MC sample
300k Events

An additional selection is applied on $M_{Miss}(\pi)$ for the $2\ell3\pi$ topology

σ of the distributions are in the [29, 37] MeV/c^2 range

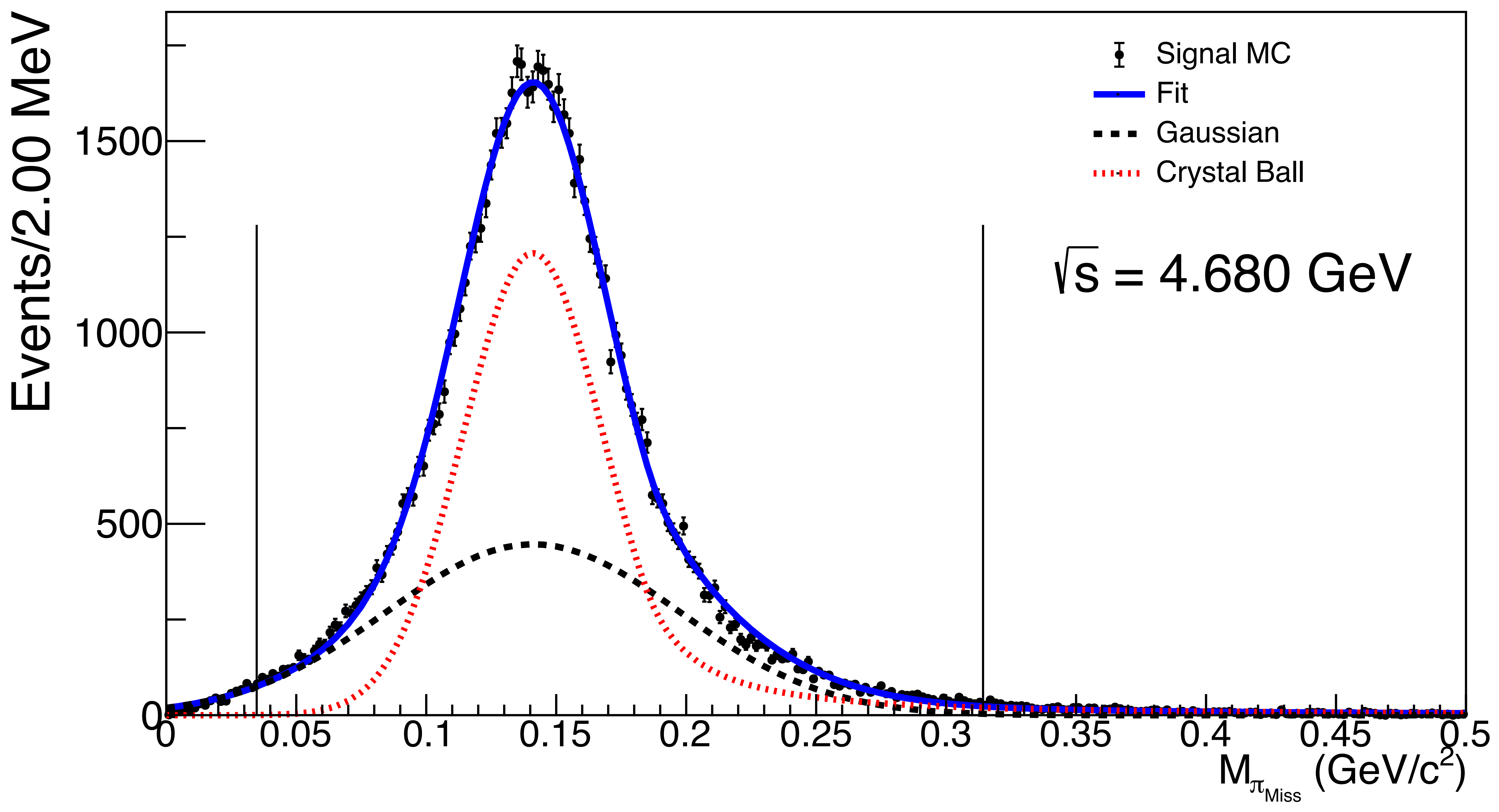

Background Rejection

$\sqrt{s}$ = 4.680 GeV

Inclusive MC sample
10x $\mathcal{L}$ data

	Decay tree	N_{Evts}	$\sum_i^{Tot} N_{Evts}$
1	$e^+e^- \to \pi^+\pi^-\psi', \psi' \to \pi^+\pi^- J/\psi, J/\psi \to \mu^+\mu^-$	3389	3389
2	$e^+e^- \to \pi^+\pi^-\psi', \psi' \to \pi^+\pi^- J/\psi, J/\psi \to e^+e^-$	2983	6372
3	$e^+e^- \to \pi^+\pi^-\psi'\gamma^I, \psi' \to \pi^+\pi^- J/\psi, J/\psi \to \mu^+\mu^-$	2875	9247
4	$e^+e^- \to \pi^+\pi^-\psi', \psi' \to \pi^+\pi^- J/\psi, J/\psi \to \mu^+\mu^-$	2528	11775
5	$e^+e^- \to \pi^+\pi^-\psi'\gamma^I, \psi' \to \pi^+\pi^- J/\psi, J/\psi \to e^+e^-$	2499	14274
6	$e^+e^- \to \pi^+\pi^-\psi', \psi' \to \pi^+\pi^- J/\psi, J/\psi \to e^+e^-$	2313	16587
7	$e^+e^- \to \pi^+\pi^-\psi', \psi' \to \pi^+\pi^- J/\psi, J/\psi \to \mu^+\mu^-$	1346	17933
8	$e^+e^- \to \pi^+\pi^-\psi', \psi' \to \pi^+\pi^- J/\psi, J/\psi \to e^+e^-$	1249	19182
9	$e^+e^- \to \pi^+\pi^-\psi', \psi' \to \pi^+\pi^- J/\psi, J/\psi \to \mu^+\mu^-$	1037	20219
10	$e^+e^- \to \pi^+\pi^-\psi', \psi' \to \pi^+\pi^- J/\psi, J/\psi \to e^+e^-$	907	21126
11	$e^+e^- \to \pi^+\pi^-\psi', \psi' \to \pi^+\pi^- J/\psi, J/\psi \to \mu^+\mu^-$	307	21433
12	$e^+e^- \to \pi^+\pi^-\psi', \psi' \to \pi^+\pi^- J/\psi, J/\psi \to e^+e^-$	289	21722
13	$e^+e^- \to \pi^+\pi^-\psi', \psi' \to \pi^+\pi^- J/\psi, J/\psi \to \mu^+\mu^-$	276	21998
14	$e^+e^- \to \pi^+\pi^-\psi', \psi' \to \pi^+\pi^- J/\psi, J/\psi \to e^+e^-$	245	22243
15	$e^+e^- \to \pi^+\pi^-\psi', \psi' \to \pi^+\pi^- J/\psi, J/\psi \to \mu^+\mu^-$	240	22483
16	$e^+e^- \to \pi^+\pi^-\psi', \psi' \to \pi^+\pi^- J/\psi, J/\psi \to e^+e^-$	197	22680
17	$e^+e^- \to \pi^+\pi^-\psi', \psi' \to \pi^+\pi^- J/\psi, J/\psi \to \mu^+\mu^-$	188	22868
18	$e^+e^- \to \pi^+\pi^-\psi', \psi' \to \pi^+\pi^- J/\psi, J/\psi \to \mu^+\mu^-$	161	23029
19	$e^+e^- \to \pi^+\pi^-\psi', \psi' \to \pi^+\pi^- J/\psi, J/\psi \to e^+e^-$	156	23185
20	$e^+e^- \to \pi^+\pi^+\pi^+\pi^-\pi^-\pi^-$	144	23329
21	$e^+e^- \to \pi^+\pi^-\psi', \psi' \to \pi^+\pi^- J/\psi, J/\psi \to \mu^+\mu^-$	132	23461
22	$e^+e^- \to \pi^+\pi^-\psi', , \psi' \to \pi^+\pi^- J/\psi, J/\psi \to e^+e^-$	109	23570
23	$e^+e^- \to \pi^+\pi^-\psi', \psi' \to \pi^+\pi^- J/\psi, J/\psi \to \mu^+\mu^-$	104	23674
24	$e^+e^- \to \pi^+\pi^+\pi^+\pi^-\pi^-\pi^-\gamma^I$	103	23777
25	$e^+e^- \to \pi^+\pi^-\psi', \psi' \to \pi^+\pi^- J/\psi, J/\psi \to \mu^+\mu^-$	96	23873
26	...	...	...

From 1.3 billion inclusive MC events, **28136 survive**, with a survival rate of [4, 28] ppm

Virtually **only the hadron component** is surviving after the selection criteria

Out of 28136 total **IncMC events**, the events are from

- > 90% Non-resonant **ππψ(2S)** signal
- < 10% Multi-π states

Background Rejection

$\sqrt{s}$ = 4.680 GeV

Inclusive MC sample
10x $\mathcal{L}$ data

	Decay tree	N_{Evts}	$\sum_i^{Tot} N_{Evts}$
1	$e^+e^- \to \pi^+\pi^+\pi^+\pi^-\pi^-\pi^-$	50	50
2	$e^+e^- \to \pi^+\pi^+\pi^+\pi^-\pi^-\pi^-\gamma^I$	39	89
3	$e^+e^- \to \pi^+\pi^+\pi^+\pi^-\pi^-\pi^-$	19	108
4	$e^+e^- \to \pi^+\pi^+\pi^+\pi^-\pi^-\pi^-$	16	124
5	$e^+e^- \to K_S^0K_S^0J/\psi\gamma^I, K_S^0 \to \pi^+\pi^-, J/\psi \to \mu^+\mu^-$	10	134
6	$e^+e^- \to K_S^0K_S^0J/\psi, K_S^0 \to \pi^+\pi^-, J/\psi \to \mu^+\mu^-$	7	144
7	$e^+e^- \to \pi^+b_1^-\gamma^f, b_1^- \to \pi^-\omega, \omega \to \pi^0\pi^+\pi^-$	5	149
8	$e^+e^- \to \pi^+\pi^+\pi^+\pi^-\pi^-\pi^-$	5	151
9	$e^+e^- \to K_S^0K_S^0J/\psi, K_S^0 \to \pi^+\pi^-, J/\psi \to e^+e^-$	5	156
10	$e^+e^- \to K_S^0K_S^0J/\psi, K_S^0 \to \pi^+\pi^-, J/\psi \to \mu^+\mu^-$	4	160
11	$e^+e^- \to \pi^-b_1^+\gamma^f, b_1^+ \to \pi^+\omega, \omega \to \pi^0\pi^+\pi^-$	4	164
12	$e^+e^- \to \pi^+\pi^+\pi^+\pi^-\pi^-\pi^-$	4	168
13	$e^+e^- \to \pi^+\pi^-f_0'\gamma^f, f_0' \to \pi^+\pi^+\pi^-\pi^-$	4	172
14	$e^+e^- \to K_S^0K_S^0J/\psi\gamma^I, K_S^0 \to \pi^+\pi^-, J/\psi \to e^+e^-$	4	176
15	$e^+e^- \to K_S^0K_S^0J/\psi, K_S^0 \to \pi^+\pi^-, J/\psi \to e^+e^-$	3	179
16	$e^+e^- \to \pi^+b_1^-\gamma^f, b_1^- \to \pi^-\omega, \omega \to \pi^0\pi^+\pi^-$	3	182
17	$e^+e^- \to \pi^+a_0^-\gamma^f, a_0^- \to \pi^-\eta, \eta \to \pi^0\pi^+\pi^-$	3	185
18	$e^+e^- \to \pi^+\pi^-\psi', \psi' \to \chi_{c1}\gamma, \chi_{c1} \to J/\psi\gamma, J/\psi \to \mu^+\mu^-$	3	188
19	$e^+e^- \to \pi^+\pi^-f_0'\gamma^f, f_0' \to \pi^+\pi^+\pi^-\pi^-$	2	190
20	$e^+e^- \to \pi^+\pi^-f_0', f_0' \to \rho^0\rho^0, \rho^0 \to \pi^+\pi^-$	2	192
21	$e^+e^- \to \pi^+\pi^+\pi^+\pi^-\pi^-\pi^-$	2	194
22	$e^+e^- \to \pi^+f_0'a_1^-, f_0' \to \pi^+\pi^-, a_1^- \to \rho^0\pi^-, \rho^0 \to \pi^+\pi^-$	2	196
23	$e^+e^- \to \pi^0\pi^0\pi^+\pi^+\pi^-\pi^-$	2	198
24	$e^+e^- \to \pi^+b_1^-\gamma^f, b_1^- \to \pi^-\omega, \omega \to \pi^0\pi^+\pi^-$	2	200
25	$e^+e^- \to \pi^+b_1^-, b_1^- \to \pi^-\omega, \omega \to \pi^+\pi^+\pi^-\pi^-$	2	202
26	...	...	...

Removing the signal component to the inclusive MC samples

The resulting contribution is of the order O(1 ppm) over the total number of simulated event

The background oscillates between 2% and 23%

Cut Flow of Event Selection

Cuts [$\sqrt{s} = 4.680$ GeV]	Events	Efficiency [%]
Total Tracks	300000	100
Fiducial	253871	84.62
Kinetic PID	215785	71.93
5 Trks Events - Kalman Fit 1C	38643	12.88
6 Trks Events - Kalman Fit 1C	76189	25.40
5&6 Trks Events	114832	38.28

Table 9: Cut-flow for the $e^+e^- \to \pi^+\pi^-\psi(2S)$ process at $\sqrt{s} = 4.680$ GeV.

Cuts [$\sqrt{s} = 4.700$ GeV]	Events	Efficiency [%]
Total Tracks	300000	100
Fiducial	254488	84.83
Kinetic PID	215839	71.95
5 Trks Events - Kalman Fit 1C	38900	12.97
6 Trks Events - Kalman Fit 1C	76203	25.40
5&6 Trks Events	115103	38.37

Table 10: Cut-flow for the $e^+e^- \to \pi^+\pi^-\psi(2S)$ process at $\sqrt{s} = 4.700$ GeV.

Cuts [$\sqrt{s} = 4.740$ GeV]	Events	Efficiency [%]
Total Tracks	300000	100
Fiducial	256133	85.38
Kinetic PID	217253	72.42
5 Trks Events - Kalman Fit 1C	34636	11.55
6 Trks Events - Kalman Fit 1C	72349	24.12
5&6 Trks Events	106985	35.66

Table 11: Cut-flow for the $e^+e^- \to \pi^+\pi^-\psi(2S)$ process at $\sqrt{s} = 4.740$ GeV.

Cuts [$\sqrt{s} = 4.750$ GeV]	Events	Efficiency [%]
Total Tracks	300000	100
Fiducial	256091	85.36
Kinetic PID	216867	72.29
5 Trks Events - Kalman Fit 1C	33433	11.14
6 Trks Events - Kalman Fit 1C	71096	23.70
5&6 Trks Events	104529	34.84

Table 12: Cut-flow for the $e^+e^- \to \pi^+\pi^-\psi(2S)$ process at $\sqrt{s} = 4.750$ GeV.

Extraction of the $\sigma(e^+e^- \longrightarrow \pi^+\pi^-\psi(2S))$

Extraction of the σ($e^+e^- \longrightarrow \pi^+\pi^-\psi(2S)$)

Signal Shape & Efficiency

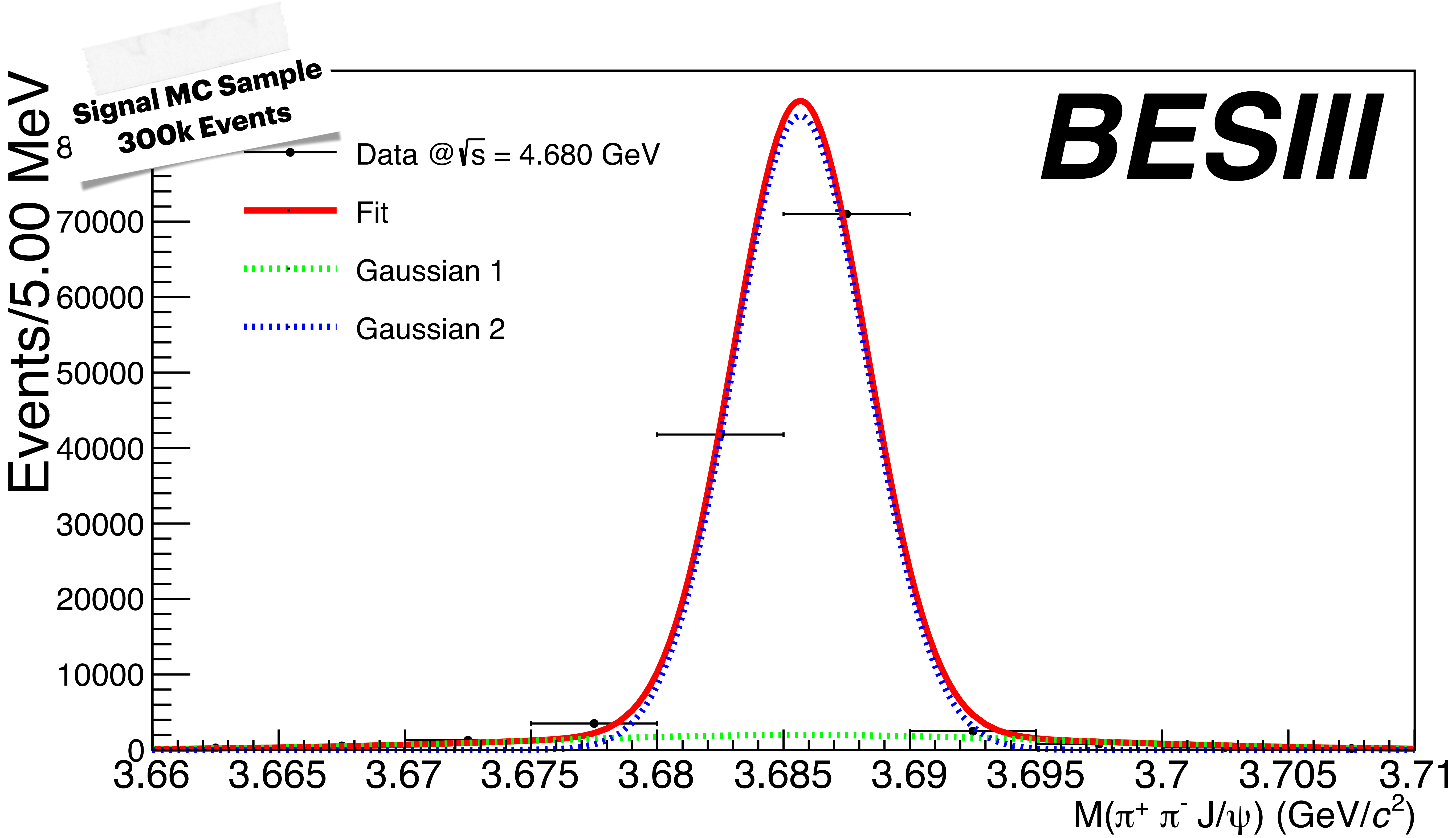

For **each √s**, the **signal** is modelled via a signal MC sample with a **sum of Gaussian and Crystal Ball** functions

<Efficiency> ~36%$_{\text{Conexc}}$

σ (from Ref. [11]) is used as input to estimate the vacuum polarisation factor and the ISR correction, an iterative procedure is performed based on the relation

The final σ_{Born} is obtained when the n^{th} iteration is consistent with a previous iteration within 0.5% for each centre-of-mass energy

[11] Phys. Rev. D **104**, 052012

Extraction of the σ($e^+e^- \longrightarrow \pi^+\pi^-\psi(2S)$)

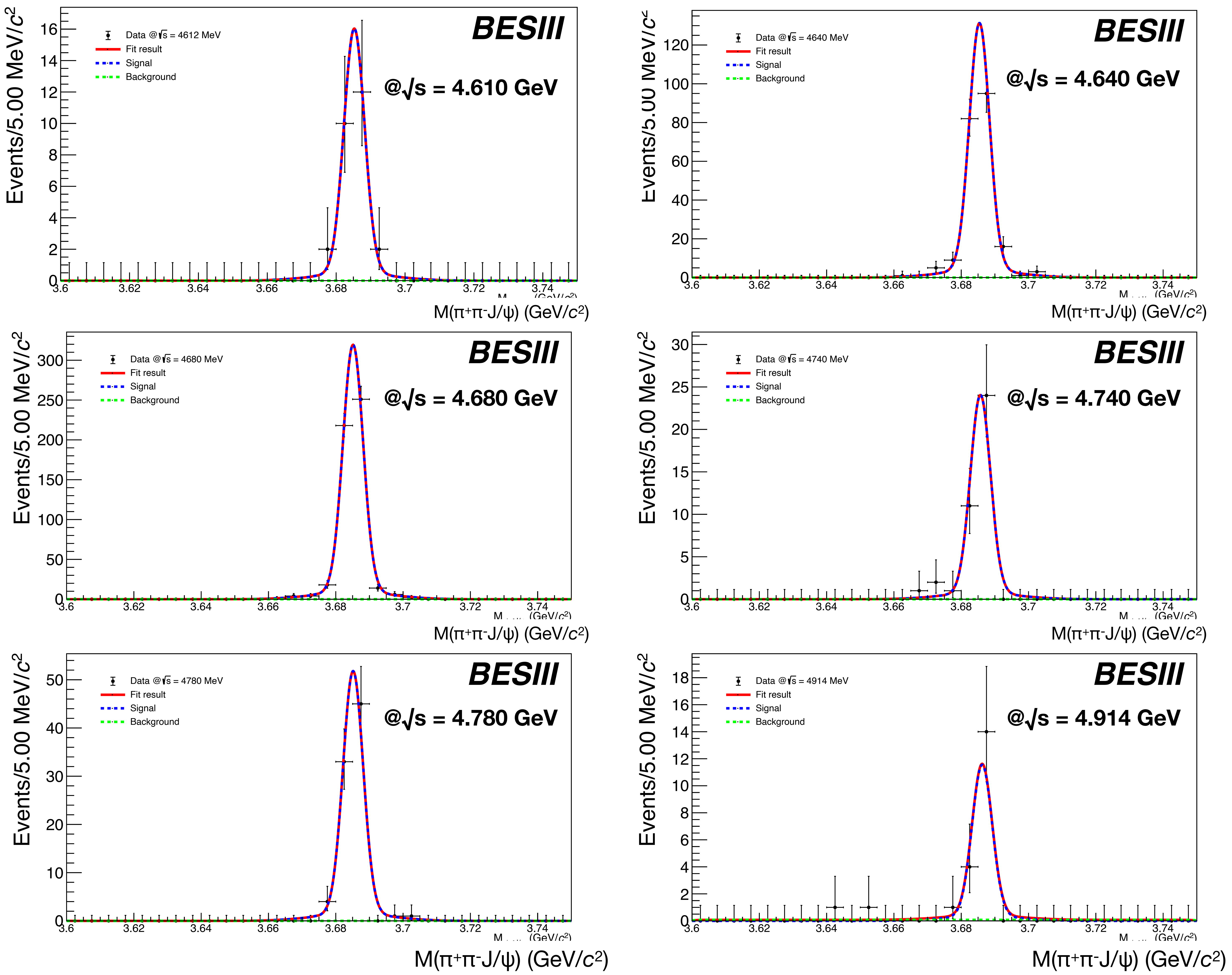

Data Fits

For **each √s**, the ππψ(2S) contribution is extracted by **fitting the M(ππJ/ψ)** invariant spectrum

The **signal** is modelled with a **sum of Gaussian and Crystal Ball**

A **polynomial** function is used to describe the **background**

Extraction of the $\sigma(e^+e^- \longrightarrow \pi^+\pi^-\psi(2S))$

$\pi\pi\psi(2S)$ cross-section

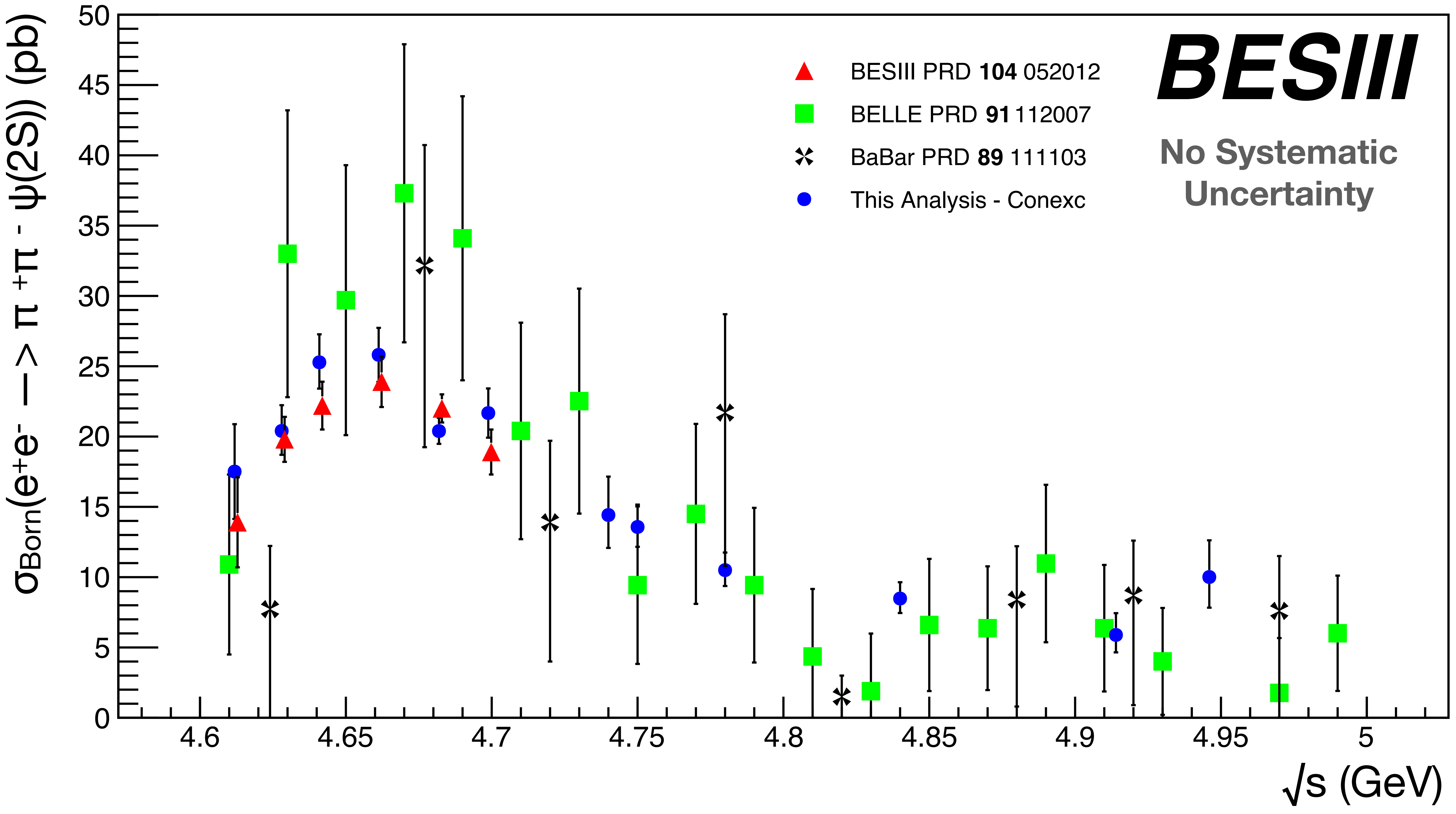

$$\sigma_{\text{Born}} = \frac{N_{\text{Obs}}}{\mathcal{L}(1+\delta)\frac{1}{|1-\Pi^2|}\epsilon\mathcal{B}}$$

The observed **cross-section** is **compatible with** the previous result of **Ref. [11]**

Results from BELLE and BaBar are reported too, further **confirming the compatibility** of this thesis' results with the published literature

[11] Phys. Rev. D **104**, 052012

Extraction of the $\sigma(e^+e^- \longrightarrow \pi^+\pi^-\psi(2S))$

$\pi\pi\,\psi(2S)$ cross-section

E_{CoM} (MeV)	$\mathcal{L}$ (pb^{-1})	N_{Obs}	ϵ (%)	$\sigma_{Observed}$ (pb)	$(1+\delta)$	$\frac{1}{\lvert 1-\Pi \rvert^2}$	σ_{Born} (pb)
4611.86	103.65	26^{+5}_{-5}	38.00	$16.49^{+3.17}_{-3.17}$	0.893	1.05453	$17.51^{+3.37}_{-3.37}$
4628.00	521.53	156^{+14}_{-13}	39.22	$19.06^{+1.71}_{-1.59}$	0.886	1.05444	$20.40^{+1.83}_{-1.70}$
4640.91	551.65	203^{+16}_{-15}	40.36	$22.78^{+1.80}_{-1.68}$	0.854	1.05442	$25.28^{+1.99}_{-1.87}$
4661.24	529.43	202^{+15}_{-15}	39.88	$23.90^{+1.77}_{-1.77}$	0.878	1.05441	$25.81^{+1.92}_{-1.92}$
4681.92	1667.39	518^{+24}_{-23}	37.99	$20.43^{+0.95}_{-0.91}$	0.950	1.05448	$20.39^{+0.95}_{-0.91}$
4698.82	535.54	173^{+14}_{-14}	38.21	$21.12^{+1.71}_{-1.71}$	0.925	1.05453	$21.67^{+1.75}_{-1.75}$
4739.70	163.87	37^{+7}_{-6}	35.51	$15.89^{+3.01}_{-2.58}$	1.045	1.05484	$14.42^{+2.73}_{-2.34}$
4750.05	366.55	77^{+9}_{-8}	34.79	$15.09^{+1.76}_{-1.57}$	1.054	1.05493	$13.57^{+1.59}_{-1.41}$
4780.54	511.47	84^{+10}_{-9}	32.90	$12.47^{+1.48}_{-1.34}$	1.126	1.05518	$10.50^{+1.25}_{-1.13}$
4843.07	525.16	66^{+9}_{-8}	30.52	$10.29^{+1.40}_{-1.25}$	1.150	1.05570	$8.48^{+1.16}_{-1.03}$
4918.02	207.82	19^{+5}_{-4}	29.24	$7.81^{+2.06}_{-1.64}$	1.255	1.05623	$5.89^{+1.55}_{-1.24}$
4950.93	159.28	23^{+6}_{-5}	34.16	$10.56^{+2.76}_{-2.30}$	0.999	1.05636	$10.01^{+2.61}_{-2.18}$

Study of the Intermediate States

Study of the Intermediate States

Dalitz Plots

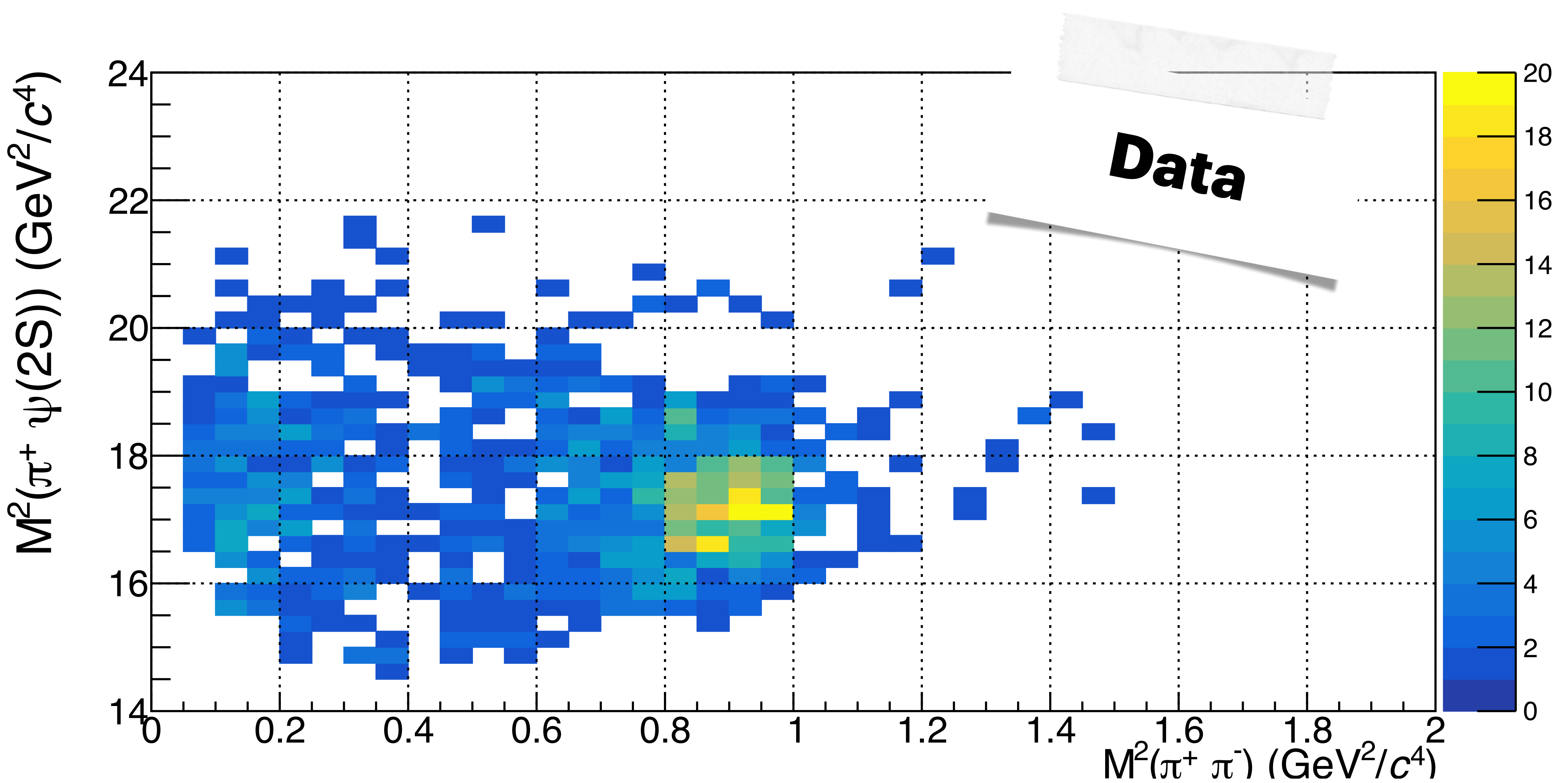

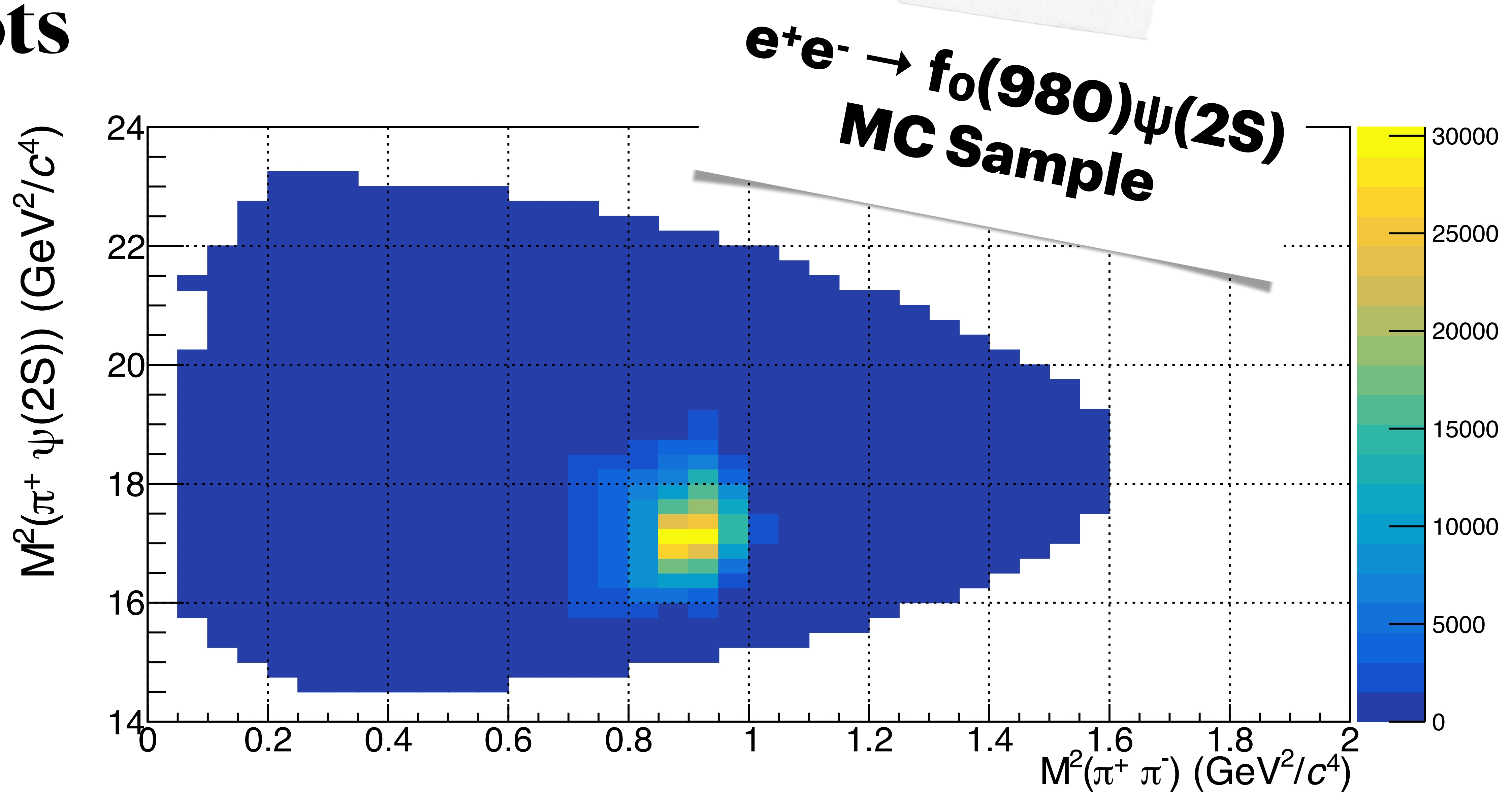

In **Ref.[11]**, a **simplified PWA** performed on the data sets highlighted **$f_0(500)$** and **$f_0(980)$** contributions

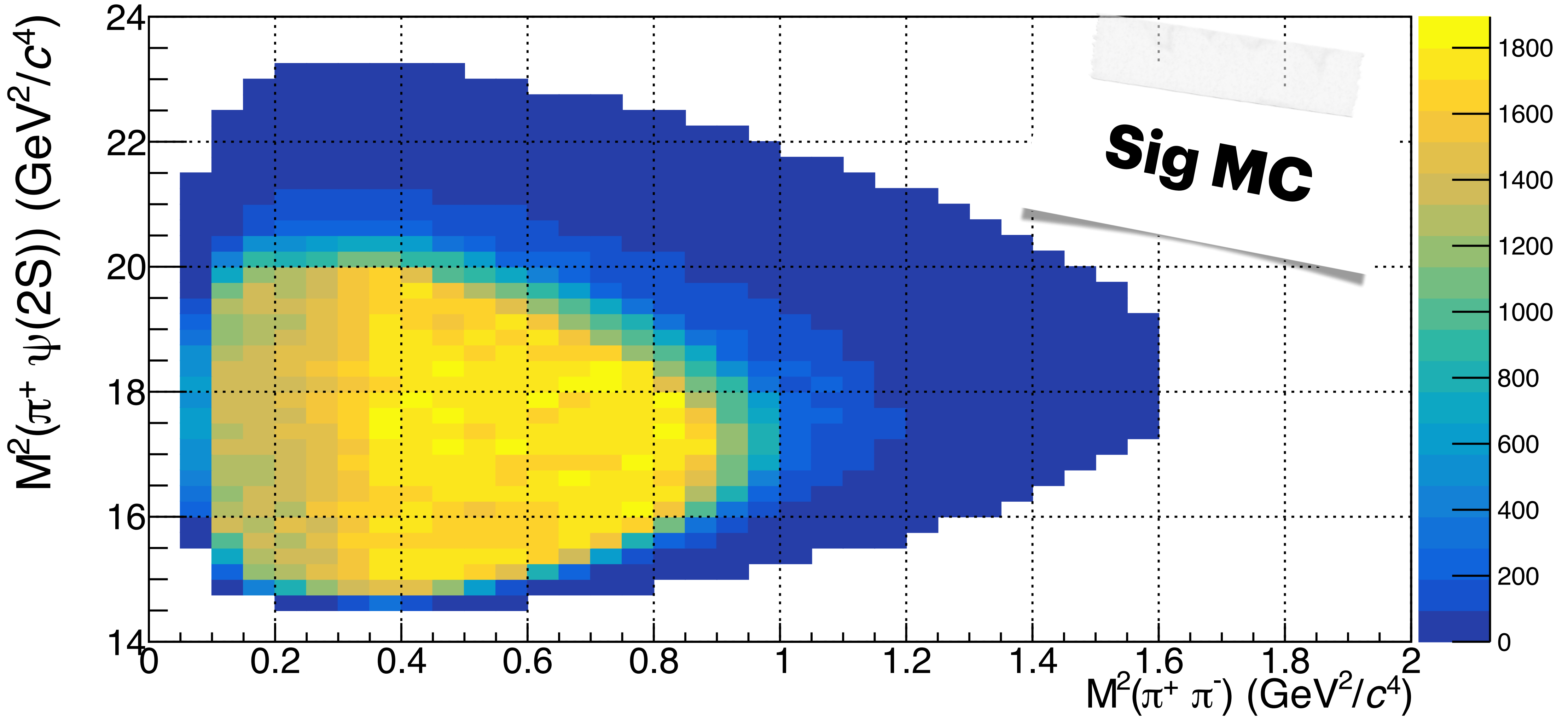

The **data samples** are **merged together** to have more significance

Study of the Intermediate States

Dalitz Plots

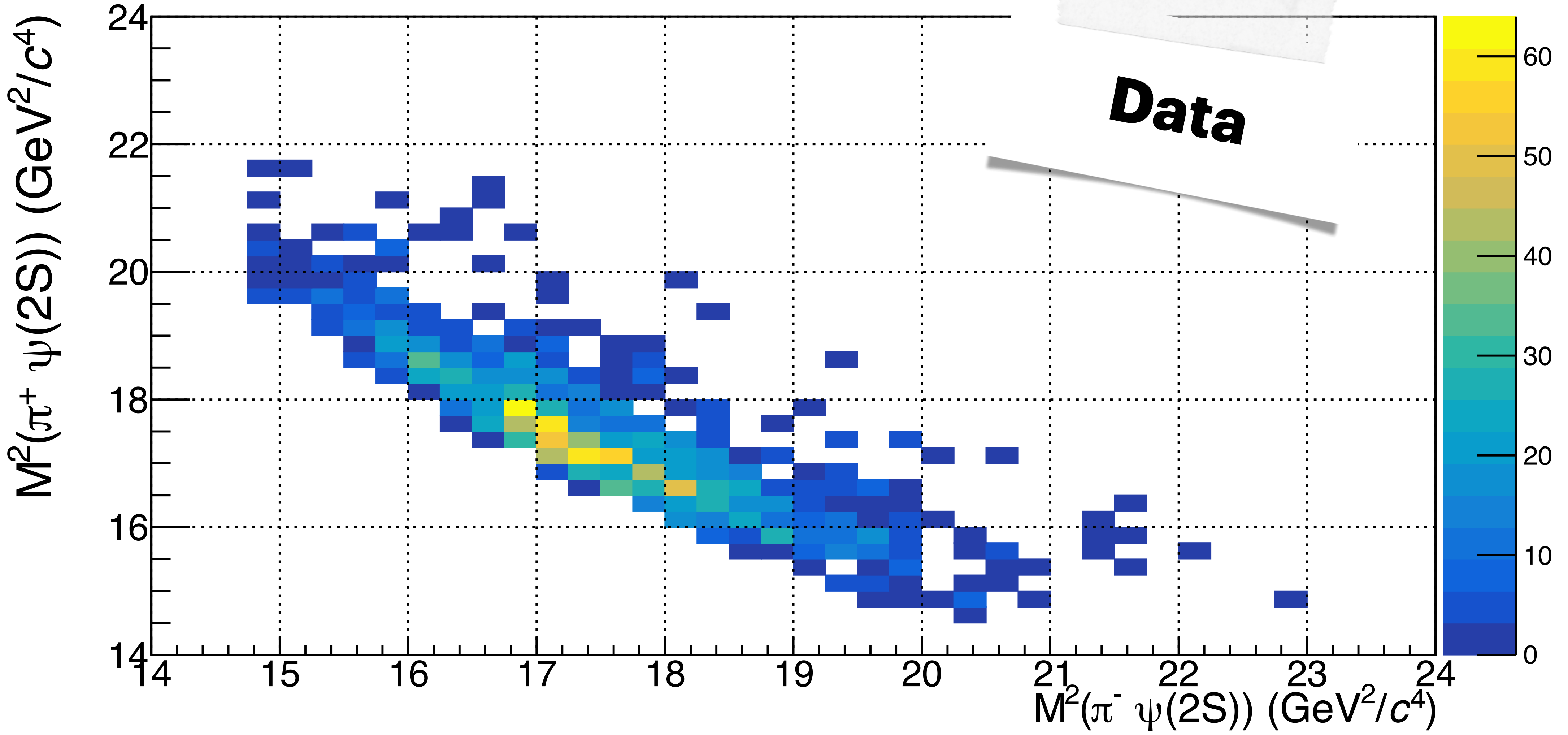

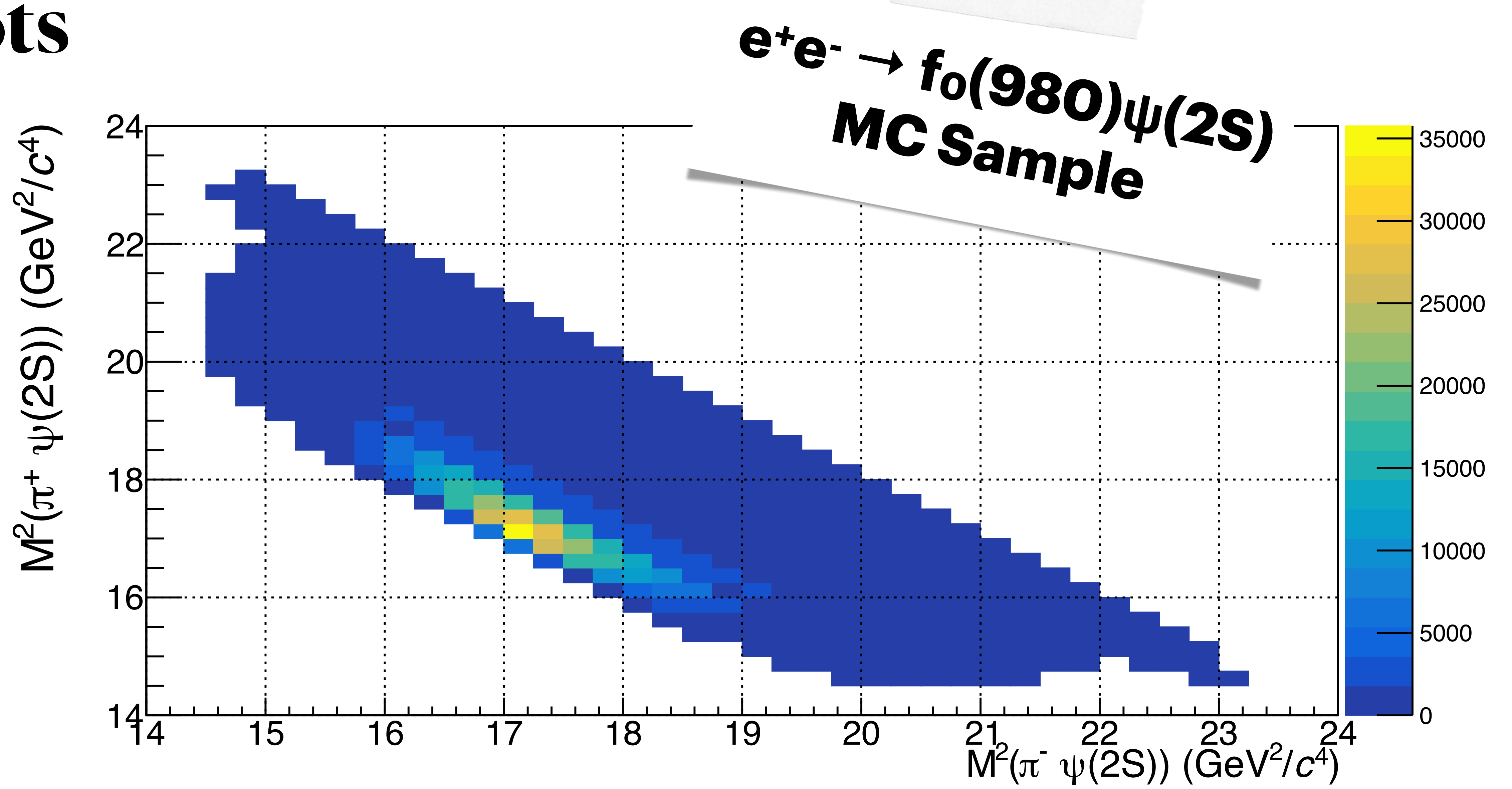

In **Ref.[11]**, a **simplified PWA** performed on the data sets highlighted **f_0(500)** and **f_0(980)** contributions

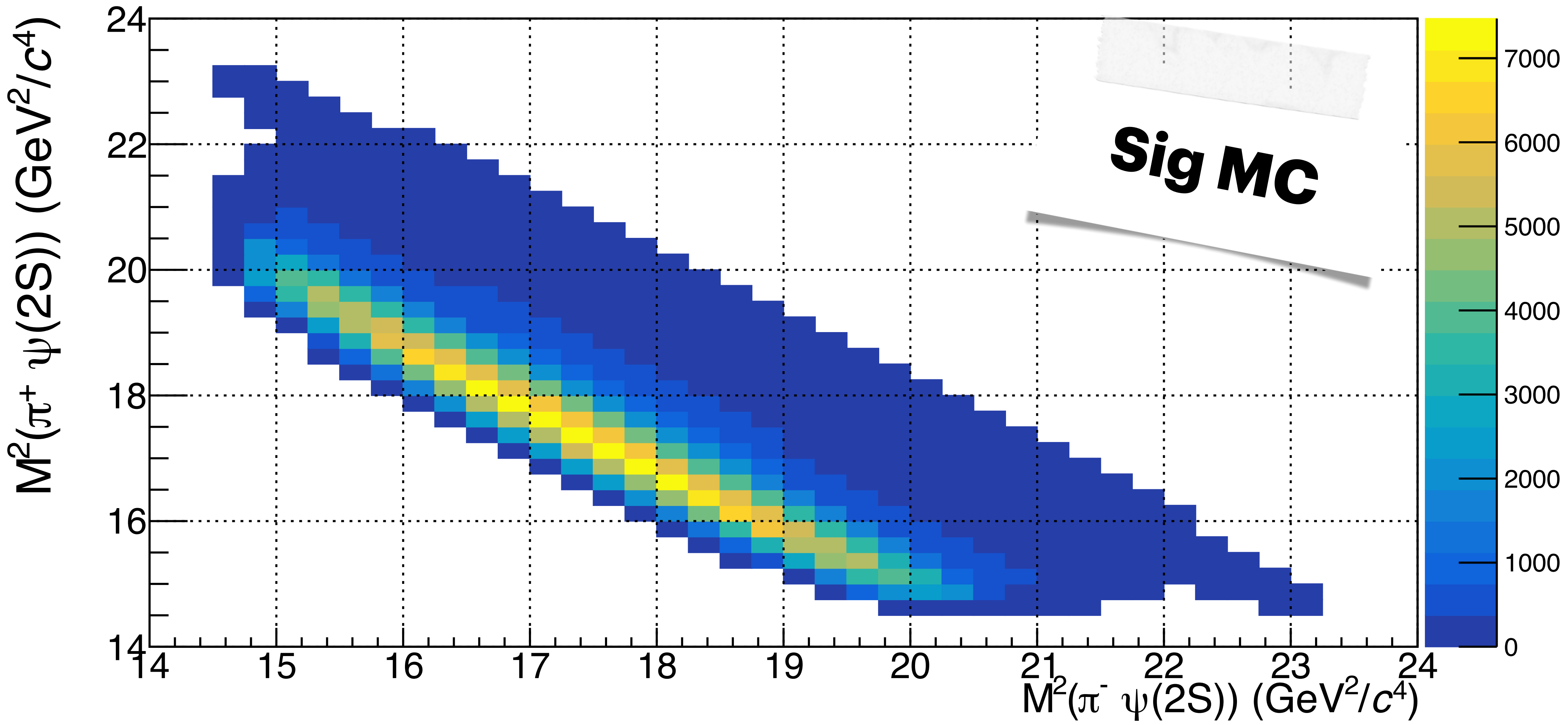

The **data samples** are **merged together** to have more significance

Cut Flow of Event Selection

Cuts [$\sqrt{s} = 4.680$ GeV]	Events	Efficiency [%]
Total Tracks	300000	100
Fiducial	252843	84.28
Kinetic PID	217074	72.36
5 Trks Events - Kalman Fit 1C	37655	12.55
6 Trks Events - Kalman Fit 1C	92285	30.76
5&6 Trks Events	129940	43.31

Table 22: Cut-flow for the $e^+e^- \to f_0(980)\psi(2S)$ process at $\sqrt{s} = 4.680$ GeV.

Cuts [$\sqrt{s} = 4.700$ GeV]	Events	Efficiency [%]
Total Tracks	300000	100
Fiducial	253827	84.61
Kinetic PID	217904	72.63
5 Trks Events - Kalman Fit 1C	37898	12.63
6 Trks Events - Kalman Fit 1C	91744	30.58
5&6 Trks Events	129642	43.21

Table 23: Cut-flow for the $e^+e^- \to f_0(980)\psi(2S)$ process at $\sqrt{s} = 4.700$ GeV.

Cuts [$\sqrt{s} = 4.740$ GeV]	Events	Efficiency [%]
Total Tracks	300000	100
Fiducial	256114	85.37
Kinetic PID	219228	73.08
5 Trks Events - Kalman Fit 1C	35609	11.87
6 Trks Events - Kalman Fit 1C	89614	29.87
5&6 Trks Events	125223	41.74

Table 24: Cut-flow for the $e^+e^- \to f_0(980)\psi(2S)$ process at $\sqrt{s} = 4.740$ GeV.

Cuts [$\sqrt{s} = 4.750$ GeV]	Events	Efficiency [%]
Total Tracks	300000	100
Fiducial	256903	85.63
Kinetic PID	220067	73.36
5 Trks Events - Kalman Fit 1C	34937	11.65
6 Trks Events - Kalman Fit 1C	87306	29.10
5&6 Trks Events	122243	40.75

Table 25: Cut-flow for the $e^+e^- \to f_0(980)\psi(2S)$ process at $\sqrt{s} = 4.750$ GeV.

Extraction of the σ(f_0(980) ψ(2S))

f_0(980) contribution

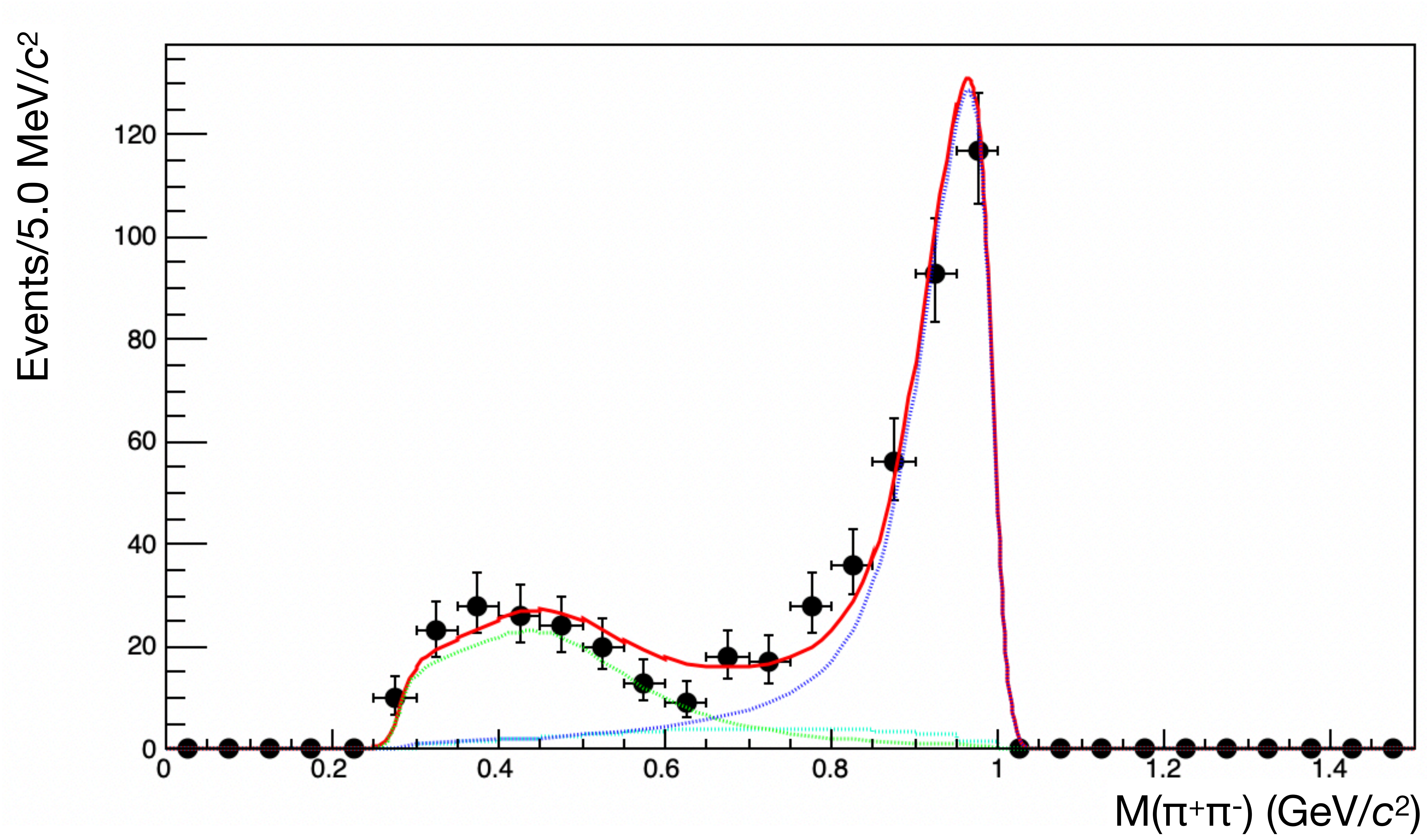

For **each √s**, the **f_0(980)** contribution is extracted by fitting the M(ππ) and M(πψ(2S)) invariant distributions

The signal is a **Flatté smeared by a Gauss(0, σ) multiplied by a threshold** function

$$BW(s) = \frac{1}{s - M^2 + i\left(g_1\rho_{\pi\pi}(s) + g_2\rho_{KK}(s)\right)}$$

The **f_0(500)** contribution is modelled with

$$BW(s) = \frac{1}{s - M_0^2 + i\sqrt{s}\Gamma}$$

with an energy-dependent width à la E791…

$$\Gamma(s) = \sqrt{1 - \frac{4m_{\pi^\pm}^2}{s}}\Gamma$$

Extraction of the $\sigma(f_0(980)\,\psi(2S))$

$f_0(980)$ contribution

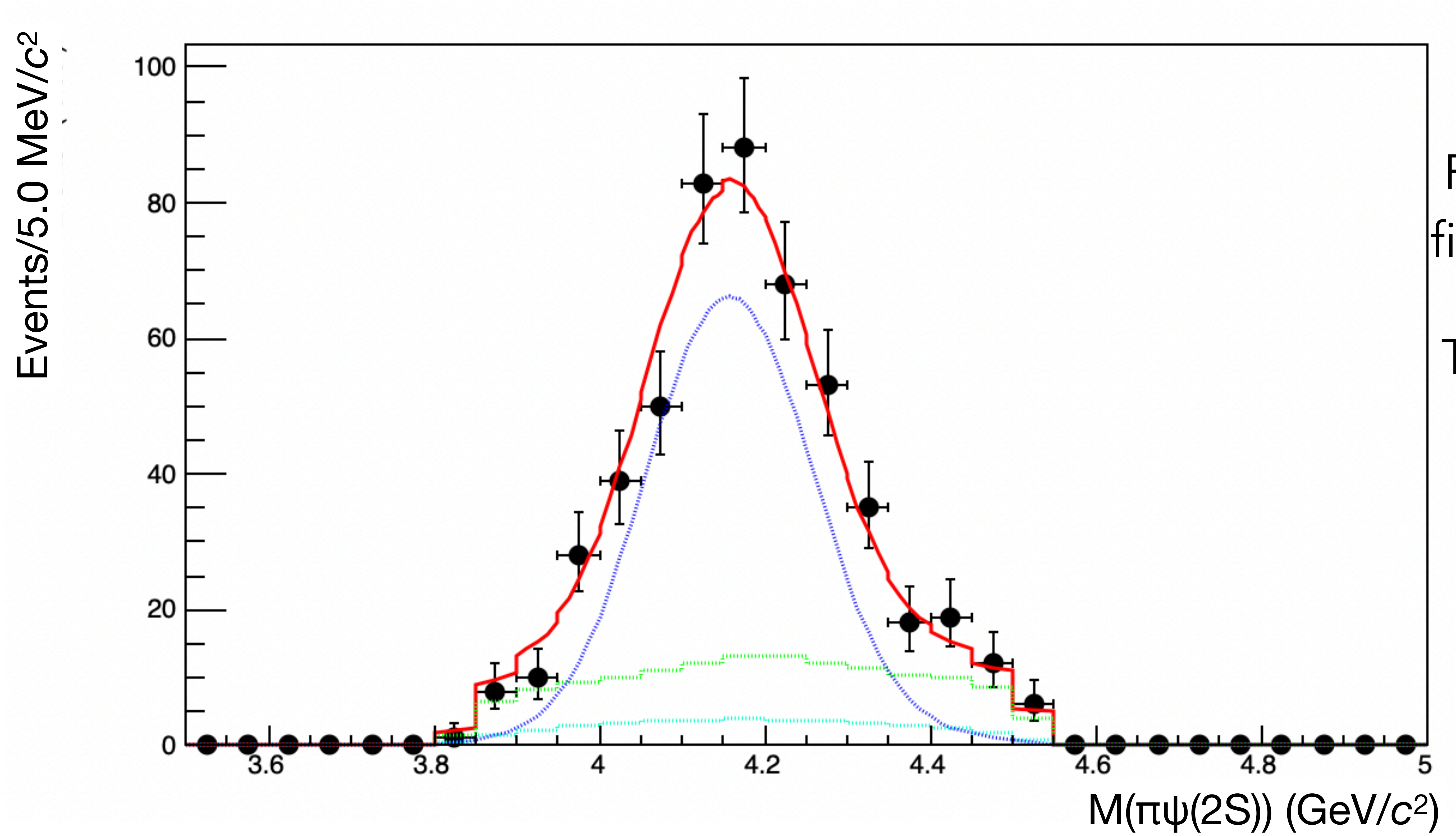

For **each √s**, the **f_0(980)** contribution is extracted by fitting the M(ππ) and M(πψ(2S)) invariant distributions

The signal is a **MS shape smeared by a Gauss(0, σ)**

The **f_0(500)** and **PHSP** contributions are modelled too by a **MS shape**

Extraction of the $\sigma(f_0(980)\,\psi(2S))$

$f_0(980)$ contribution

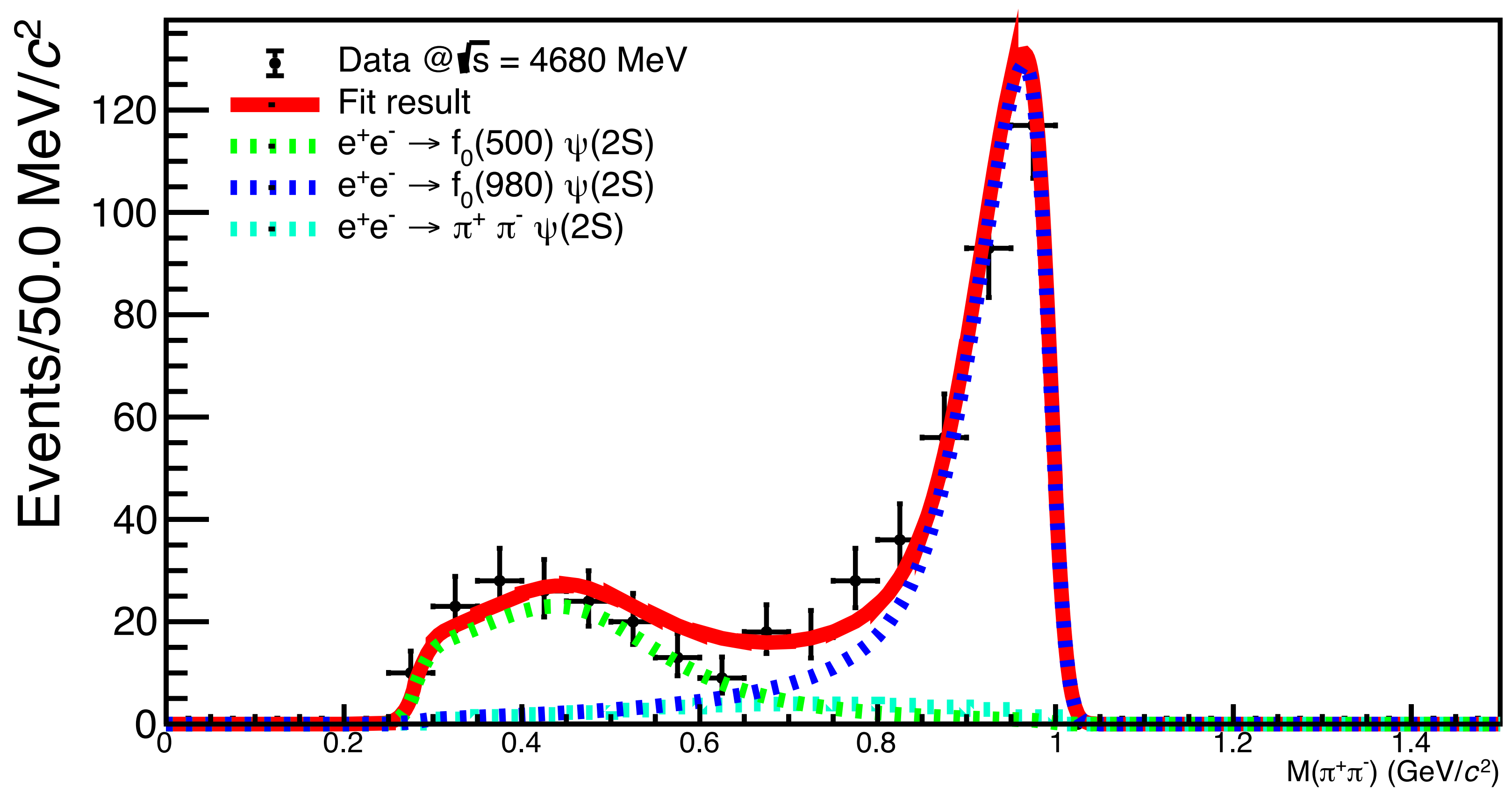

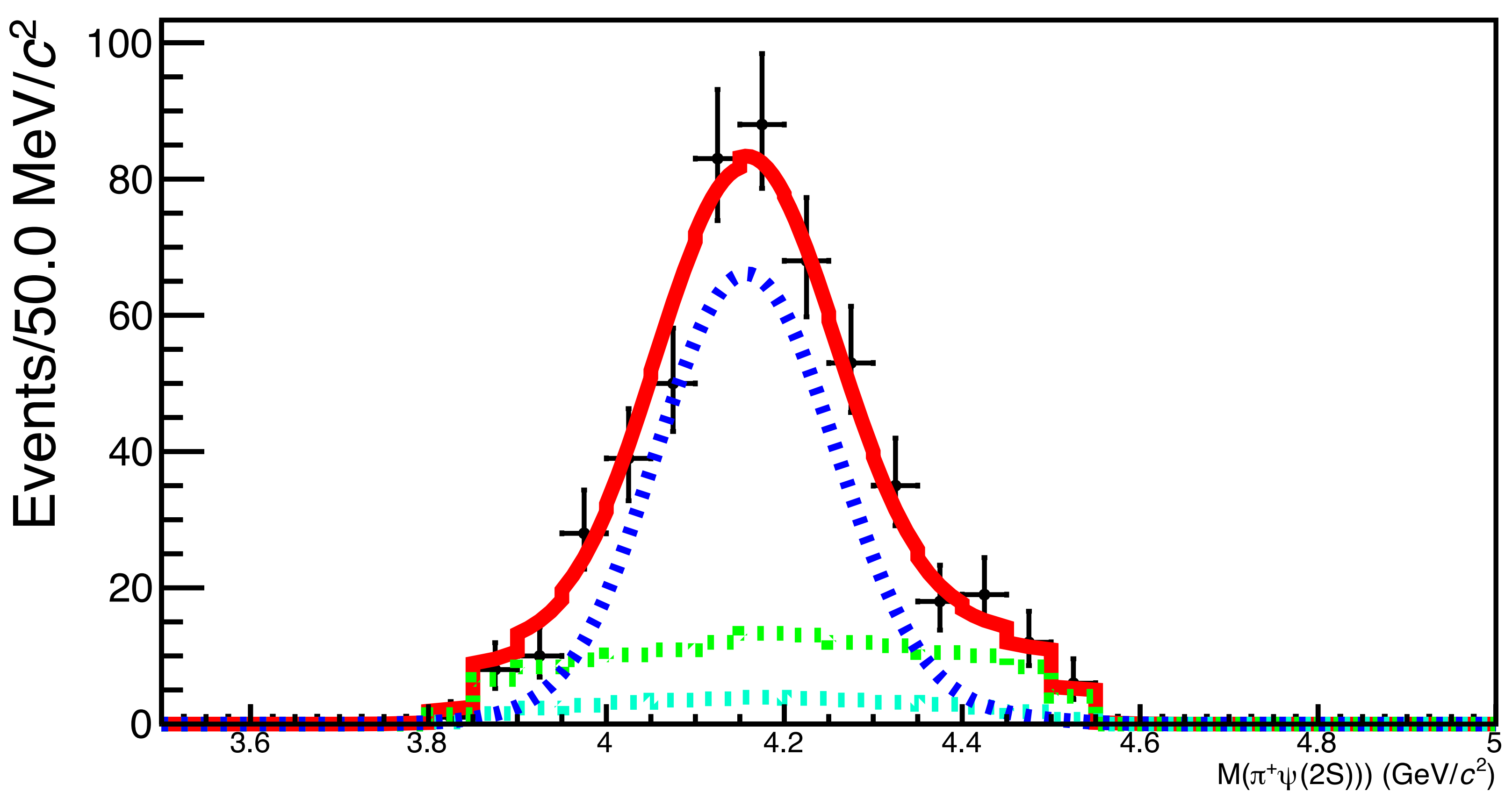

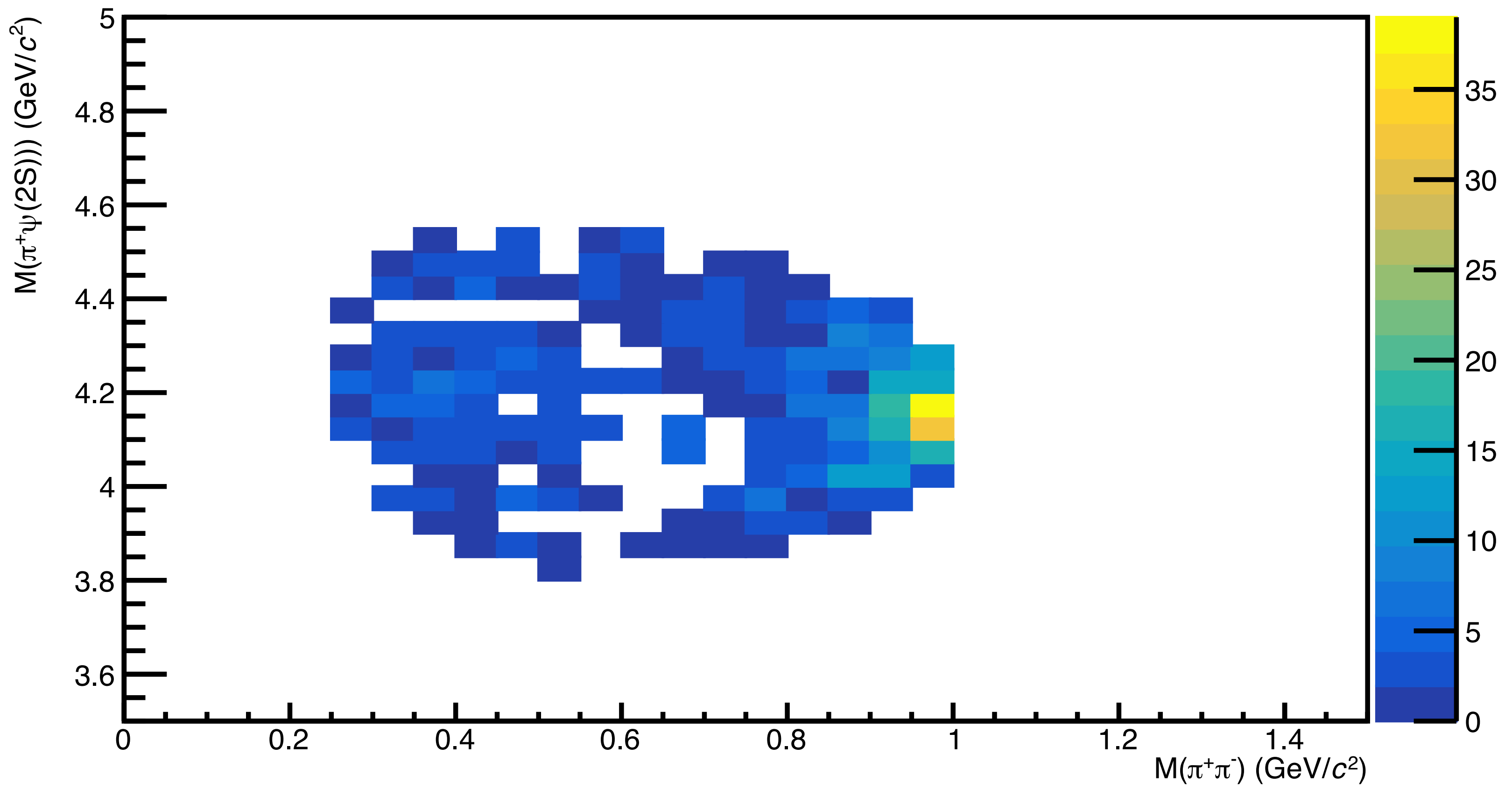

Extraction of the σ(f_0(980) ψ(2S))

f_0(980) contribution

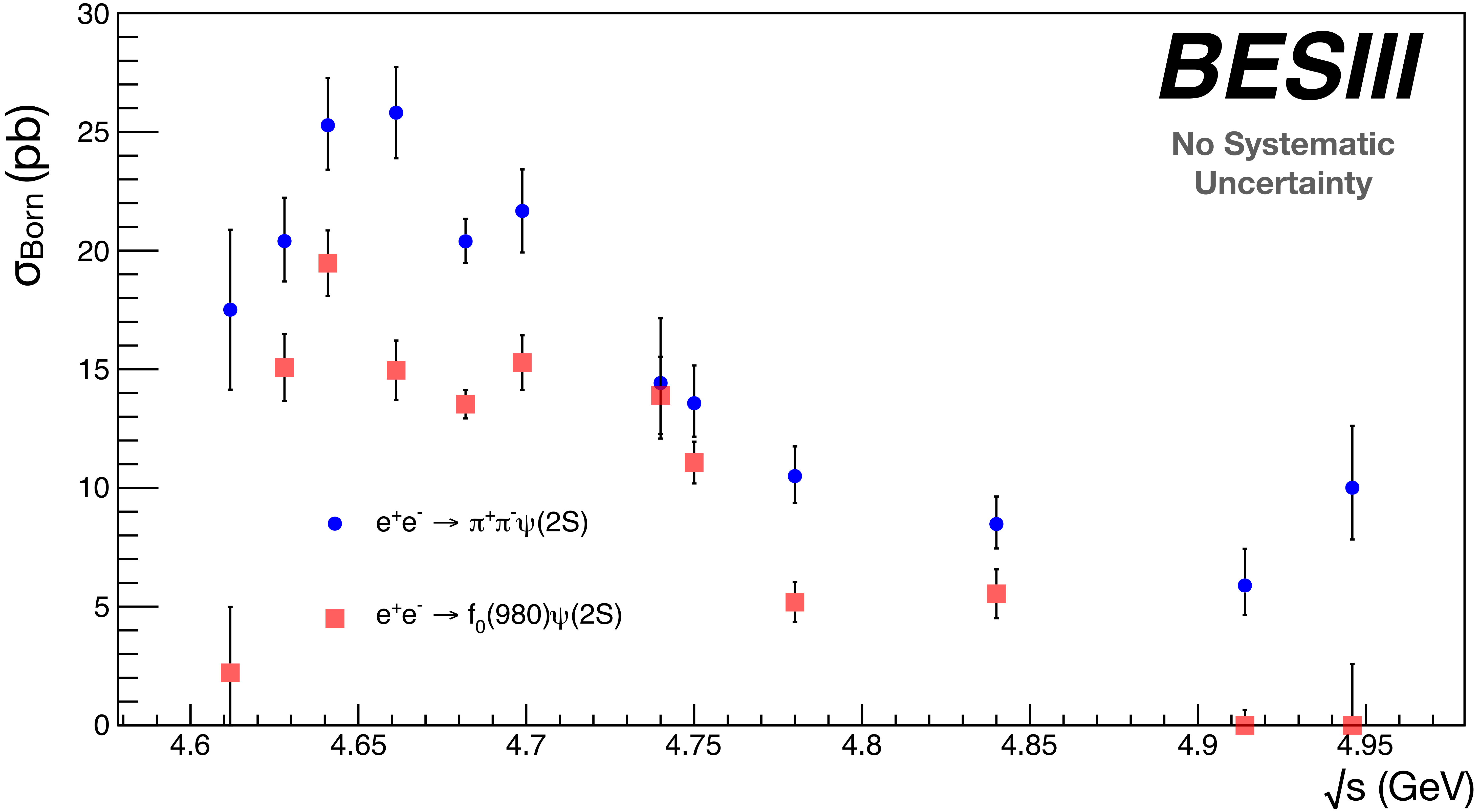

No particular structures can be recognised

Within the statistical uncertainty, ***σ_{Born}* x B** is **flat** wrt σ_{Born}(ππψ(2S))

The hypothesis of the **Y(4660)** being an ***f_0(980) - ψ(2S)* molecule**[12] **cannot be confirmed**

[12] Phys. Lett. B 665, 26-29 (2008)

Extraction of the σ(f_0(980) ψ(2S))

E_{CoM} (MeV)	$N_{\text{Obs}}^{f_0(980)}$	$\epsilon^{f_0(980)}$ (%)	$(1+\delta)$	$\frac{1}{\lvert 1-\Pi \rvert^2}$	$\sigma \times \mathcal{B}$ (pb)
4611.86	16 ± 4	0.4858	0.677	1.05453	2.21 ± 2.78
4628.00	107 ± 10	0.4795	0.673	1.05444	15.07 ± 1.41
4640.91	155 ± 11	0.4792	0.714	1.05442	19.47 ± 1.38
4661.24	120 ± 10	0.4533	0.792	1.05441	14.96 ± 1.25
4681.92	337 ± 15	0.4331	0.817	1.05448	13.53 ± 0.60
4698.82	120 ± 9	0.4321	0.804	1.05453	15.28 ± 1.15
4739.70	34 ± 4	0.4174	0.847	1.05484	13.90 ± 1.63
4750.05	63 ± 5	0.4075	0.902	1.05493	11.07 ± 0.88
4780.54	43 ± 7	0.3478	1.103	1.05518	5.19 ± 0.84
4843.07	43 ± 8	0.3601	0.972	1.05570	5.54 ± 1.03
4918.02	11 @90% C.L.	0.3963	0.889	1.05623	3.55 @90% C.L.
4950.93	12 @90% C.L.	0.3870	0.895	1.05636	5.14 @90% C.L.

[12] Phys. Lett. B 665, 26-29 (2008)

Systematic Uncertainties on the Cross-sections

- *Luminosity*: 1% as from Ref. [13]
- *Vacuum polarisation*: 0.5% from Ref. [14]
- *ISR radiative corrections*: Difference in the $(1 + \delta)$ between the between the first (flat cross-section hypothesis) and the last iterations is taken as systematic uncertainty
- *Tracking efficiency*: 1.0% per track[10], 2.0% (leptons) and 3.5% (average of 2 pion-topologies)
- *Intermediate states* branching fractions: from PDG
- *Lepton separation*, *trigger efficiency*, and *FSR*: 1.0% from Ref. [11]

[10] Phys. Rev. Lett **110**, 252001
[11] Phys. Rev. D **104**, 052012
[13] Chin. Phys. C **46**, 11, 113003
[14] Sov. J. Nucl. Phys **41**, 466-472

Systematic Uncertainties on the Cross-sections

- *Mass veto windows*: Variations in veto windows were considered up to ±6σ. No significant (< 0.5σ) deviations were observed
- *Different Generator*: With KKMC, < 0.5σ (non-significant) deviations were observed
- *Bin Size*: Differences wrt the nominal value oscillate within 1σ significance, passing the Barlow's test
- *<u>Background Shape</u>*: Inclusive MC shape was tested. Differences with respect the nominal values oscillate within 1.1σ significance for every energy point. Despite being relatively small the difference, this systematic source (taken as the difference) was added
- *f_0(500)/f_0(980) Masses and Widths*: Changed up to ±5σ from PDG. From the broad spectrum of tests all the differences oscillate within 1.5σ significance, passing the Barlow's test
- *f_0(980) Shape*: In the ππspectrum a Crystallball function was tested, while in the πψ spectrum a Gaussian with a non-zero bias and with a different spread was tried. All the tested scenarios differ from the nominal value by less than 3σ, passing the Barlow's Test

Systematic Uncertainties on the Cross-sections

$\pi\pi\,\psi(2S)$ cross-section

Sample	Luminosity	Vacuum polarisation	ISR corrections	Tracking efficiency	Intermediate States $\mathcal{B}$	Other sources	Bkg. Shape	Total
4.612	1.00	0.50	8.03	3.50	1.00	0.90	38.46	39.48
4.626	1.00	0.50	5.31	3.50	1.00	0.89	1.28	6.72
4.640	1.00	0.50	6.03	3.50	1.00	0.86	9.85	12.19
4.660	1.00	0.50	4.20	3.50	1.00	0.88	1.49	5.92
4.680	1.00	0.50	1.54	3.50	1.00	0.95	0.00	4.22
4.700	1.00	0.50	3.49	3.50	1.00	0.93	10.40	11.65
4.740	1.00	0.50	0.17	3.50	1.00	1.05	40.54	40.73
4.750	1.00	0.50	0.61	3.50	1.00	1.06	7.79	8.76
4.780	1.00	0.50	0.14	3.50	1.00	1.13	0.00	3.97
4.840	1.00	0.50	1.67	3.50	1.00	1.16	31.82	32.11
4.914	1.00	0.50	0.06	3.50	1.00	1.26	10.53	11.27
4.946	1.00	0.50	7.11	3.50	1.00	1.00	8.70	11.90

Systematic Uncertainties on the Cross-sections

$f_0(980)\ \psi(2S)$ cross-section

Sample	Luminosity	Vacuum polarisation	ISR corrections	Tracking efficiency	Intermediate States $\mathcal{B}$	Other sources	Bkg. Shape	Total
4.612	1.00	0.50	3.35	3.50	1.00	0.68	0.06	5.12
4.626	1.00	0.50	6.63	3.50	1.00	0.68	0.11	7.67
4.640	1.00	0.50	3.50	3.50	1.00	0.72	0.03	5.22
4.660	1.00	0.50	2.44	3.50	1.00	0.80	0.09	4.59
4.680	1.00	0.50	0.81	3.50	1.00	0.82	0.03	3.98
4.700	1.00	0.50	0.93	3.50	1.00	0.81	0.00	4.00
4.740	1.00	0.50	0.03	3.50	1.00	0.85	0.03	3.90
4.750	1.00	0.50	3.81	3.50	1.00	0.91	0.06	5.47
4.780	1.00	0.50	7.63	3.50	1.00	1.11	0.16	8.60
4.840	1.00	0.50	0.40	3.50	1.00	0.98	0.12	3.95
4.914	—	—	—	—	—	—	—	—
4.946	—	—	—	—	—	—	—	—

Final Born Cross-sections Results

Sample	$\sigma_{\text{Born}}(\pi^+\pi^-\psi(2S))$ (pb)	$\sigma_{\text{Born}}(f_0(980)\psi(2S))\times$ $\mathcal{B}(f_0(980)\to\pi^+\pi^-)$ (pb)
4.612	$17.51^{+3.37}_{-3.37}\pm 6.91$	$2.21^{+2.78}_{-2.78}\pm 0.11$
4.626	$20.40^{+1.83}_{-1.70}\pm 1.37$	$15.07^{+1.41}_{-1.41}\pm 1.16$
4.640	$25.28^{+1.99}_{-1.87}\pm 3.08$	$19.47^{+1.38}_{-1.38}\pm 1.02$
4.660	$25.81^{+1.92}_{-1.92}\pm 1.53$	$14.96^{+1.25}_{-1.25}\pm 0.69$
4.680	$20.39^{+0.95}_{-0.91}\pm 0.86$	$13.53^{+0.60}_{-0.60}\pm 0.54$
4.700	$21.67^{+1.75}_{-1.75}\pm 2.52$	$15.28^{+1.15}_{-1.15}\pm 0.61$
4.740	$14.42^{+2.73}_{-2.34}\pm 5.87$	$13.90^{+1.63}_{-1.63}\pm 0.54$
4.750	$13.57^{+1.59}_{-1.41}\pm 1.19$	$11.07^{+0.88}_{-0.88}\pm 0.61$
4.780	$10.50^{+1.25}_{-1.13}\pm 0.42$	$5.19^{+0.84}_{-0.84}\pm 0.45$
4.840	$8.48^{+1.16}_{-1.03}\pm 2.72$	$5.54^{+1.03}_{-1.03}\pm 0.22$
4.914	$5.89^{+1.55}_{-1.24}\pm 0.66$	3.55 @90% C.L.
4.946	$10.01^{+2.61}_{-2.18}\pm 1.19$	5.14 @90% C.L.

Analysis of the $\pi^{\pm}\psi(2S)$ Invariant Mass and Search for the $Z_c(4430)^{\pm}$

Cut Flow of Event Selection

Cuts [$\sqrt{s}$ = 4.680 GeV]	Events	Efficiency [%]
Total Tracks	300000	100
Fiducial	250531	83.51
Kinetic PID	210770	70.26
5 Trks Events - Kalman Fit 1C	51886	17.30
6 Trks Events - Kalman Fit 1C	92451	30.82
5&6 Trks Events	144337	48.11

Table 35: Cut-flow for the $e^+e^- \to \pi^\mp Z_c(4430)^\pm \to \pi^+\pi^-\psi(2S)$ process at $\sqrt{s} = 4.680$ GeV.

Cuts [$\sqrt{s}$ = 4.700 GeV]	Events	Efficiency [%]
Total Tracks	300000	100
Fiducial	252119	84.04
Kinetic PID	212800	70.93
5 Trks Events - Kalman Fit 1C	51570	17.19
6 Trks Events - Kalman Fit 1C	94101	31.37
5&6 Trks Events	145671	48.56

Table 36: Cut-flow for the $e^+e^- \to \pi^\mp Z_c(4430)^\pm \to \pi^+\pi^-\psi(2S)$ process at $\sqrt{s} = 4.700$ GeV.

Cuts [$\sqrt{s}$ = 4.740 GeV]	Events	Efficiency [%]
Total Tracks	300000	100
Fiducial	254349	84.78
Kinetic PID	214356	71.45
5 Trks Events - Kalman Fit 1C	49170	16.39
6 Trks Events - Kalman Fit 1C	97184	32.39
5&6 Trks Events	146354	48.78

Table 37: Cut-flow for the $e^+e^- \to \pi^\mp Z_c(4430)^\pm \to \pi^+\pi^-\psi(2S)$ process at $\sqrt{s} = 4.740$ GeV.

Cuts [$\sqrt{s}$ = 4.750 GeV]	Events	Efficiency [%]
Total Tracks	300000	100
Fiducial	254486	84.83
Kinetic PID	213609	71.20
5 Trks Events - Kalman Fit 1C	47993	16.00
6 Trks Events - Kalman Fit 1C	97526	32.51
5&6 Trks Events	145519	48.51

Table 38: Cut-flow for the $e^+e^- \to \pi^\mp Z_c(4430)^\pm \to \pi^+\pi^-\psi(2S)$ process at $\sqrt{s} = 4.750$ GeV.

Analysis of the $\pi^{\pm}\psi(2S)$ Invariant Mass and Search for the $Z_c(4430)^{\pm}$

Signal MC Shape Extraction

Z_c Signal MC sample
300k events

√s [GeV]	$w_{Normalised} = (\sigma \times \mathcal{L})/(\sigma \times \mathcal{L})\|_{4.680}$
4.612	0.05
4.626	0.31
4.640	0.41
4.660	0.40
4.680	1.00
4.700	0.34
4.740	0.07
4.750	0.15
4.780	0.16
4.840	0.13
4.914	0.04
4.946	0.05

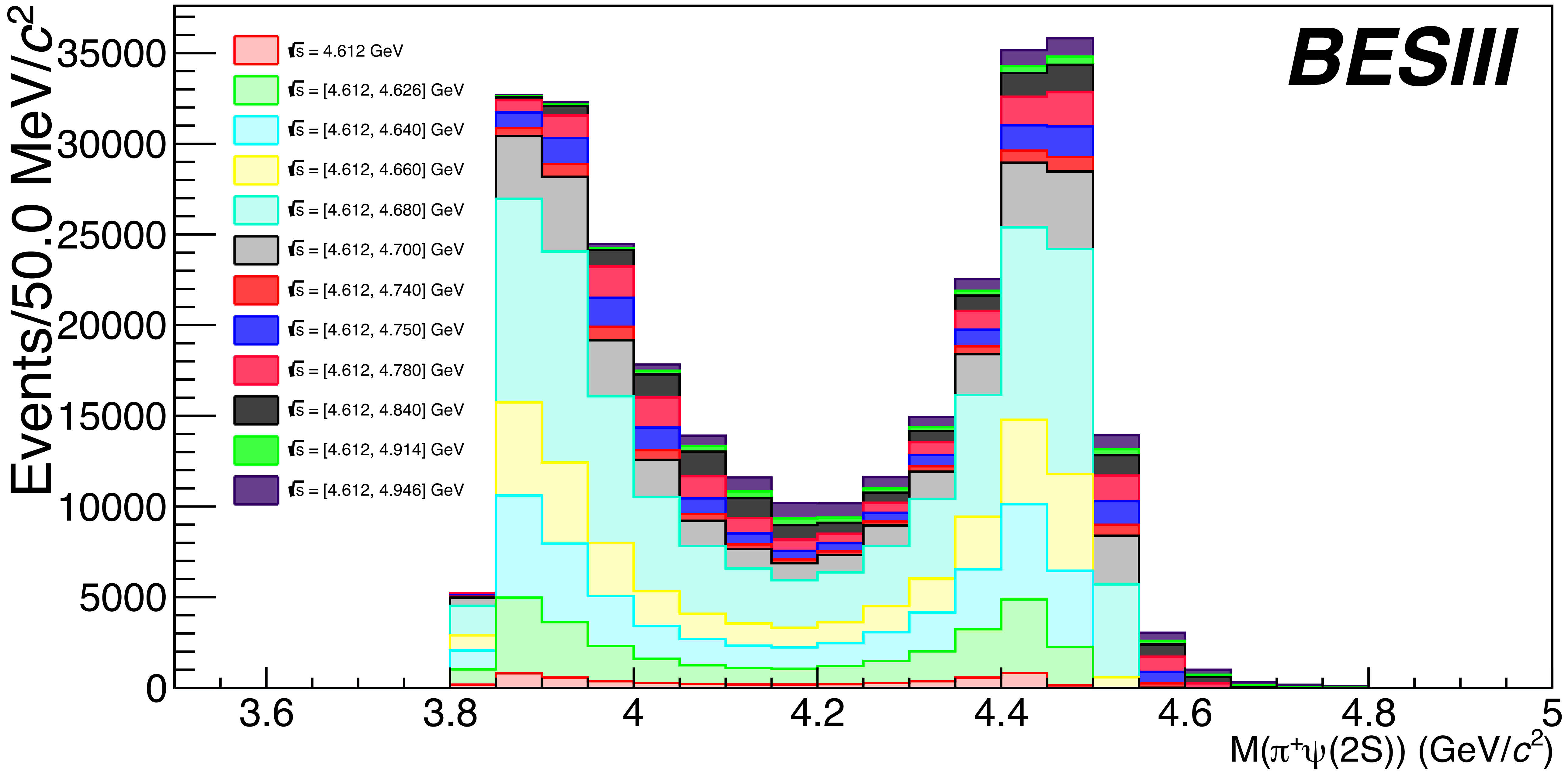

Signal function
MC Signal Shape

Analysis of the $\pi^{\pm}\psi(2S)$ Invariant Mass and Search for the $Z_c(4430)^{\pm}$

Signal MC Shape Extraction

Z_c Signal MC sample
300k events

√s [GeV]	$w_{Normalised}$ = $(\sigma \times \mathcal{L})/(\sigma \times \mathcal{L})\|_{4.680}$
4.612	0.05
4.626	0.31
4.640	0.41
4.660	0.40
4.680	1.00
4.700	0.34
4.740	0.07
4.750	0.15
4.780	0.16
4.840	0.13
4.914	0.04
4.946	0.05

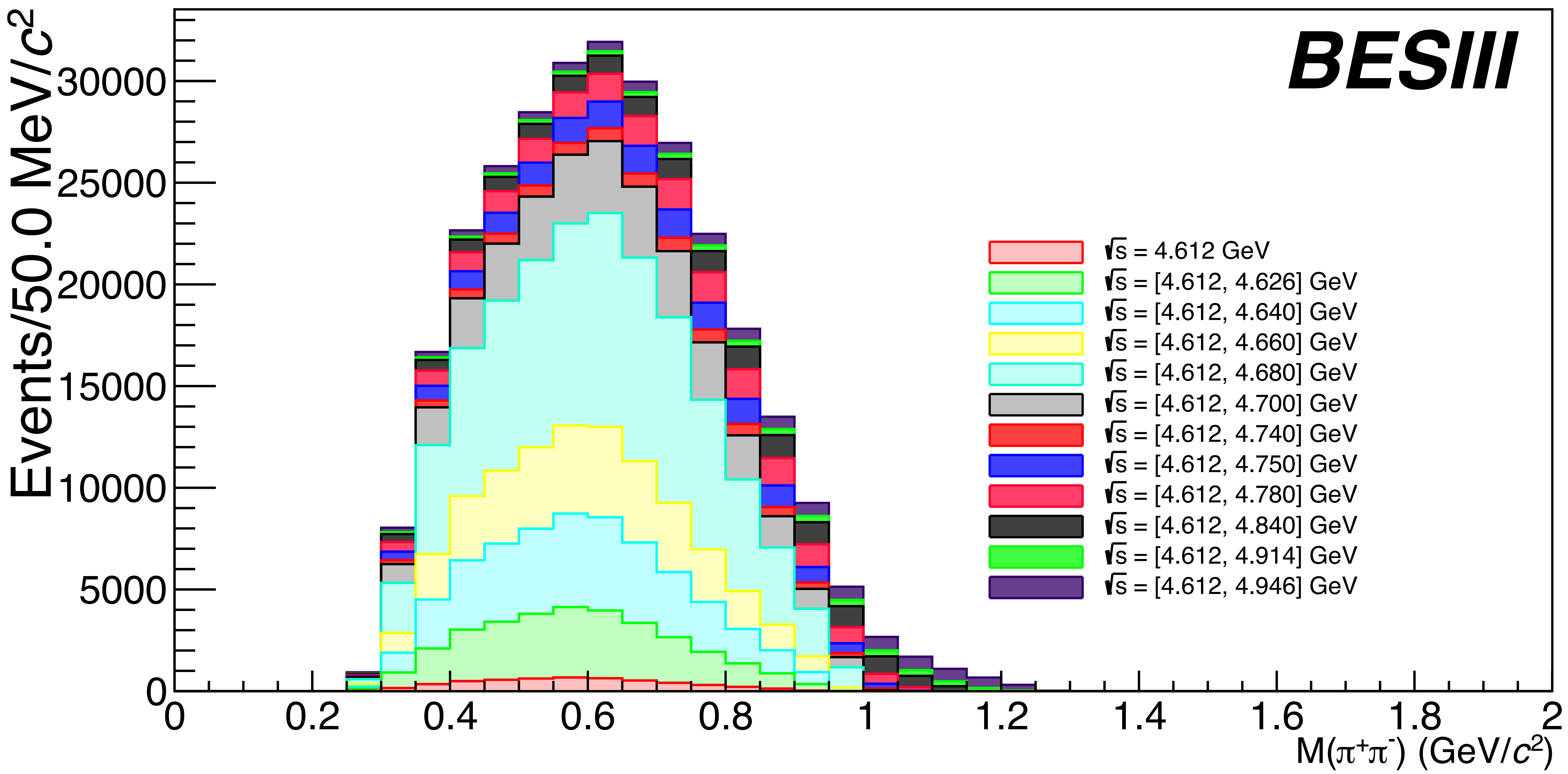

Signal function
MC Signal Shape

Analysis of the $\pi^{\pm}\psi(2S)$ Invariant Mass and Search for the $Z_c(4430)^{\pm}$

Drawing from the $f_0(980)$ study, the the **M(ππ)** and **M(πψ(2S))** invariant distributions are **fitted without Z_c(4430)** contribution

The two f_0 states are described by analytical shapes, with the $f_0(980)$ being a weighted sum of 12 Flattés

All the other shapes are taken from MC simulation

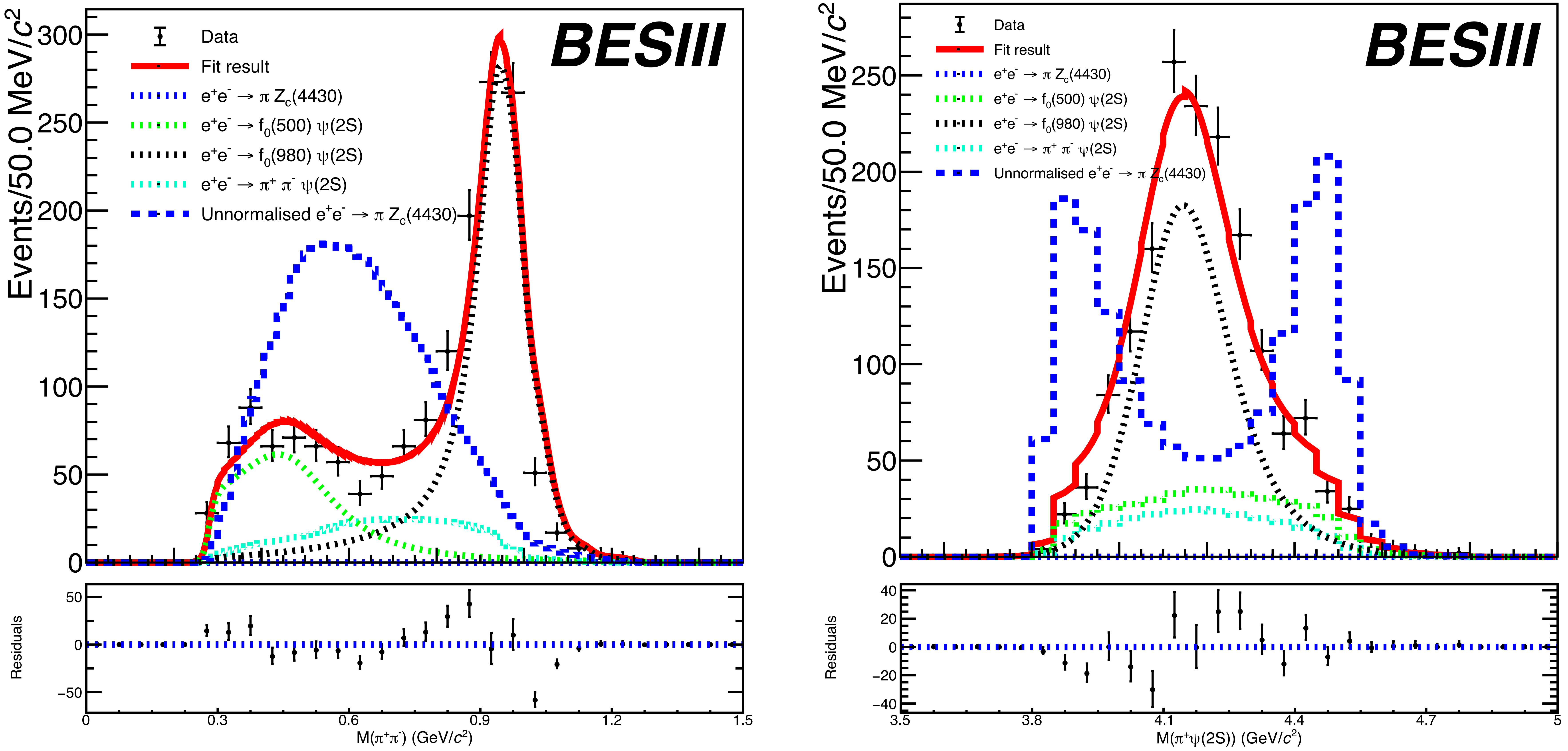

Analysis of the $\pi^{\pm}\psi(2S)$ Invariant Mass and Search for the $Z_c(4430)^{\pm}$

Drawing from the $f_0(980)$ study, the the **M(ππ)** and **M(πψ(2S))** invariant distributions are **fitted without Z_c(4430)** contribution

Adding Z_c(4430) contribution does not improve the fit significantly

	Value
N(f_0(980))	988 ± 29
N(f_0(500))	384 ± 29
N(PHSP)	248 ± 41

NB
Constrained to total number of events

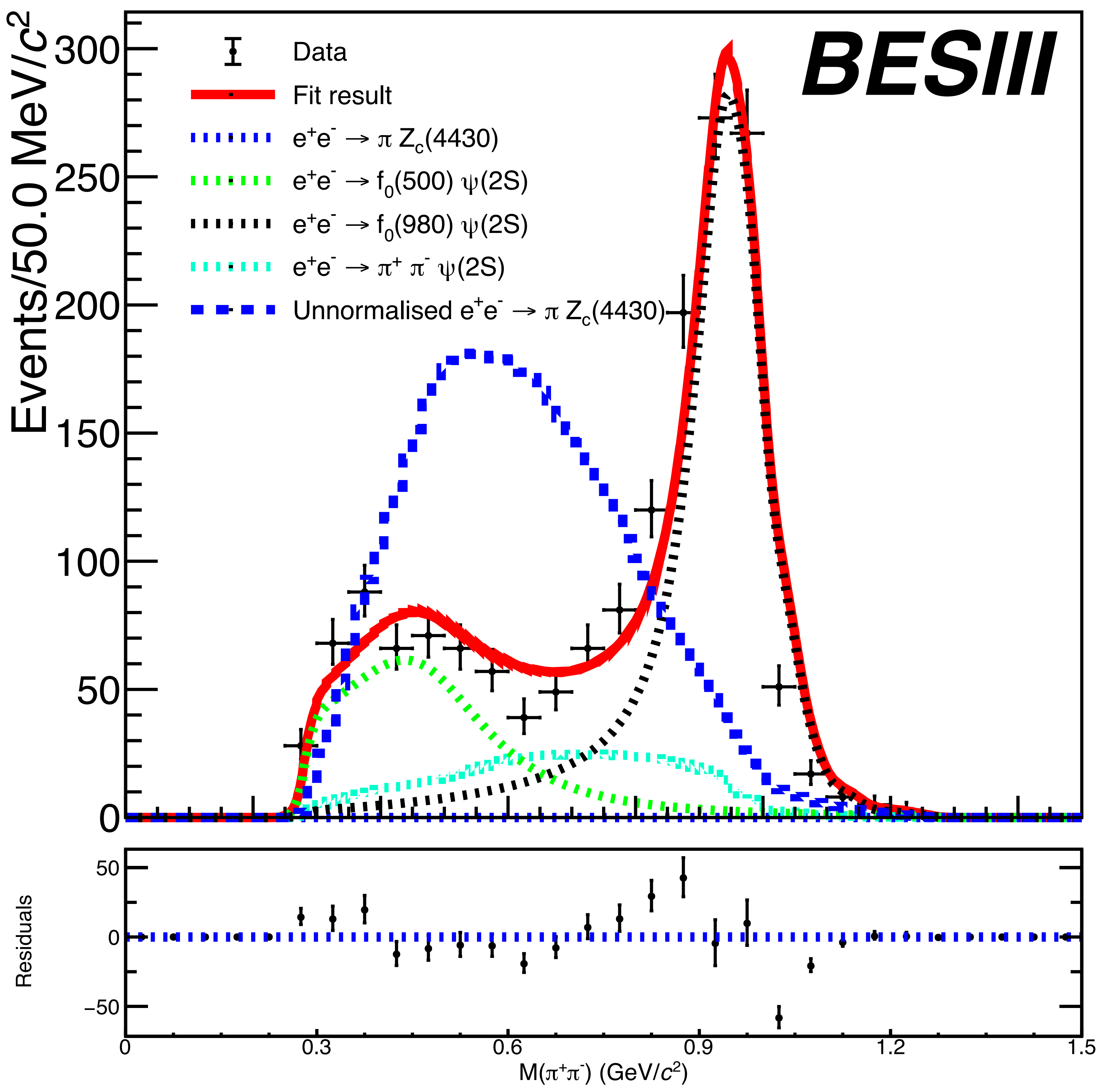

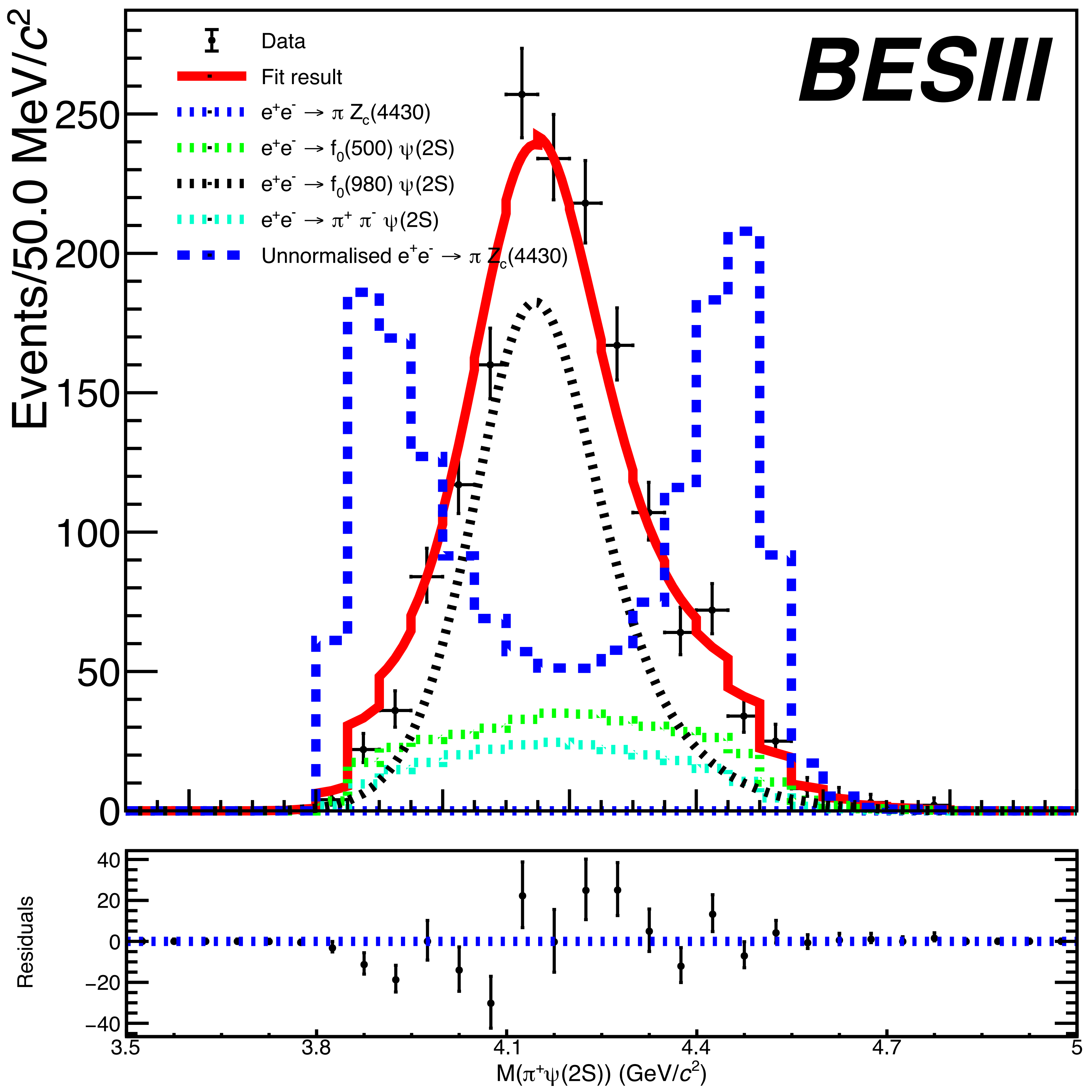

Analysis of the $\pi^{\pm}\psi(2S)$ Invariant Mass and Search for the $Z_c(4430)^{\pm}$

Bayesian U.L. @90%
$N(Z_c(4430)) < 14$

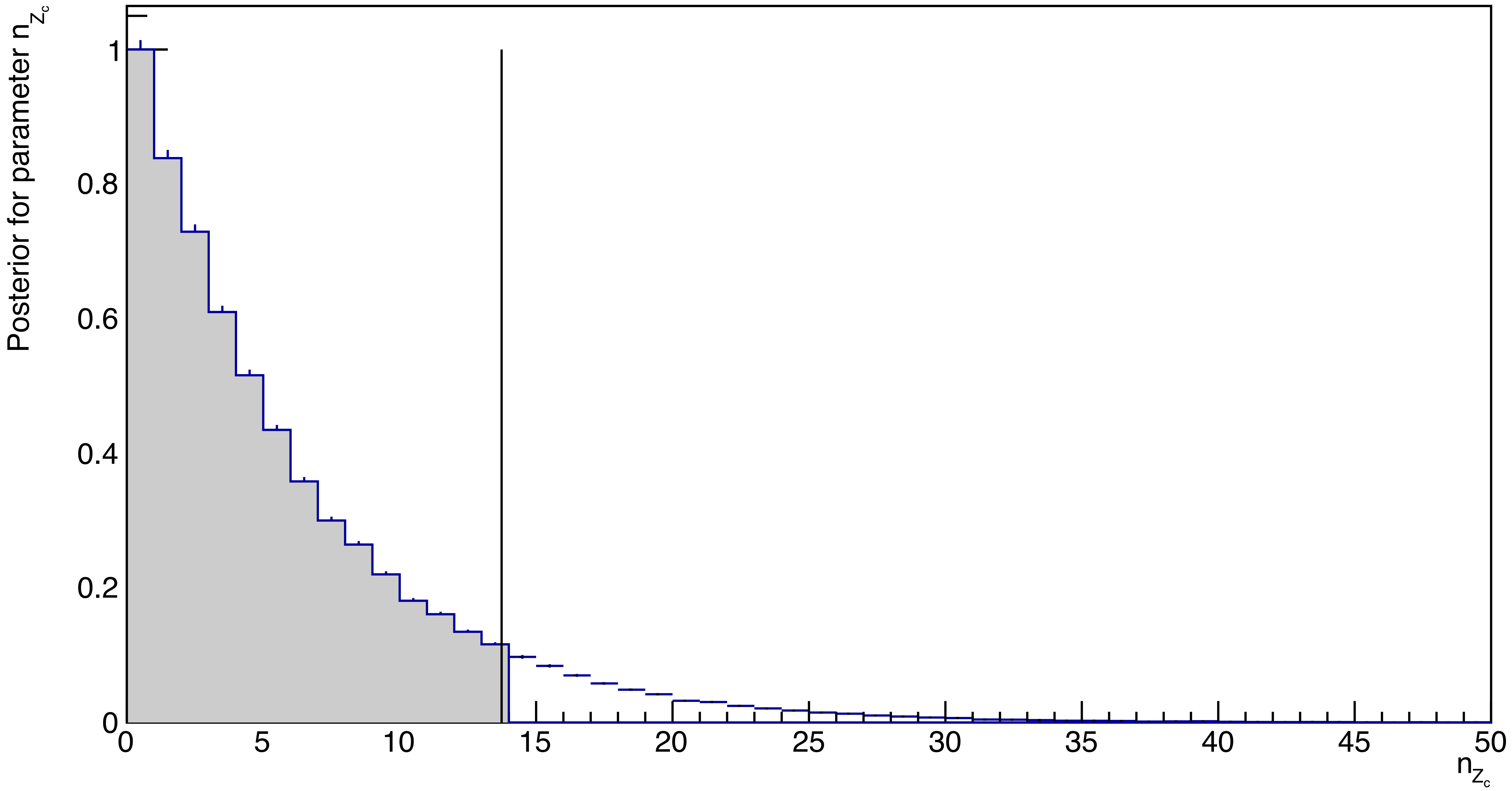

The **Bayesian U.L.** is obtained by integrating the posterior distribution using the **Metropolis-Hastings algorithm** with a **uniform proposal distribution**, a upper limit (U.L.) with a **Uniform prior** and **incorporating the systematic** uncertainties

Analysis of the $\pi^{\pm}\psi(2S)$ Invariant Mass and Search for the $Z_c(4430)^{\pm}$

Production Ratio Estimation

Bayesian U.L. @90%
$N(Z_c(4430)) < 14$

$$R = \frac{\sigma_{\text{Born}}(e^+e^- \to \pi^{\pm} Z_c(4430)^{\mp} \to \pi^+\pi^-\psi(2S))}{\sigma_{\text{Born}}(e^+e^- \to \pi^+\pi^-\psi(2S))} < 0.7\ \%$$

When **compared with the paper**[10] used as motivation for this analysis, the **$Z_c(4430)^{\pm}$** state **production** in the $e^+e^- \to \pi^+\pi^-\psi(2S)$ channel is **suppressed by** at least **20 times with respect to** that of the **$Z_c(3900)^{\pm}$** hadron in $e^+e^- \to \pi^+\pi^- J/\psi$

Conclusions and Outlook

Using twelve data samples with a total integrated luminosity of ~5 fb^{-1} @$\sqrt{s}$ = [4.612, 4.946]

The **$e^+e^- \rightarrow \pi^+\pi^-\psi(2S)$** reaction is studied GeV, **below 4.7 GeV** the reaction is **consistent** with the results of Ref. [11], while **above** the cross-section is **measured for the first time**

The contribution of the **$e^+e^- \rightarrow f_0(980)\psi(2S)$** process is found **for the first time** and its cross section is measured, a structure can be recognised **around 4.666 GeV**

The **non trivial structure suggest** some kind of link between the Y(4660) state and the $f_0(980) - \psi(2S)$ bound state, but the statistical un certainty prevents conclusion

A **search for the $Z_c(4430)$** exotic state @$\sqrt{s}$ < 5.0 GeV is performed via the **$e^+e^- \rightarrow \pi^+\pi^-\psi(2S)$** reaction, but **no evident $Z_c(4430)$** is found and a Bayesian upper limit at the 90% confidence level (C.L.) is set

Thanks for your attention!

Back-up Slides

Event Selection

Charged Particles Momentum Optimisation

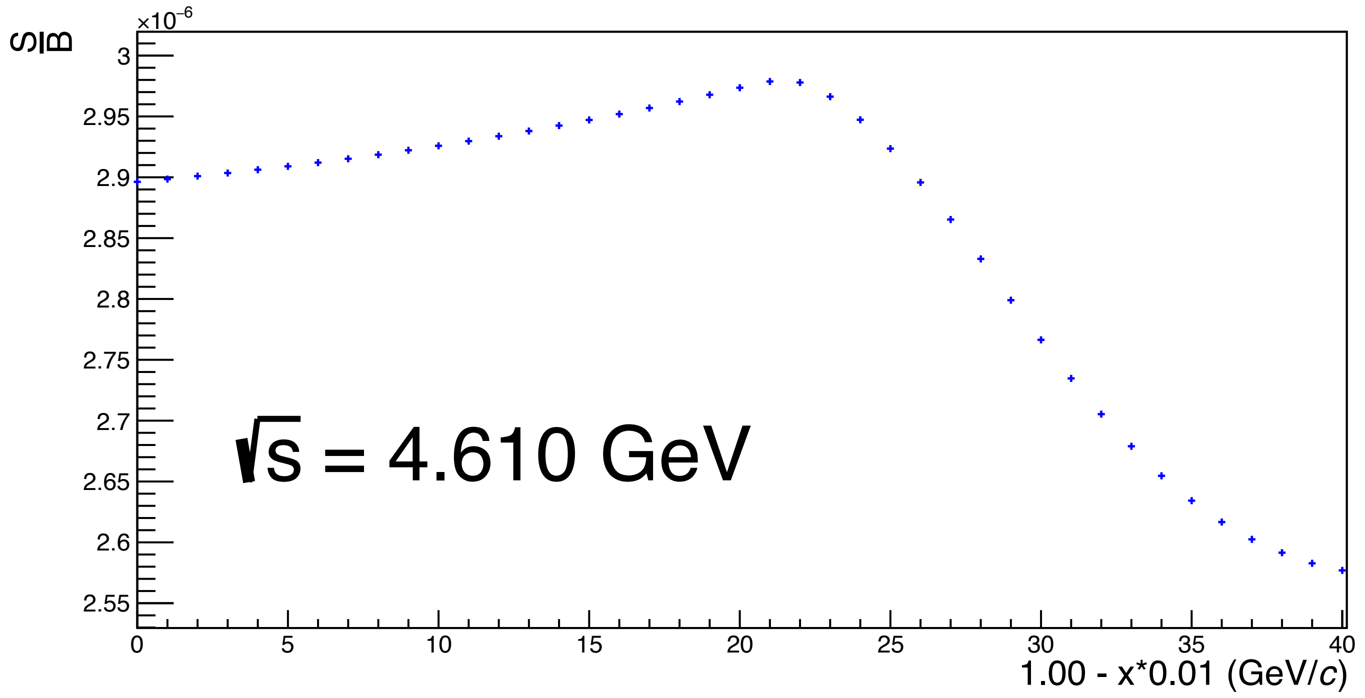

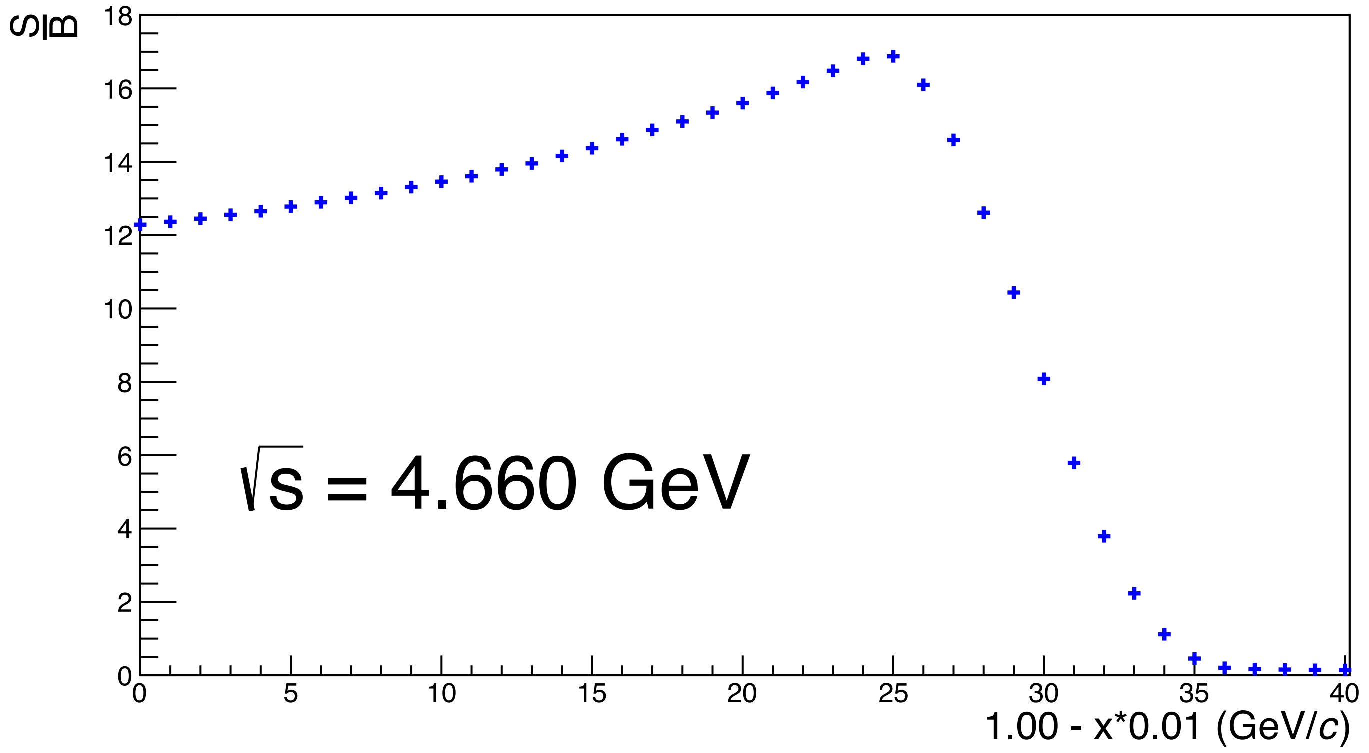

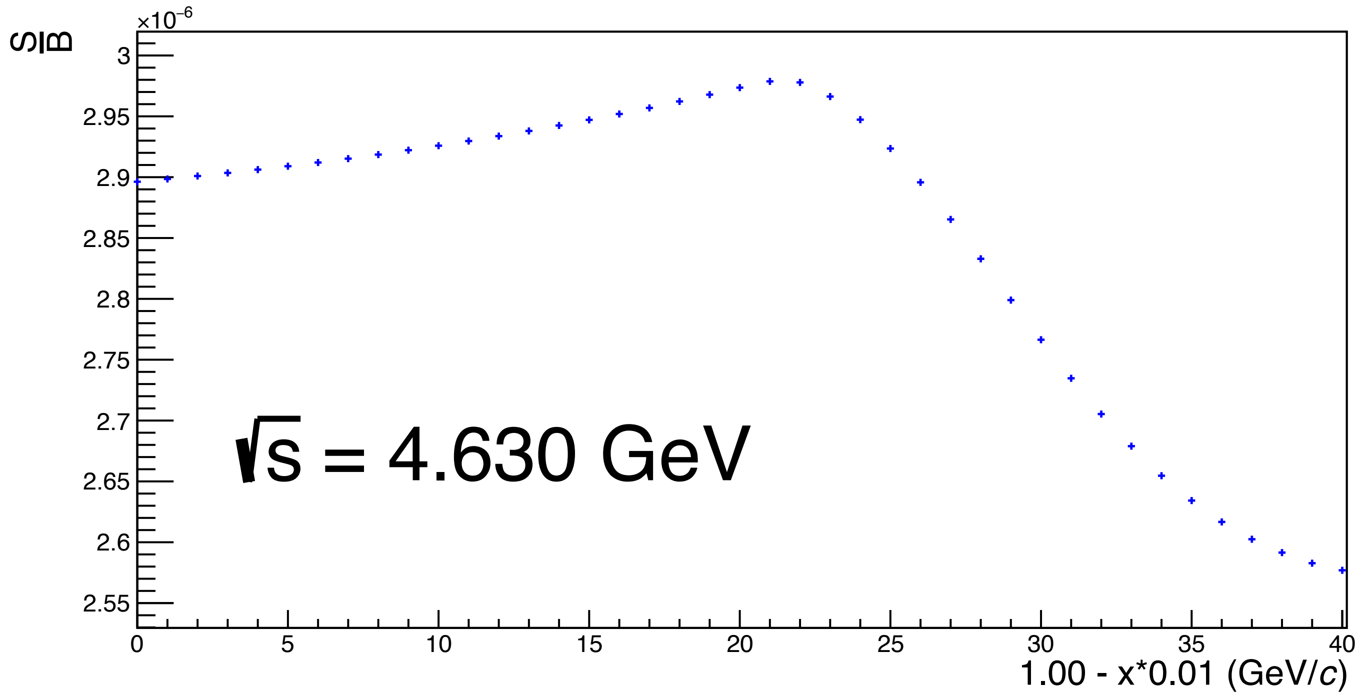

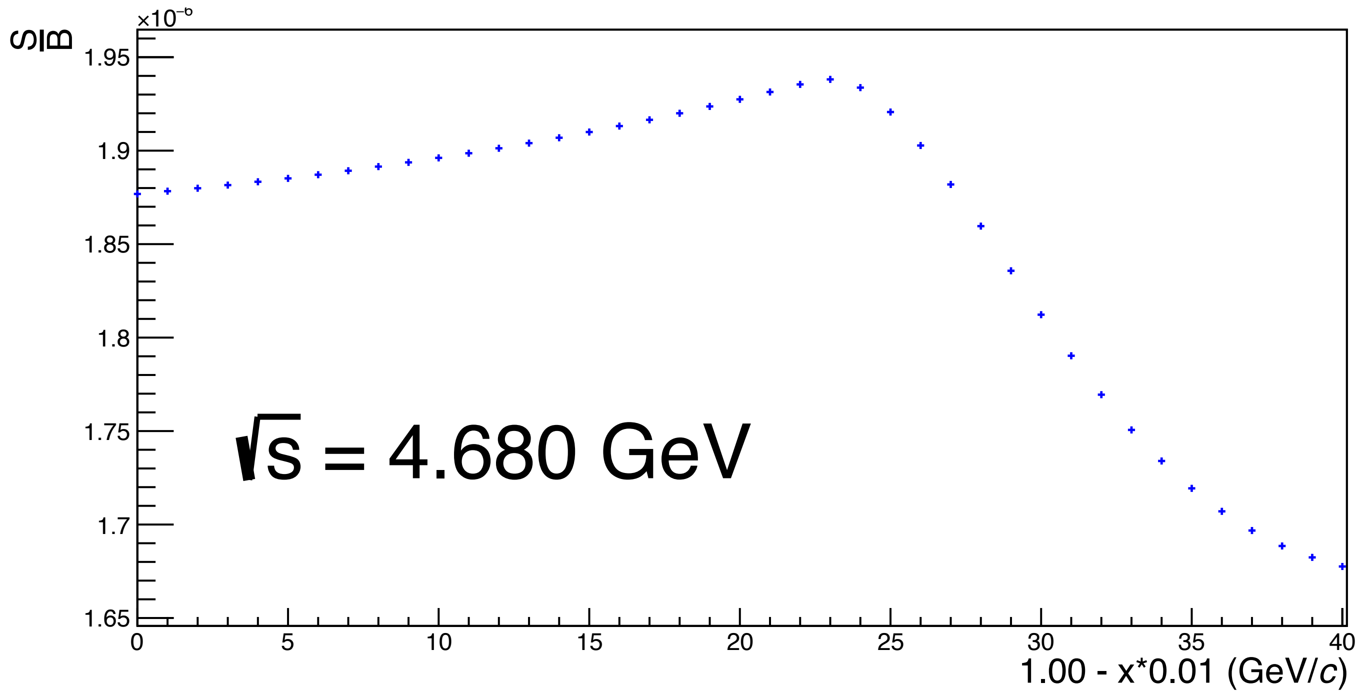

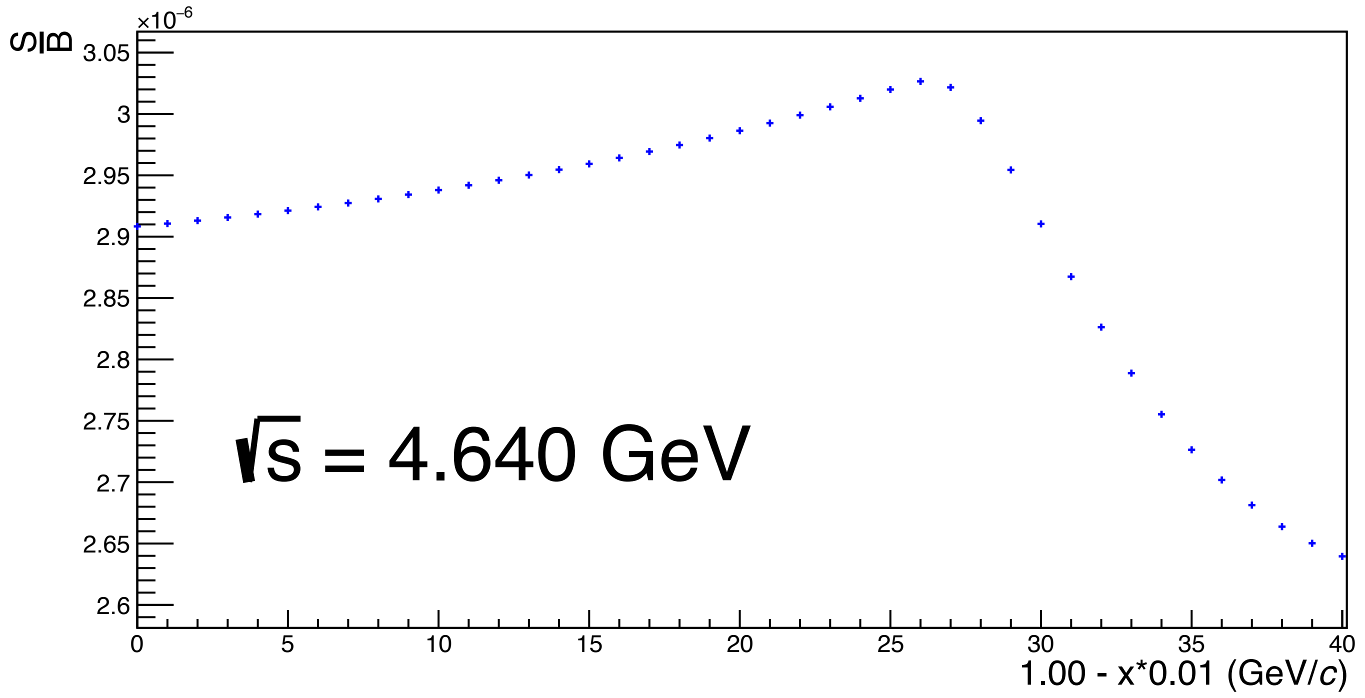

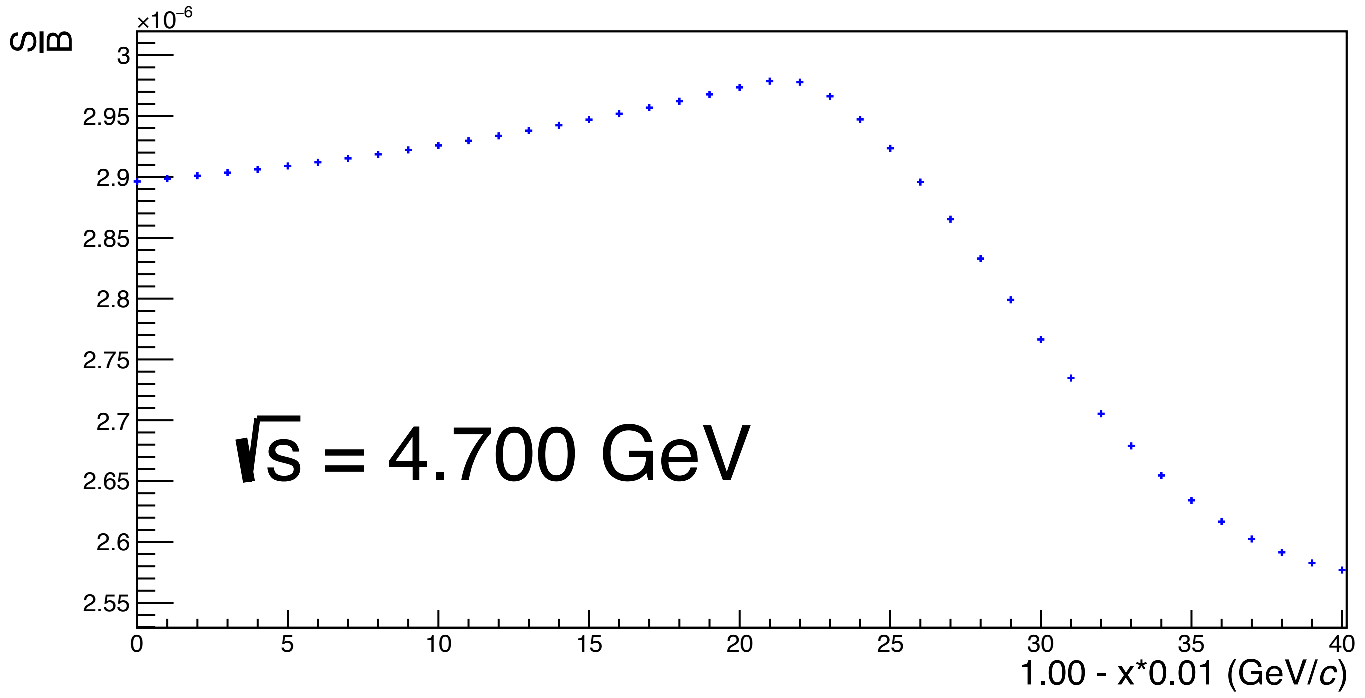

Event Selection

Charged Particles Momentum Optimisation

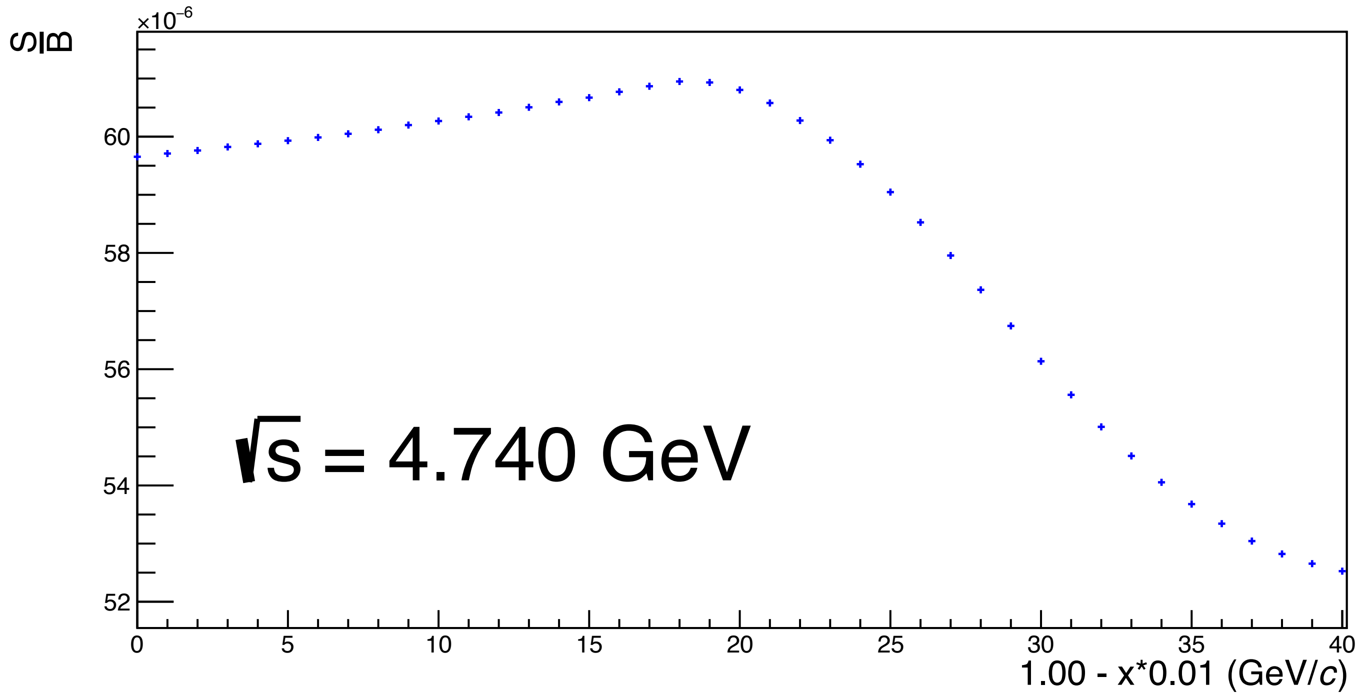

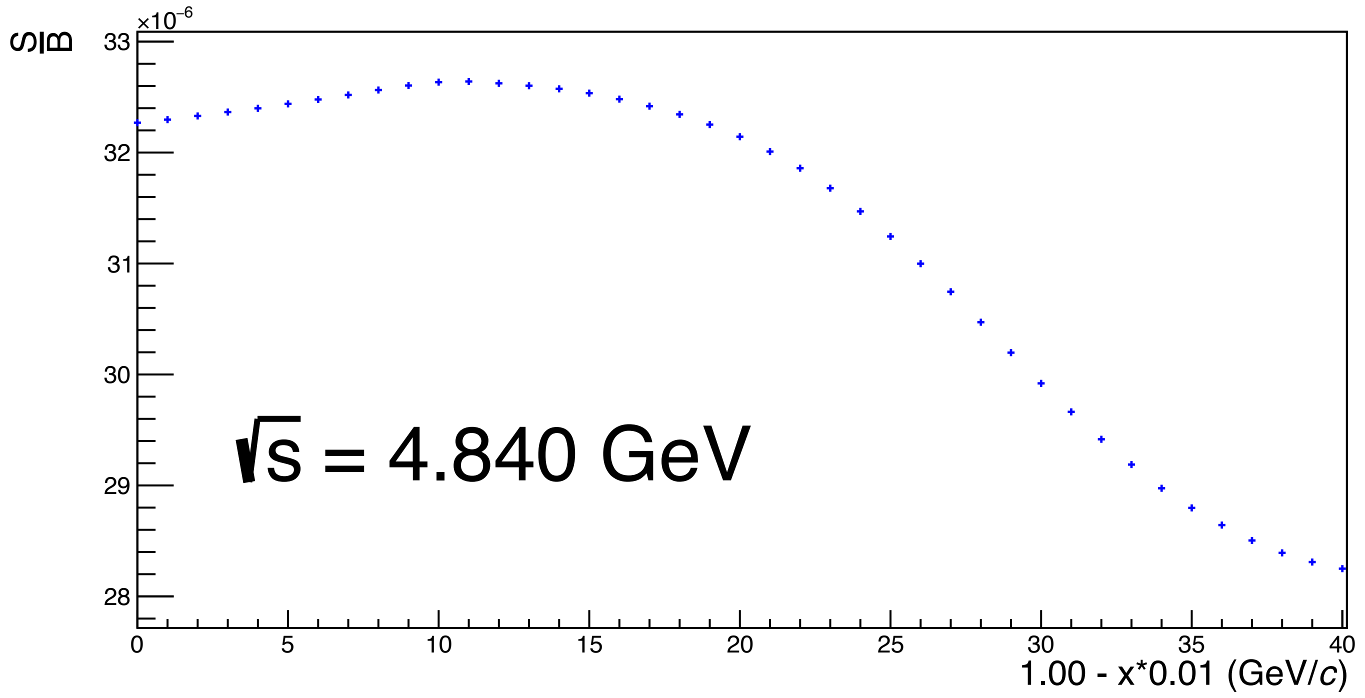

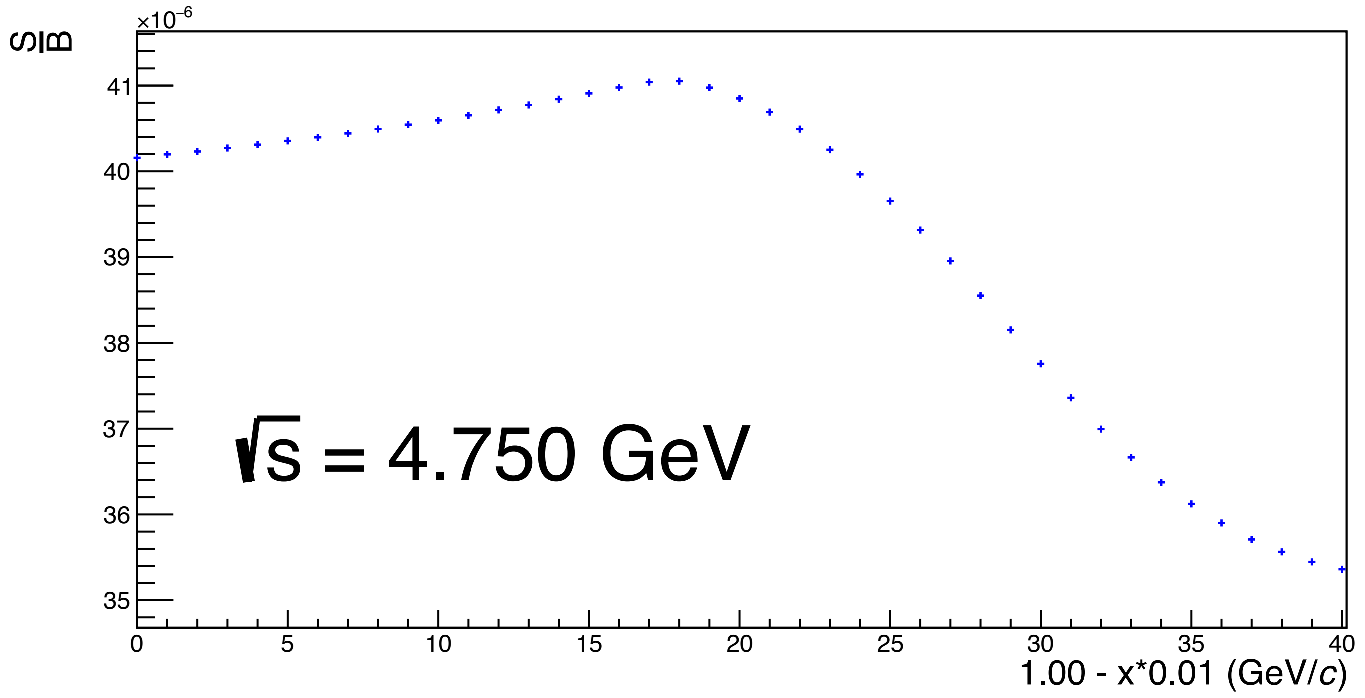

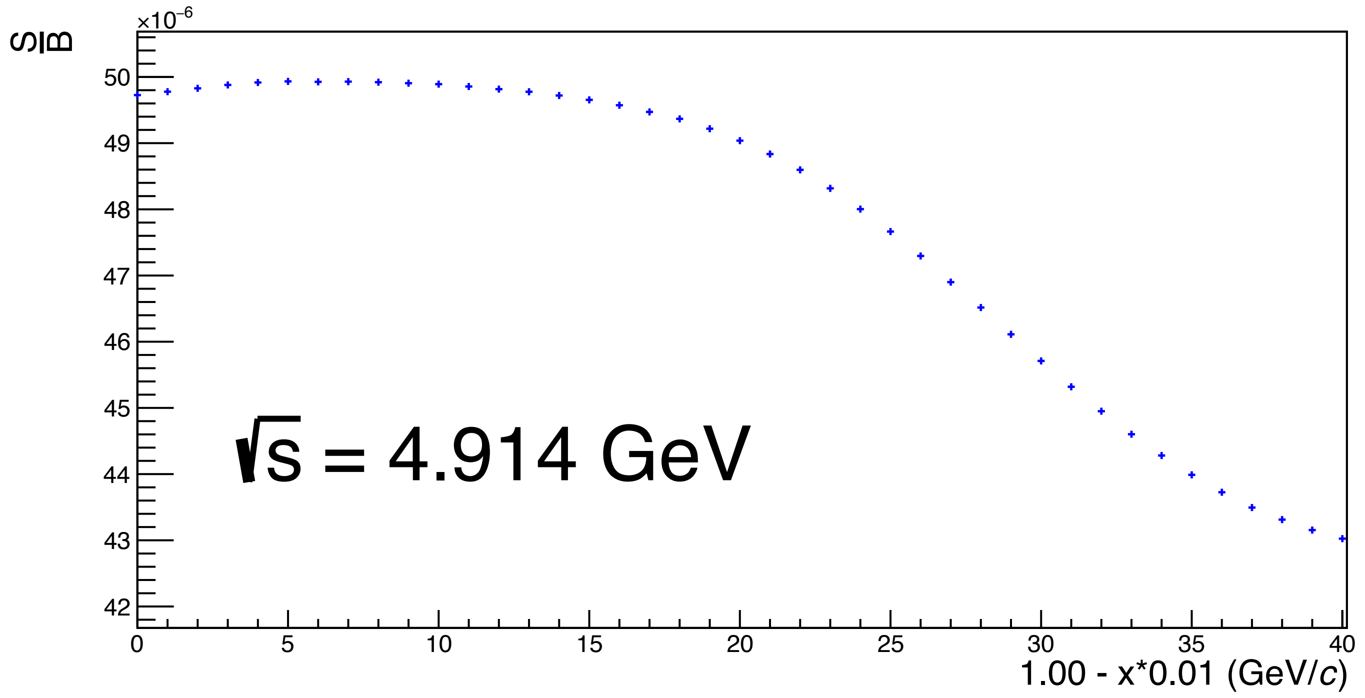

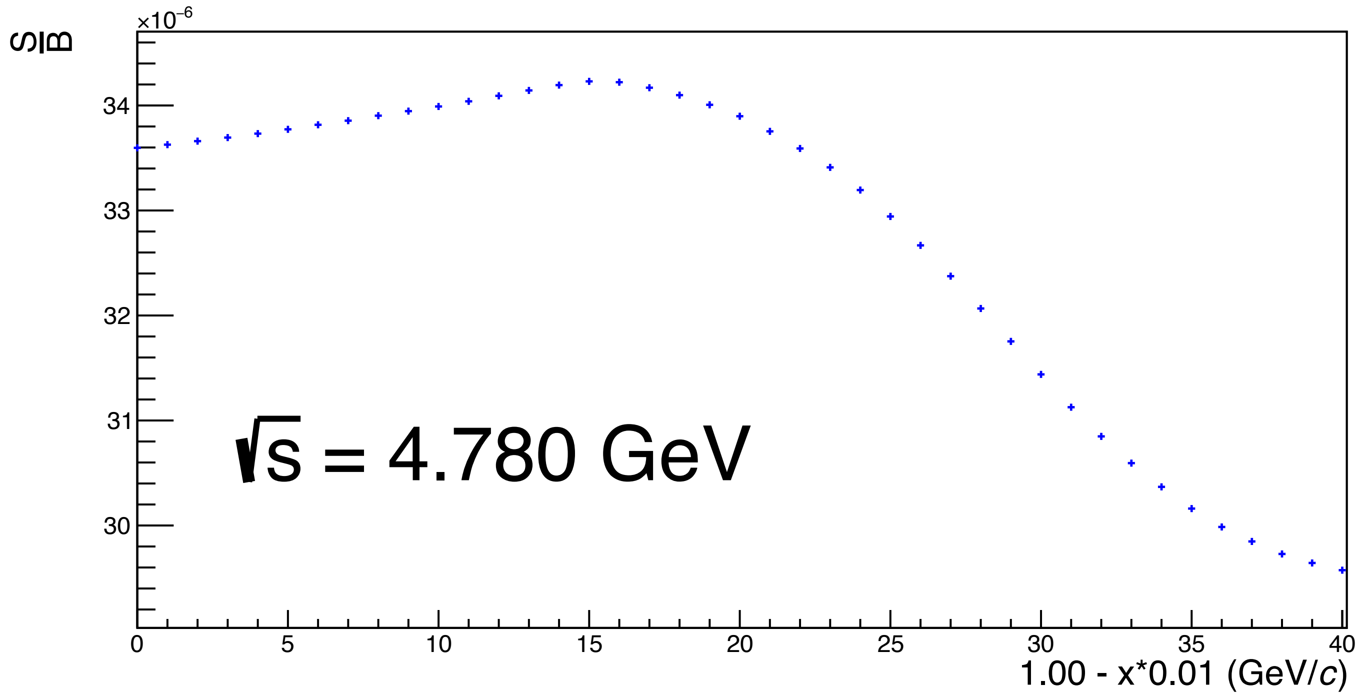

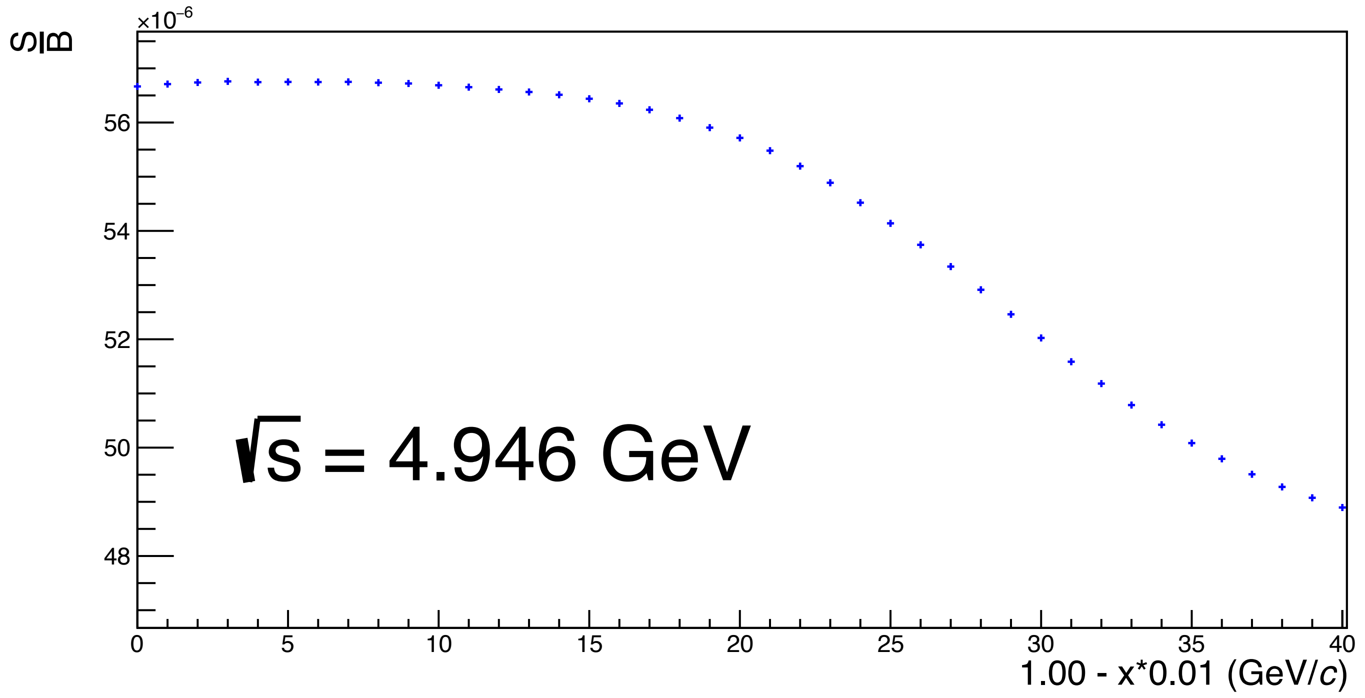

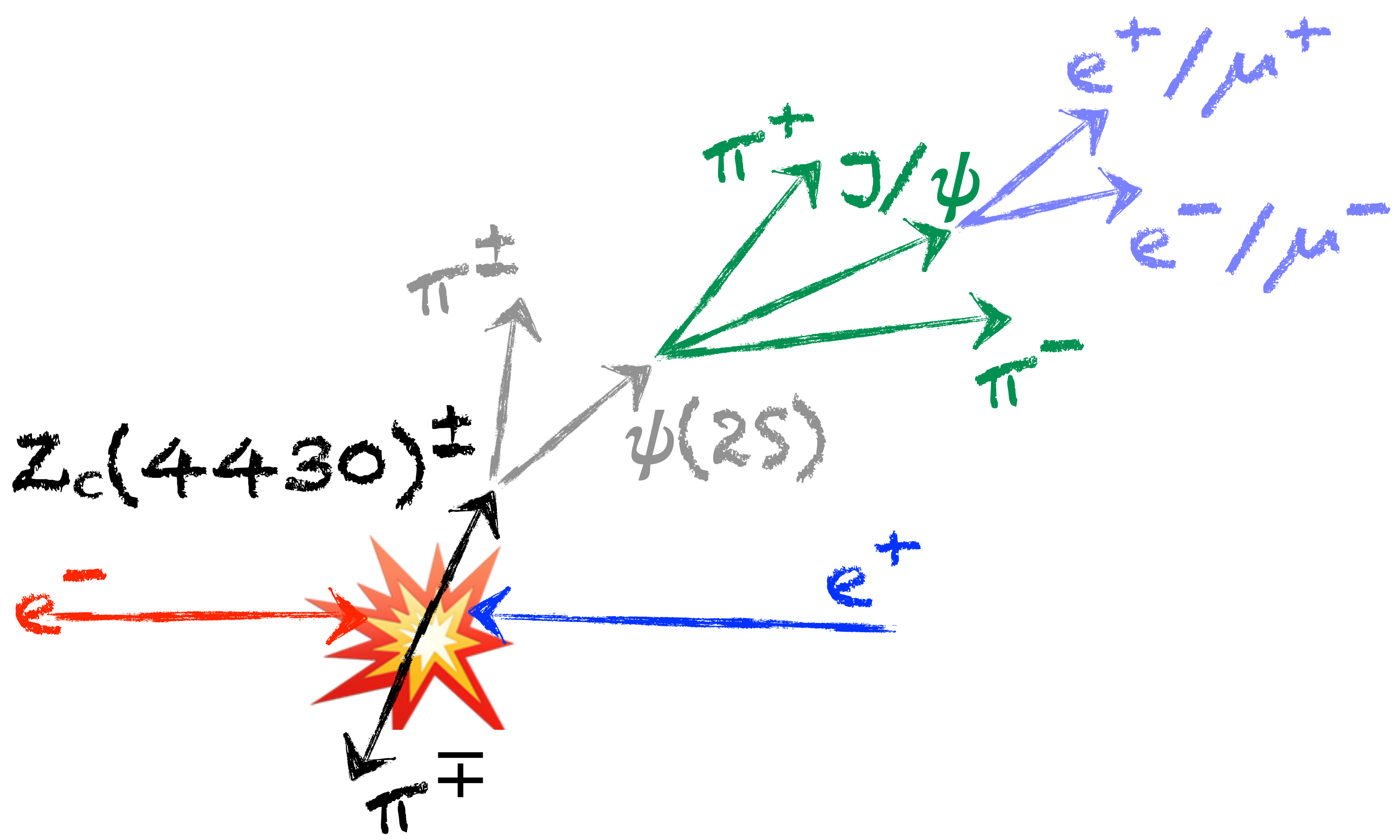

Event Selection

$p(\pi_{Miss})$ Cut

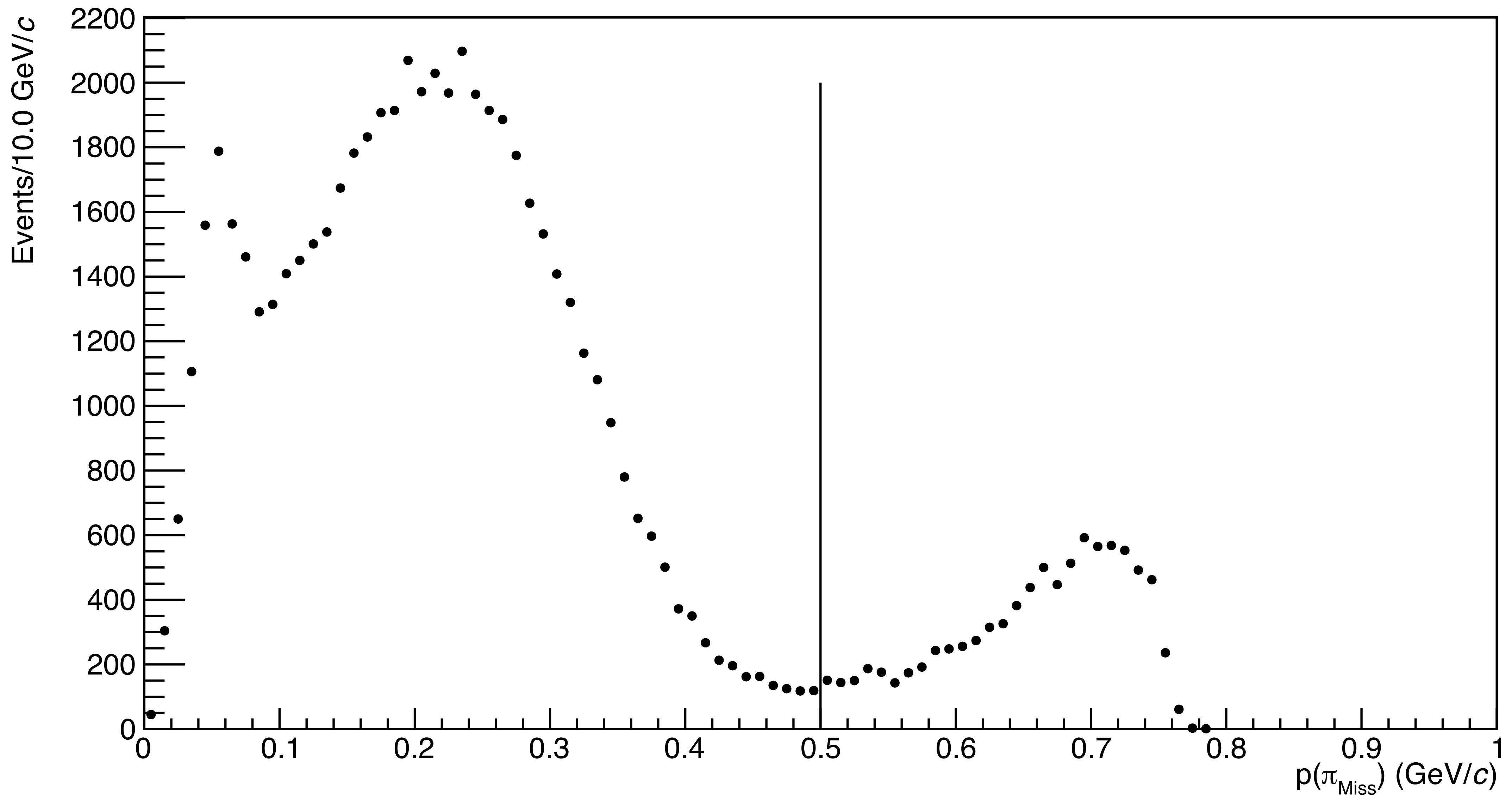

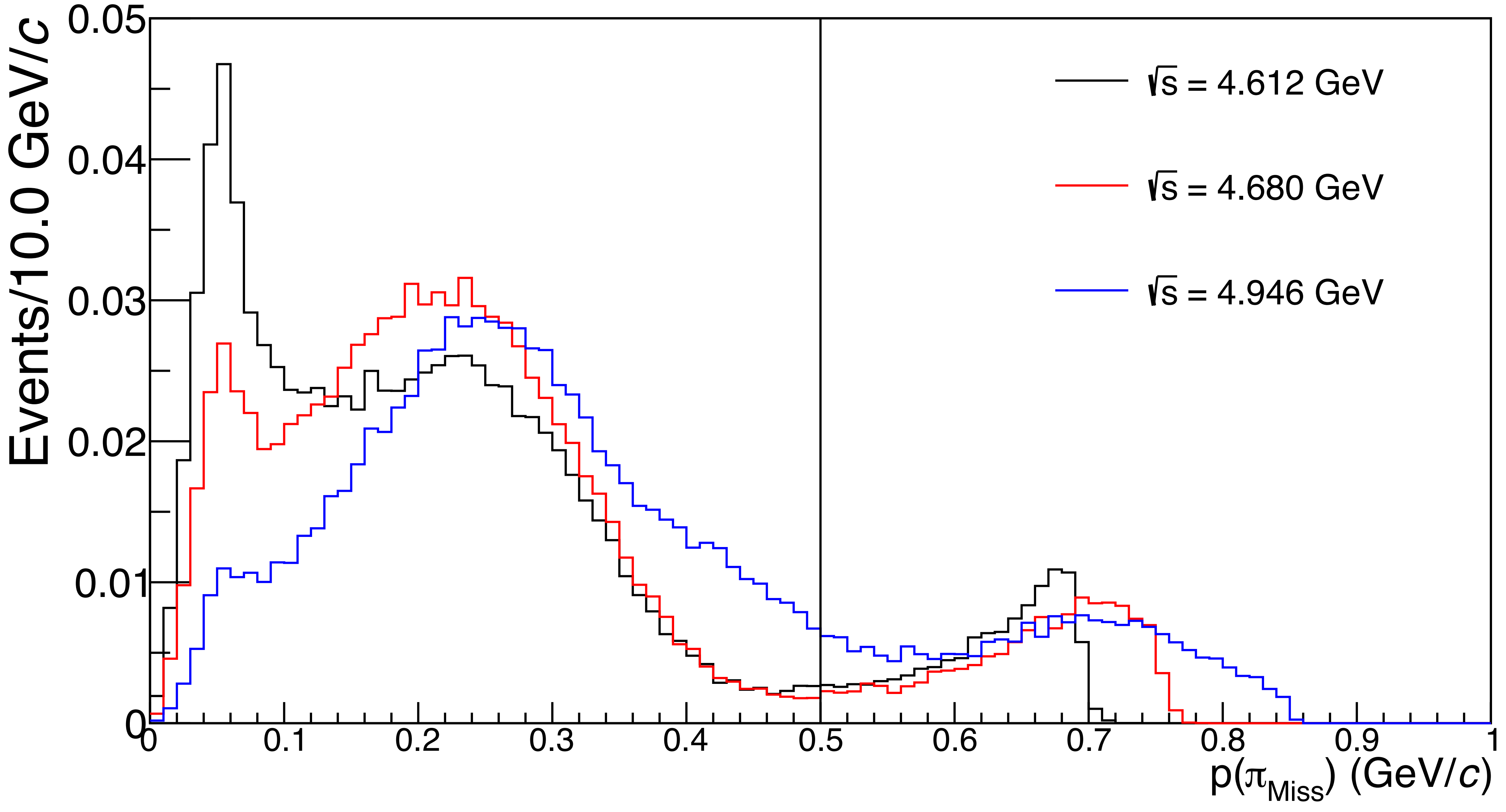

After Selection Comparison

Inclusive MC / Signal MC [no Z_c]/ Data

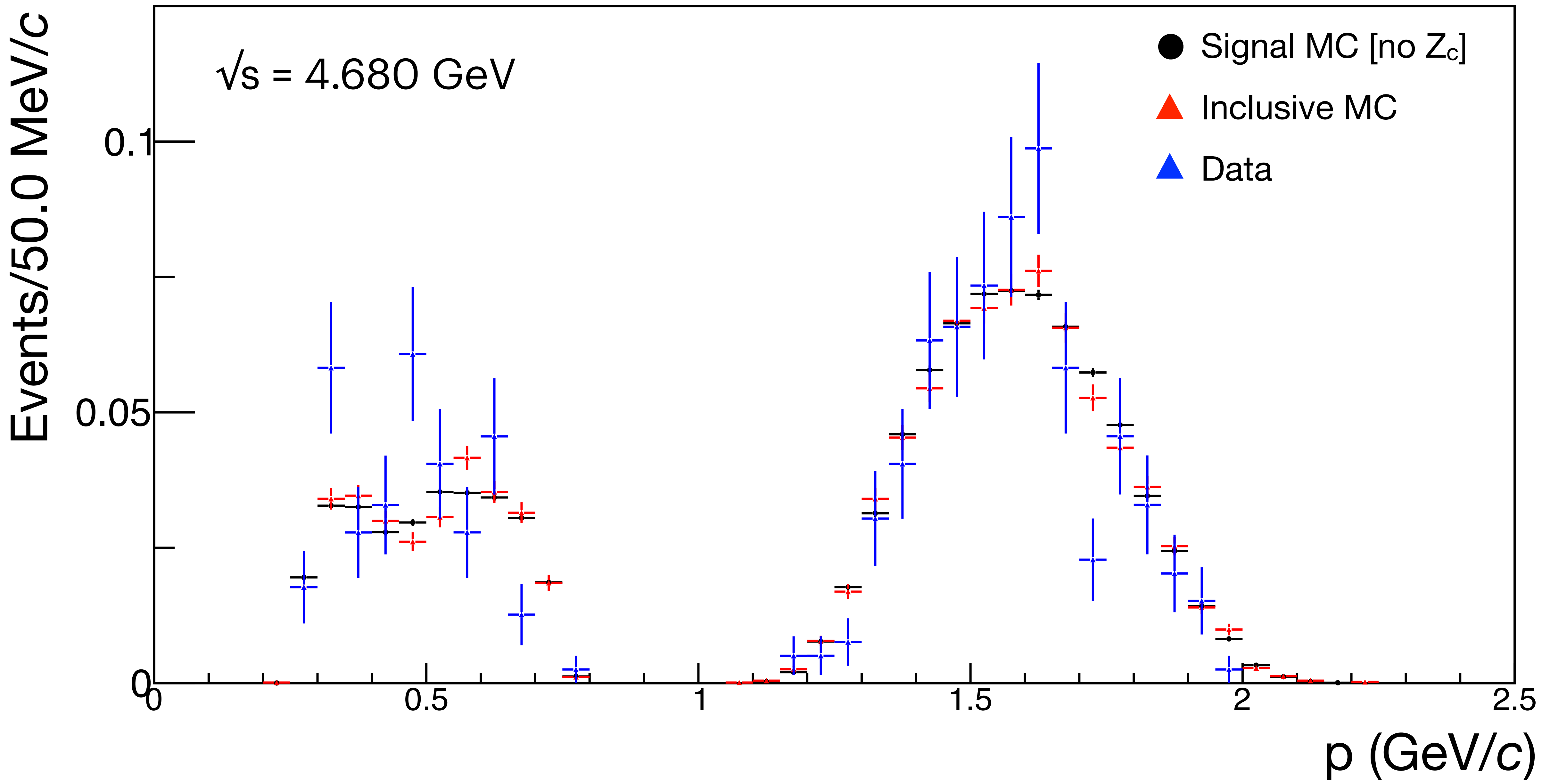

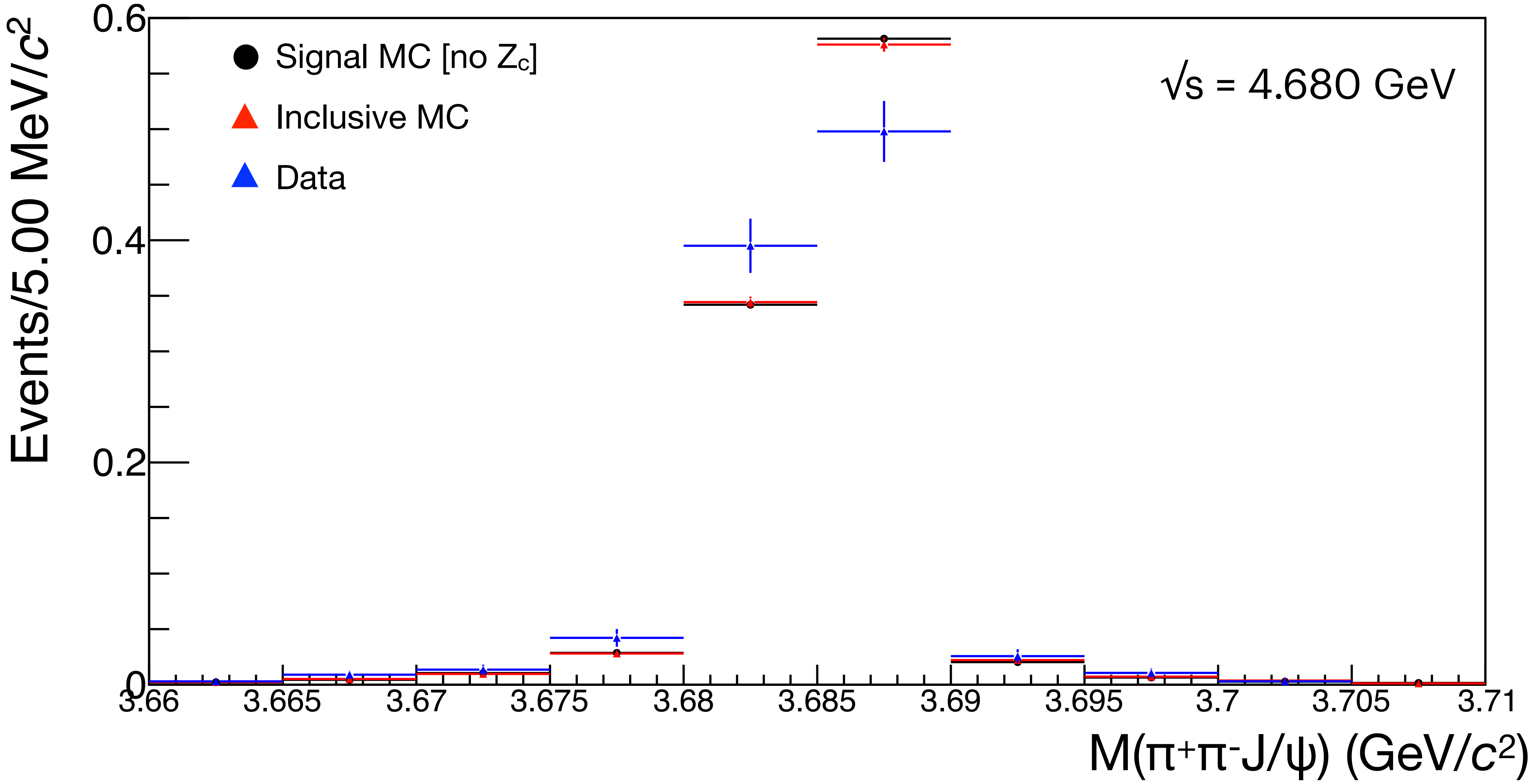

Cut Flow of Event Selection

Cuts [$\sqrt{s} = 4.612$ GeV]	Events	Efficiency [%]
Total Tracks	300000	100
Fiducial	252731	84.24
Kinetic PID	215256	71.75
5 Trks Events - Kalman Fit 1C	40301	13.43
6 Trks Events - Kalman Fit 1C	74211	24.74
5&6 Trks Events	114512	38.17

Table 5: Cut-flow for the $e^+e^- \to \pi^+\pi^-\psi(2S)$ process at $\sqrt{s} = 4.612$ GeV.

Cuts [$\sqrt{s} = 4.626$ GeV]	Events	Efficiency [%]
Total Tracks	300000	100
Fiducial	252435	84.15
Kinetic PID	215129	71.71
5 Trks Events - Kalman Fit 1C	41271	13.76
6 Trks Events - Kalman Fit 1C	76882	25.63
5&6 Trks Events	118153	39.38

Table 6: Cut-flow for the $e^+e^- \to \pi^+\pi^-\psi(2S)$ process at $\sqrt{s} = 4.626$ GeV.

Cuts [$\sqrt{s} = 4.640$ GeV]	Events	Efficiency [%]
Total Tracks	300000	100
Fiducial	253398	84.47
Kinetic PID	215811	71.94
5 Trks Events - Kalman Fit 1C	42034	14.01
6 Trks Events - Kalman Fit 1C	79623	26.54
5&6 Trks Events	121657	40.55

Table 7: Cut-flow for the $e^+e^- \to \pi^+\pi^-\psi(2S)$ process at $\sqrt{s} = 4.640$ GeV.

Cuts [$\sqrt{s} = 4.660$ GeV]	Events	Efficiency [%]
Total Tracks	300000	100
Fiducial	253456	84.49
Kinetic PID	215117	71.71
5 Trks Events - Kalman Fit 1C	40847	13.62
6 Trks Events - Kalman Fit 1C	79447	26.48
5&6 Trks Events	120294	40.10

Table 8: Cut-flow for the $e^+e^- \to \pi^+\pi^-\psi(2S)$ process at $\sqrt{s} = 4.660$ GeV.

Cut Flow of Event Selection

Cuts [$\sqrt{s}$ = 4.780 GeV]	Events	Efficiency [%]
Total Tracks	300000	100
Fiducial	256749	85.58
Kinetic PID	217568	72.52
5 Trks Events - Kalman Fit 1C	31676	10.56
6 Trks Events - Kalman Fit 1C	67410	22.47
5&6 Trks Events	99086	33.03

Table 13: Cut-flow for the $e^+e^- \to \pi^+\pi^-\psi(2S)$ process at $\sqrt{s} = 4.780$ GeV.

Cuts [$\sqrt{s}$ = 4.840 GeV]	Events	Efficiency [%]
Total Tracks	300000	100
Fiducial	257237	85.75
Kinetic PID	215498	71.83
5 Trks Events - Kalman Fit 1C	27921	9.31
6 Trks Events - Kalman Fit 1C	63999	21.33
5&6 Trks Events	91920	30.64

Table 14: Cut-flow for the $e^+e^- \to \pi^+\pi^-\psi(2S)$ process at $\sqrt{s} = 4.840$ GeV.

Cuts [$\sqrt{s}$ = 4.914 GeV]	Events	Efficiency [%]
Total Tracks	300000	100
Fiducial	257593	85.86
Kinetic PID	217033	72.34
5 Trks Events - Kalman Fit 1C	26535	8.85
6 Trks Events - Kalman Fit 1C	61331	20.44
5&6 Trks Events	87866	29.29

Table 15: Cut-flow for the $e^+e^- \to \pi^+\pi^-\psi(2S)$ process at $\sqrt{s} = 4.914$ GeV.

Cuts [$\sqrt{s}$ = 4.946 GeV]	Events	Efficiency [%]
Total Tracks	300000	100
Fiducial	256900	85.63
Kinetic PID	216006	72.00
5 Trks Events - Kalman Fit 1C	30792	10.26
6 Trks Events - Kalman Fit 1C	71913	23.97
5&6 Trks Events	102705	34.24

Table 16: Cut-flow for the $e^+e^- \to \pi^+\pi^-\psi(2S)$ process at $\sqrt{s} = 4.946$ GeV.

Extraction of the σ(e^+e^- —> $\pi^+\pi^-\psi(2S)$)

Signal Shape & Efficiency

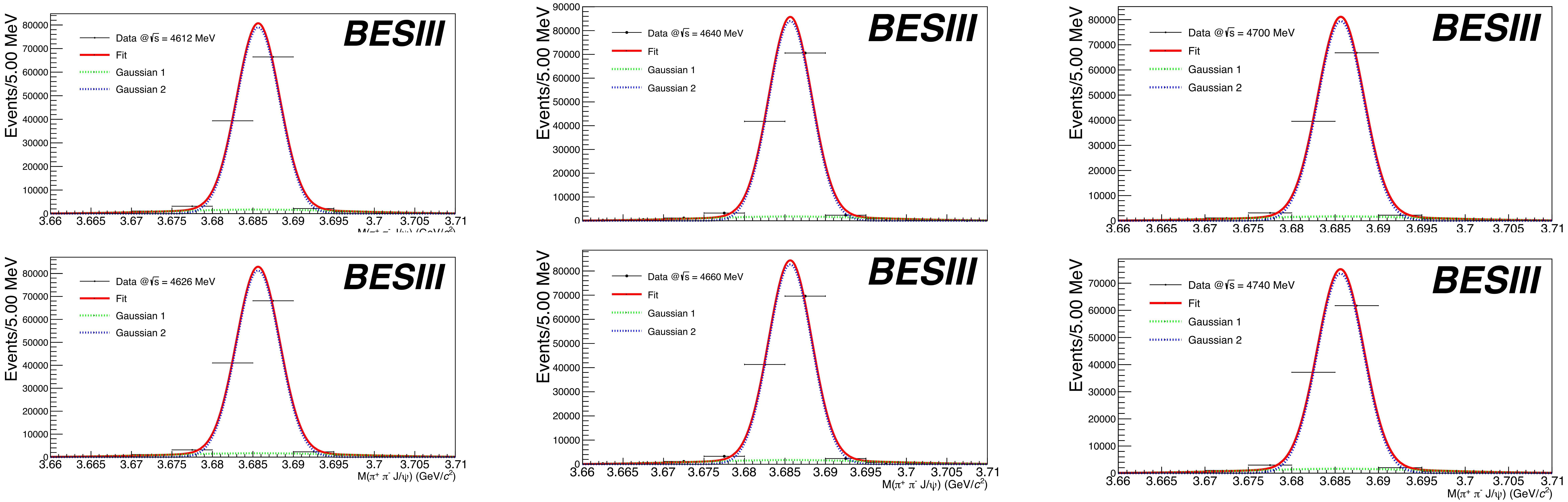

Extraction of the σ(e^+e^- —> $\pi^+\pi^-\psi(2S)$)

Signal Shape & Efficiency

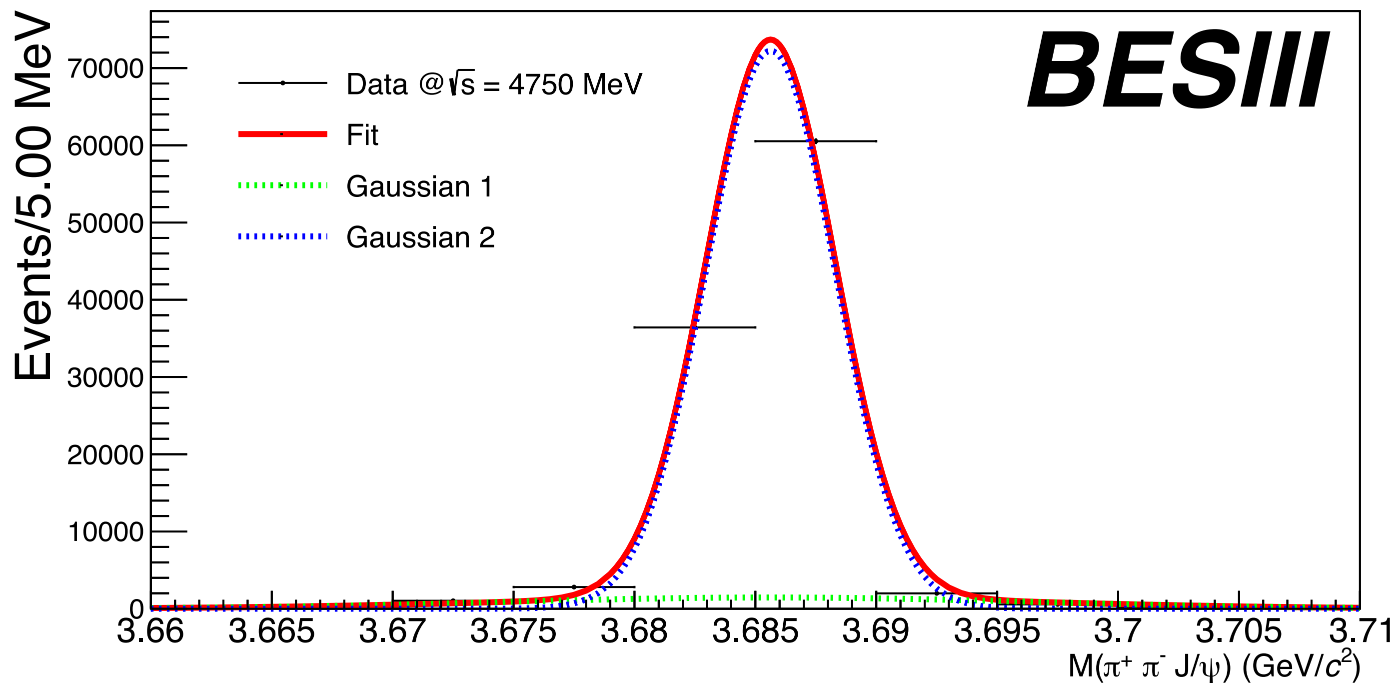

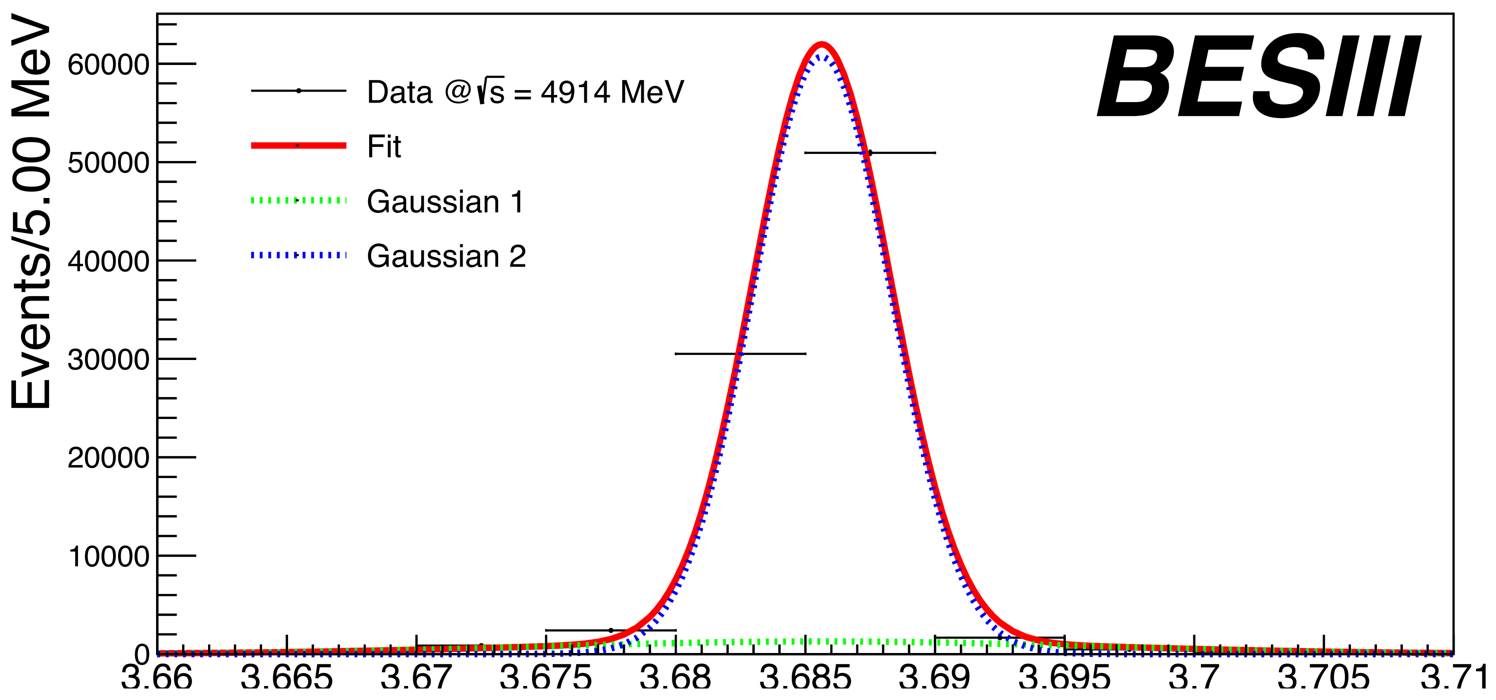

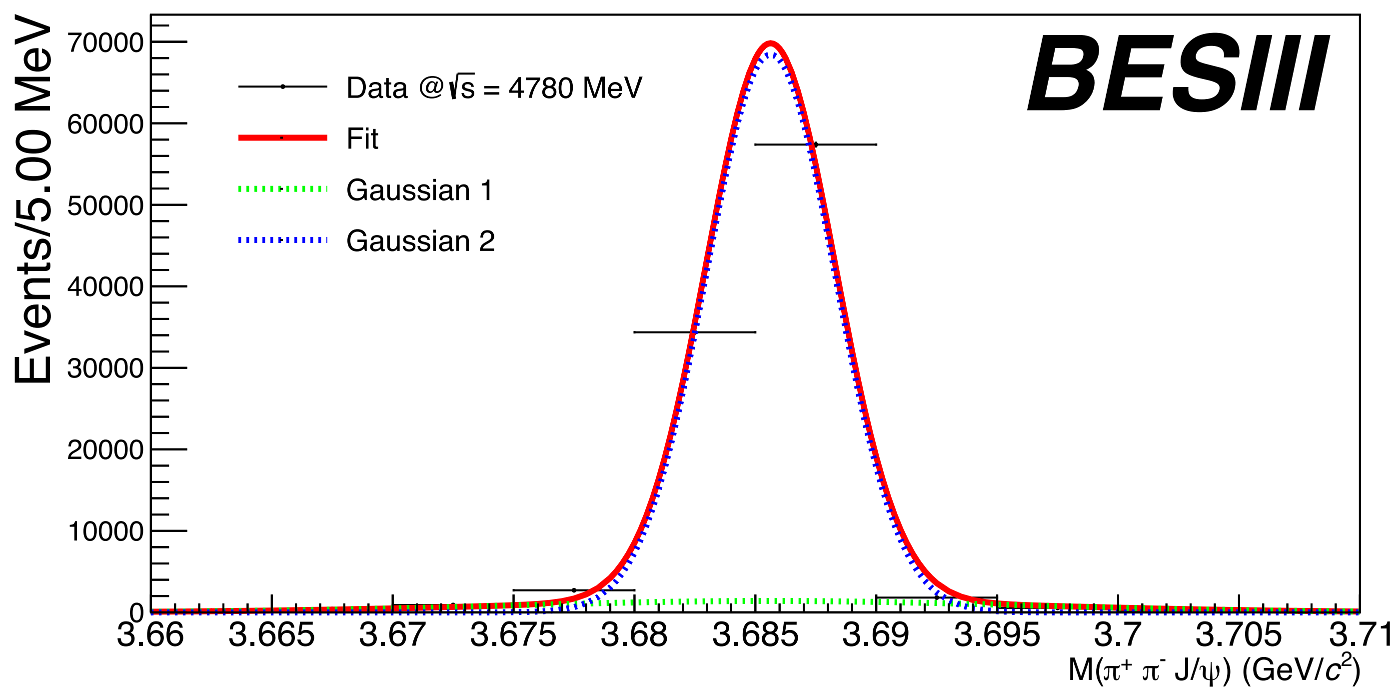

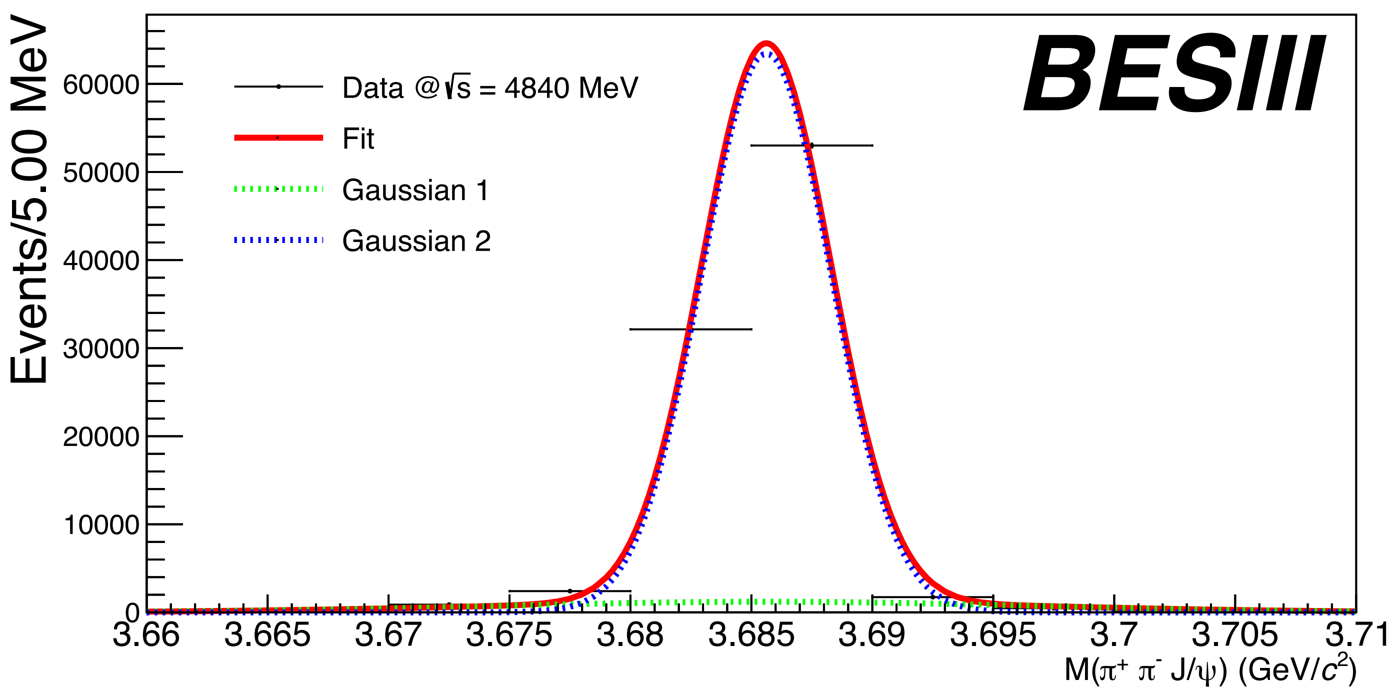

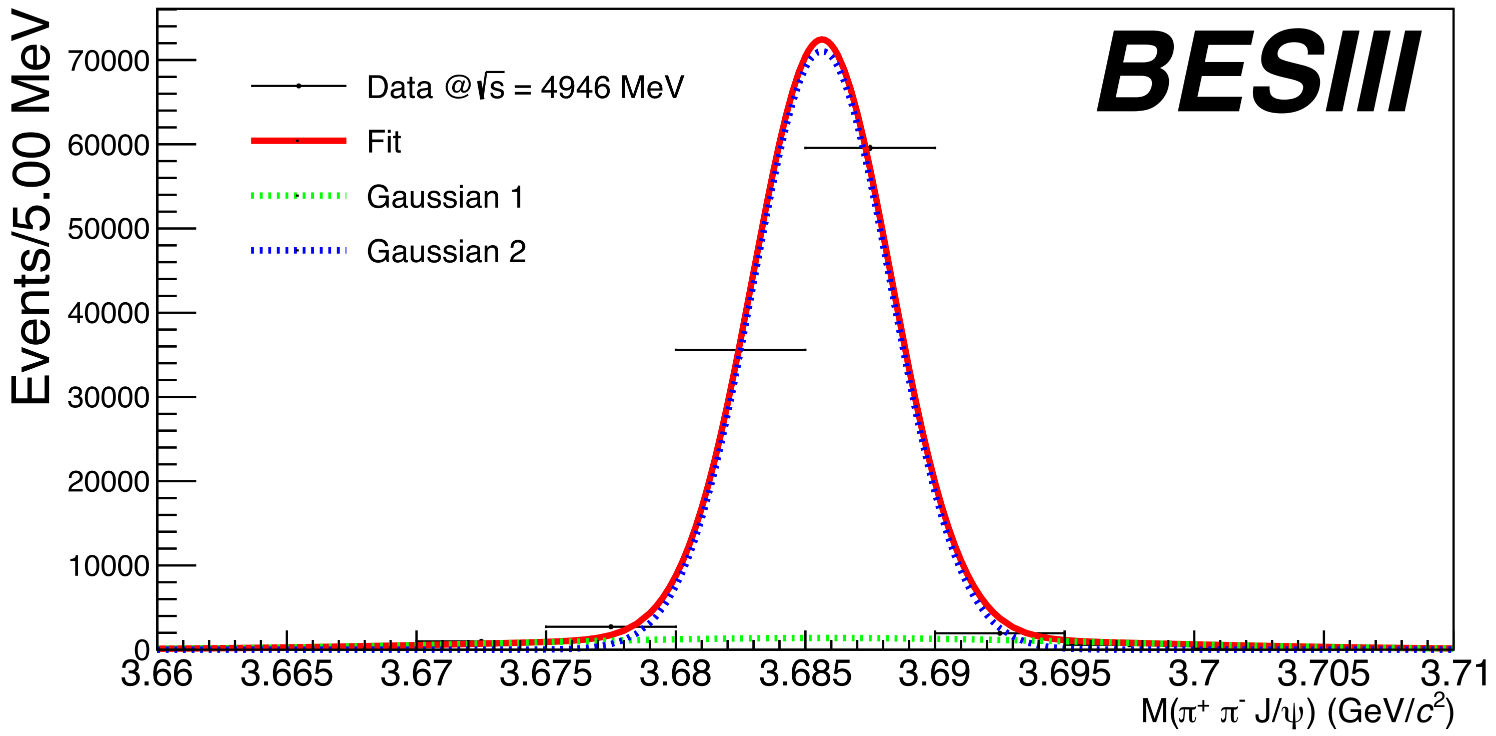

Extraction of the $\sigma(e^+e^- \rightarrow \pi^+\pi^-\psi(2S))$

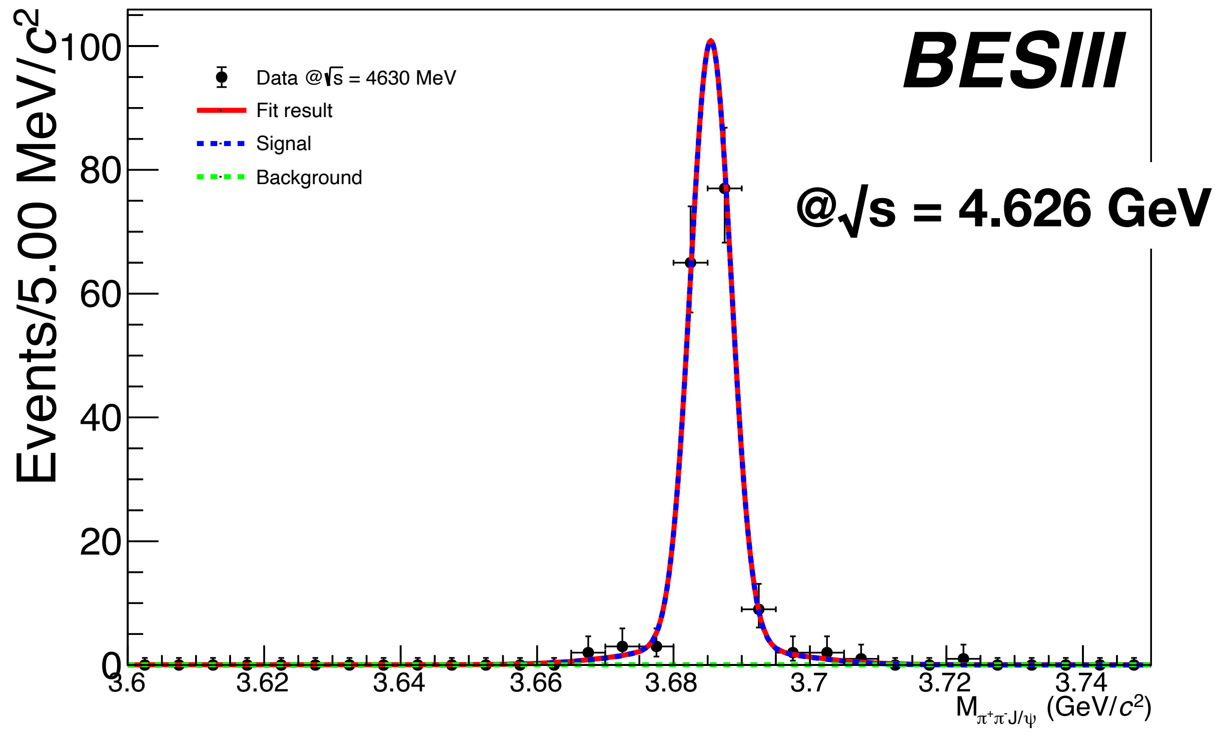

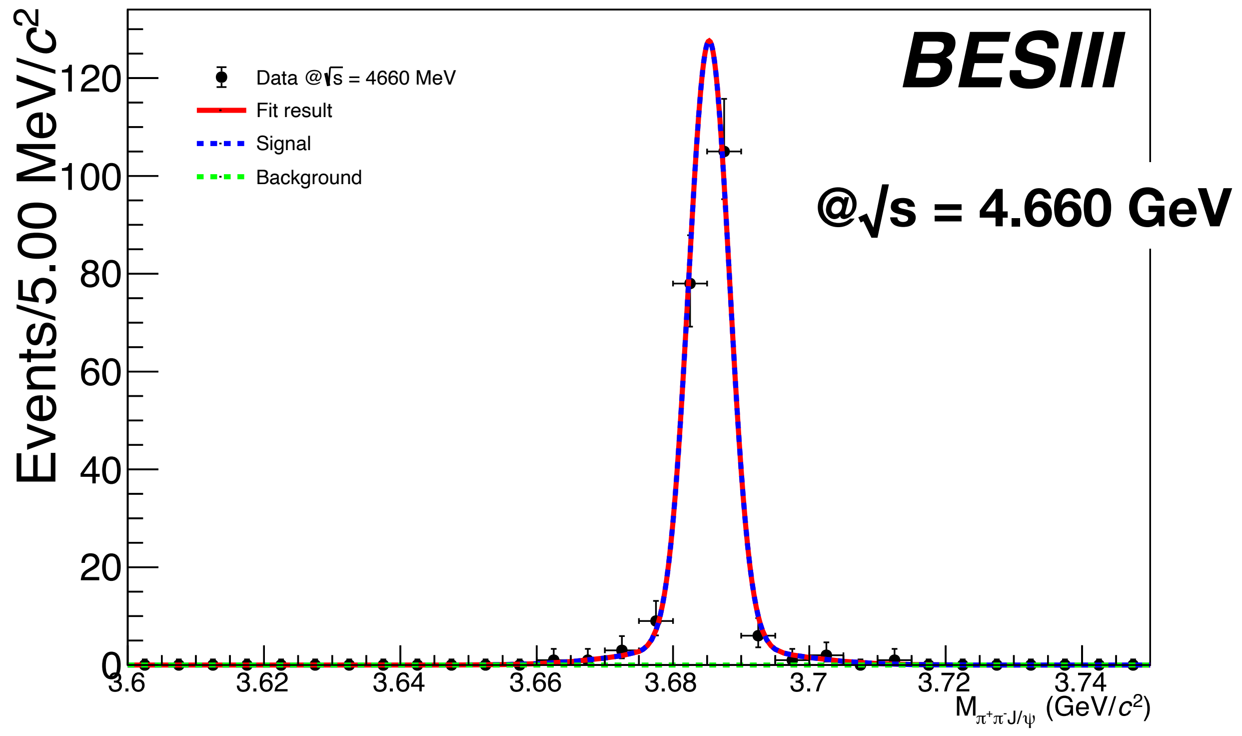

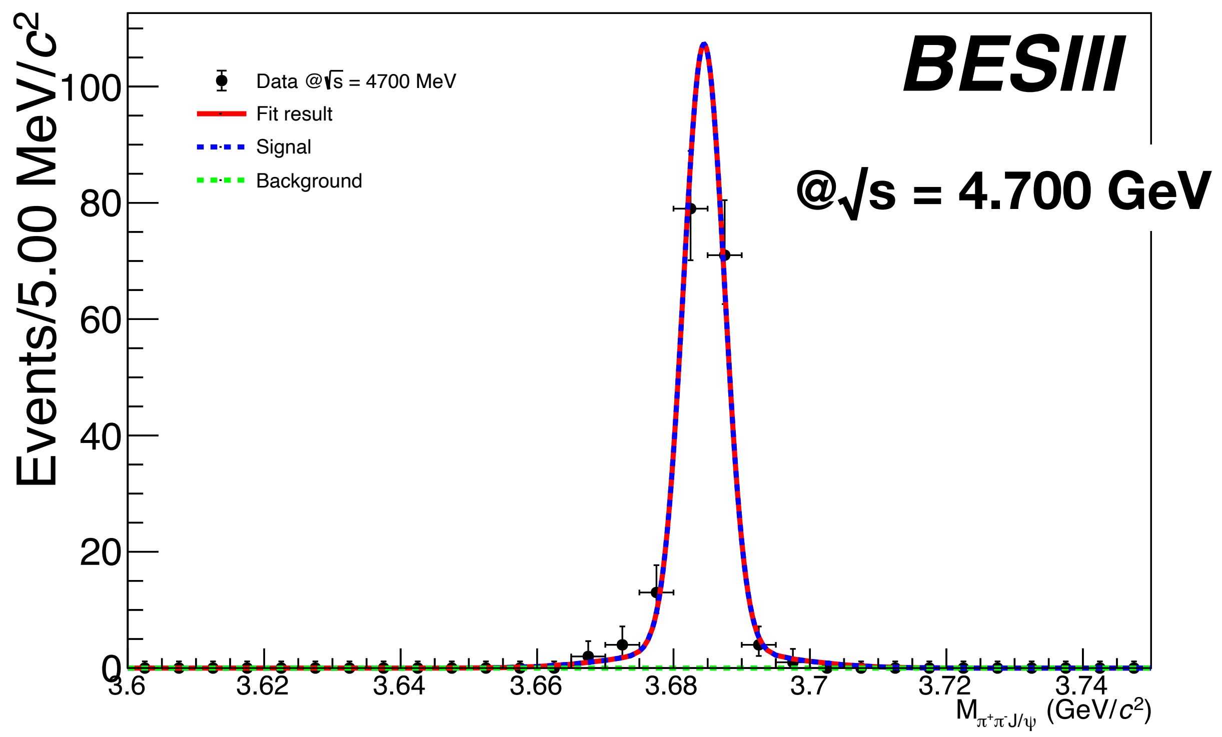

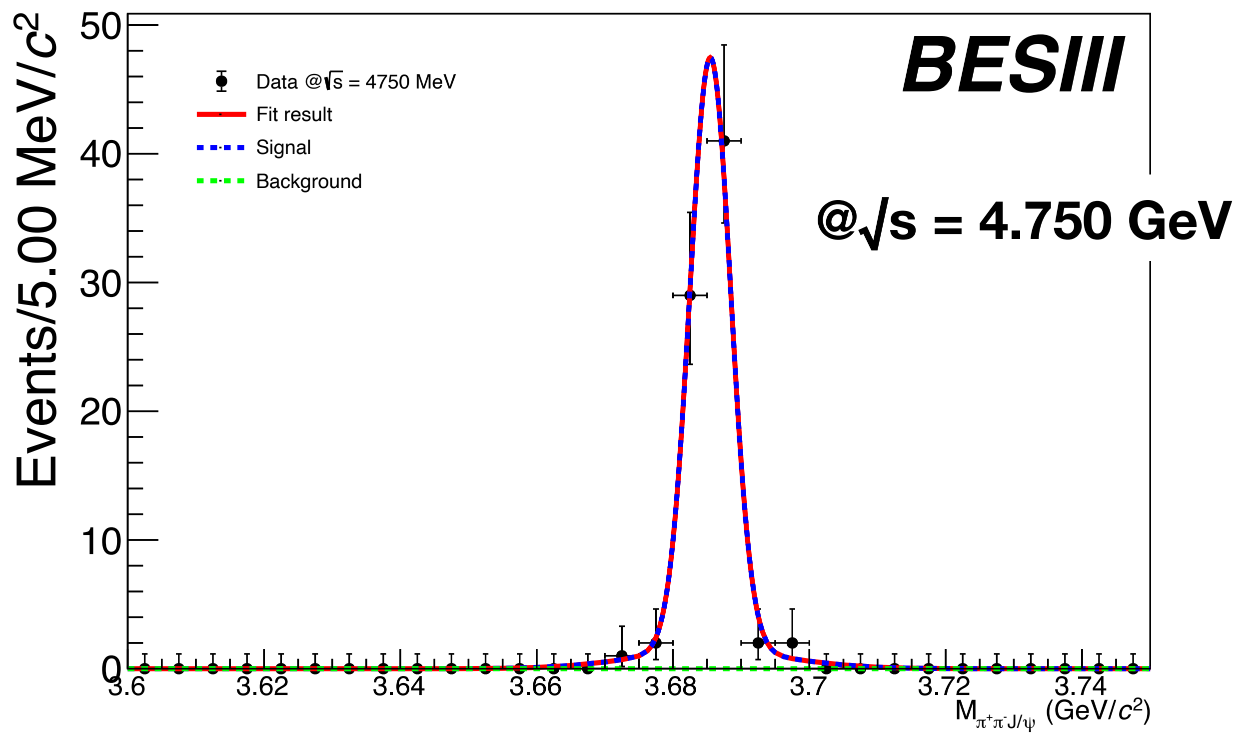

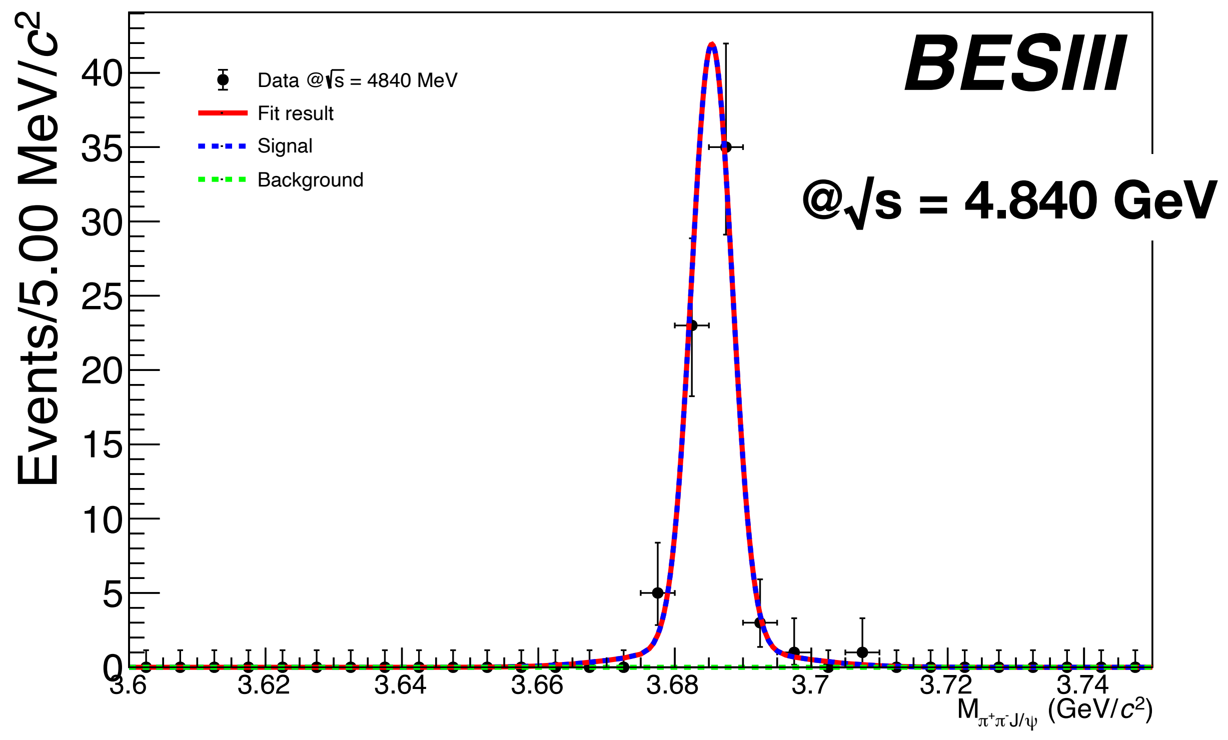

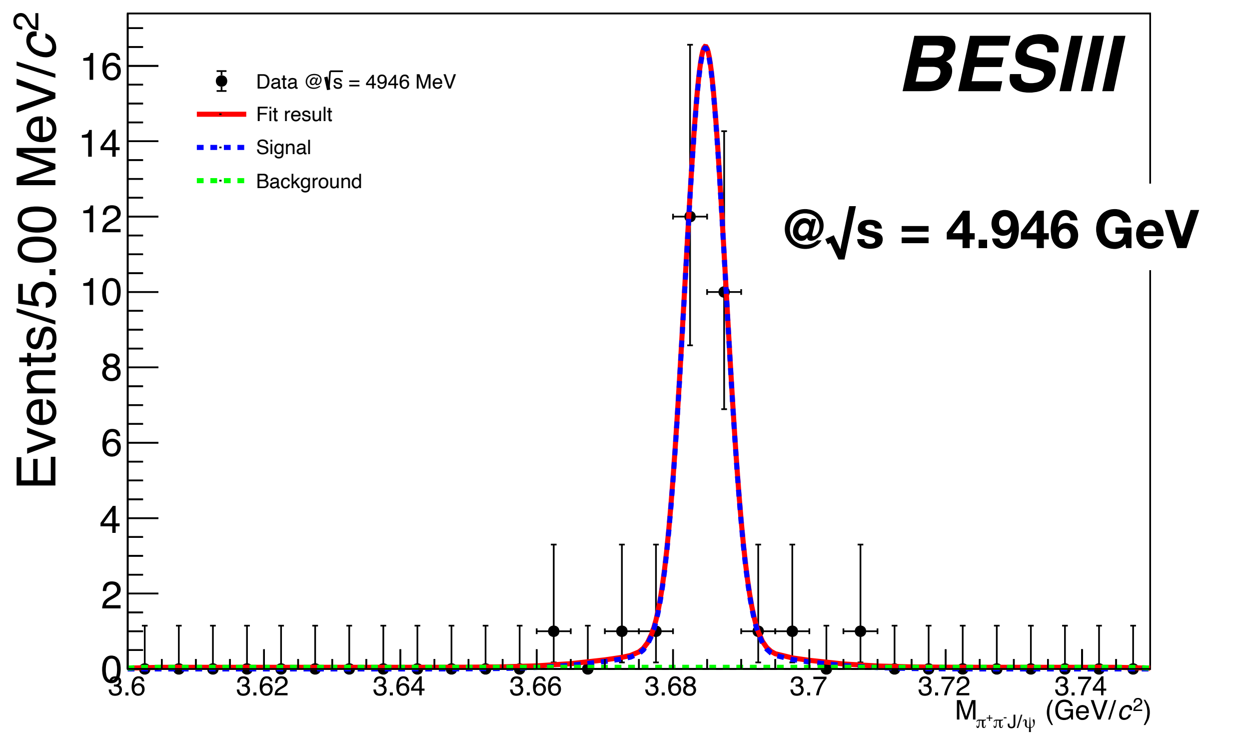

Extraction of the σ(e^+e^- —> $\pi^+\pi^-\psi(2S)$)

$\pi\pi\,\psi(2S)$ cross-section

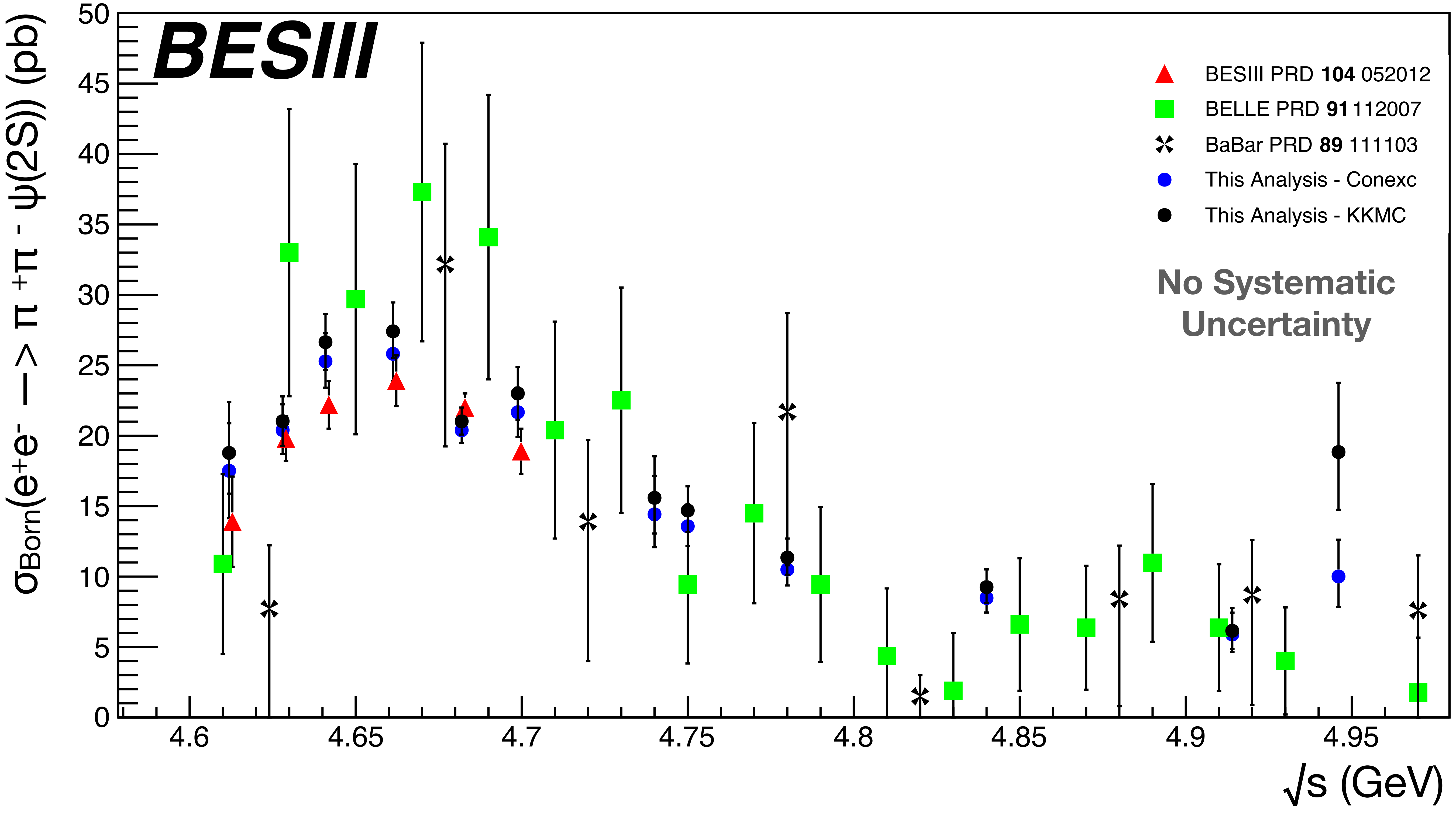

$$\sigma_{\text{Born}} = \frac{N_{\text{Obs}}}{\mathcal{L}(1+\delta)\frac{1}{|1-\Pi^2|}\epsilon\mathcal{B}}$$

The observed **cross-section** is **compatible with** the previous result of **Ref. [11]**

Results from BELLE and BaBar are reported too, further **confirming the compatibility** of this thesis' results with the published literature

[11] Phys. Rev. D **104**, 052012

Study of the invariant masses profiles

Inclusive MC / Non-resonant MC/ Data

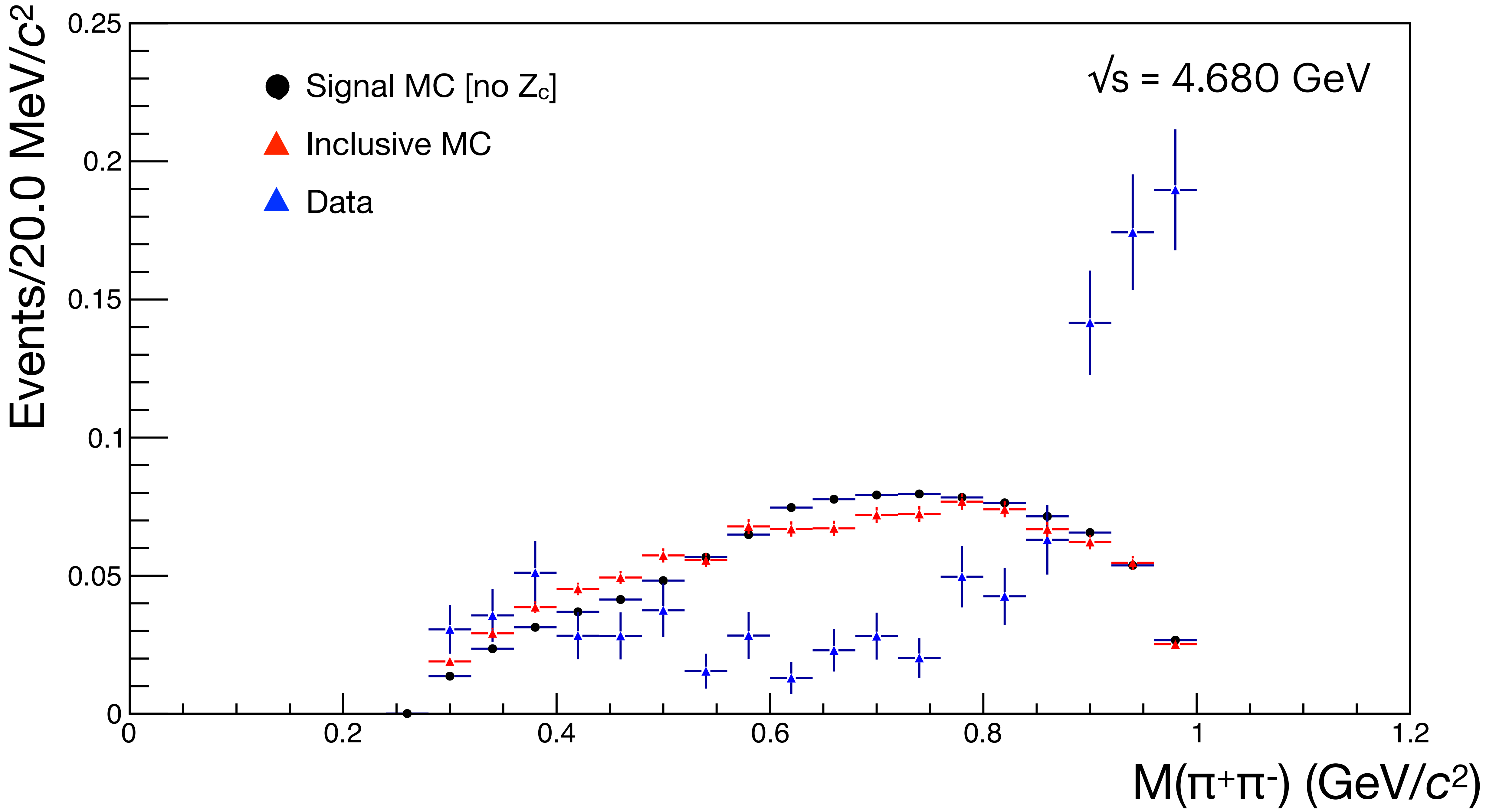

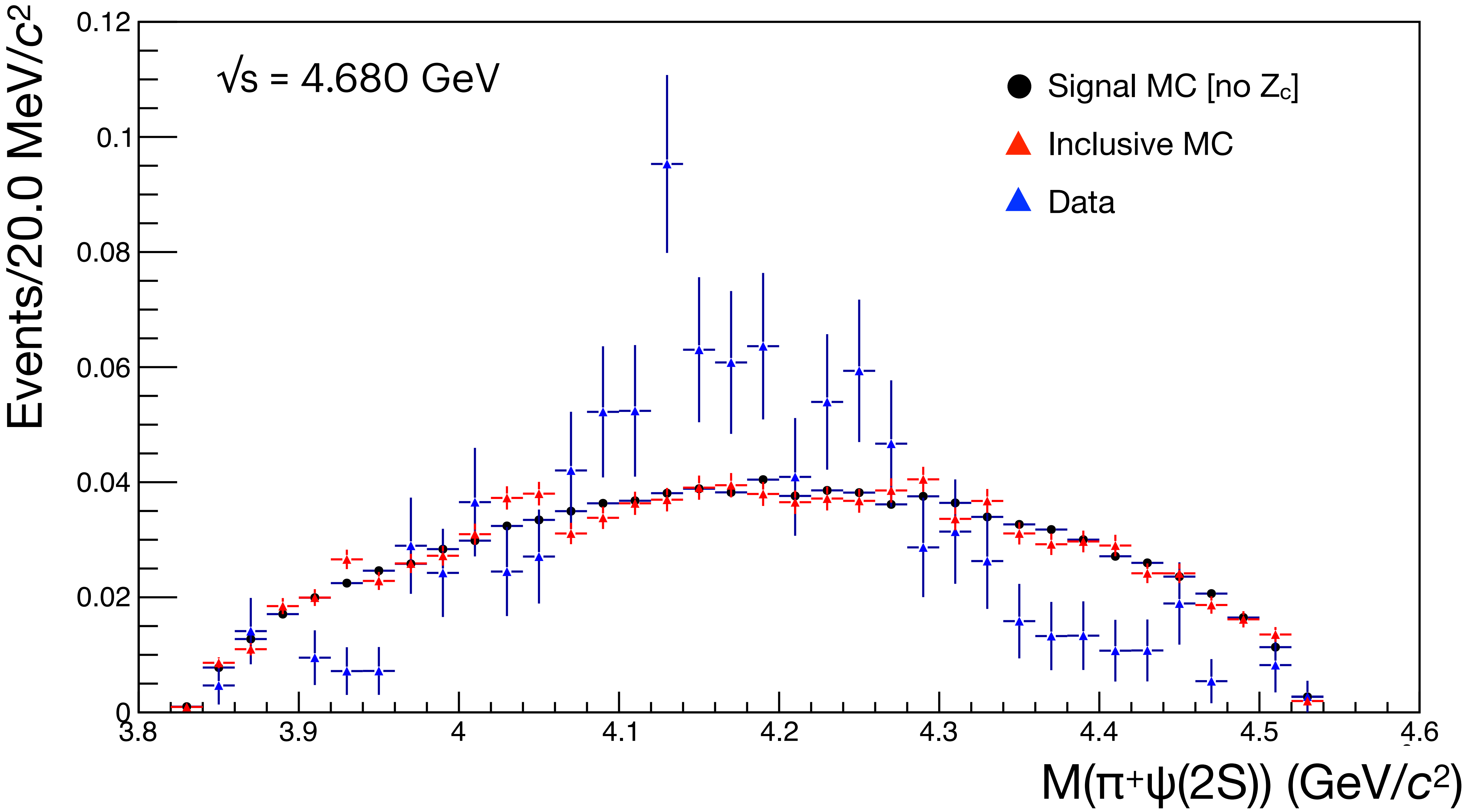

Cut Flow of Event Selection

$f_0(980)\ \psi(2S)$ cross-section

Cuts [$\sqrt{s}=4.612$ GeV]	Events	Efficiency [%]
Total Tracks	300000	100
Fiducial	251862	83.95
Kinetic PID	216412	72.14
5 Trks Events - Kalman Fit 1C	45052	15.02
6 Trks Events - Kalman Fit 1C	100675	33.56
5&6 Trks Events	145727	48.58

Table 18: Cut-flow for the $e^+e^- \to f_0(980)\psi(2S)$ process at $\sqrt{s}=4.612$ GeV.

Cuts [$\sqrt{s}=4.626$ GeV]	Events	Efficiency [%]
Total Tracks	300000	100
Fiducial	251229	83.74
Kinetic PID	215973	71.99
5 Trks Events - Kalman Fit 1C	43881	14.63
6 Trks Events - Kalman Fit 1C	99976	33.33
5&6 Trks Events	143857	47.95

Table 19: Cut-flow for the $e^+e^- \to f_0(980)\psi(2S)$ process at $\sqrt{s}=4.626$ GeV.

Cuts [$\sqrt{s}=4.640$ GeV]	Events	Efficiency [%]
Total Tracks	300000	100
Fiducial	251922	83.97
Kinetic PID	216537	72.18
5 Trks Events - Kalman Fit 1C	43047	14.35
6 Trks Events - Kalman Fit 1C	100703	33.57
5&6 Trks Events	143750	47.92

Table 20: Cut-flow for the $e^+e^- \to f_0(980)\psi(2S)$ process at $\sqrt{s}=4.640$ GeV.

Cuts [$\sqrt{s}=4.660$ GeV]	Events	Efficiency [%]
Total Tracks	300000	100
Fiducial	251800	83.93
Kinetic PID	216310	72.10
5 Trks Events - Kalman Fit 1C	39434	13.14
6 Trks Events - Kalman Fit 1C	96558	32.19
5&6 Trks Events	135992	45.33

Table 21: Cut-flow for the $e^+e^- \to f_0(980)\psi(2S)$ process at $\sqrt{s}=4.660$ GeV.

Cut Flow of Event Selection

$f_0(980)\ \psi(2S)$ cross-section

Cuts [$\sqrt{s}$ = 4.780 GeV]	Events	Efficiency [%]
Total Tracks	300000	100
Fiducial	257277	85.76
Kinetic PID	220006	73.34
5 Trks Events - Kalman Fit 1C	30045	10.02
6 Trks Events - Kalman Fit 1C	74291	24.76
5&6 Trks Events	104336	34.78

Table 26: Cut-flow for the $e^+e^- \to f_0(980)\psi(2S)$ process at $\sqrt{s} = 4.780$ GeV.

Cuts [$\sqrt{s}$ = 4.840 GeV]	Events	Efficiency [%]
Total Tracks	300000	100
Fiducial	258147	86.05
Kinetic PID	219406	73.14
5 Trks Events - Kalman Fit 1C	30713	10.24
6 Trks Events - Kalman Fit 1C	77319	25.77
5&6 Trks Events	108032	36.01

Table 27: Cut-flow for the $e^+e^- \to f_0(980)\psi(2S)$ process at $\sqrt{s} = 4.840$ GeV.

Cuts [$\sqrt{s}$ = 4.914 GeV]	Events	Efficiency [%]
Total Tracks	300000	100
Fiducial	259012	86.34
Kinetic PID	219647	73.22
5 Trks Events - Kalman Fit 1C	33805	11.27
6 Trks Events - Kalman Fit 1C	85079	28.36
5&6 Trks Events	118884	39.63

Table 28: Cut-flow for the $e^+e^- \to f_0(980)\psi(2S)$ process at $\sqrt{s} = 4.914$ GeV.

Cuts [$\sqrt{s}$ = 4.946 GeV]	Events	Efficiency [%]
Total Tracks	300000	100
Fiducial	258200	86.07
Kinetic PID	218228	72.74
5 Trks Events - Kalman Fit 1C	33605	11.20
6 Trks Events - Kalman Fit 1C	82487	27.50
5&6 Trks Events	116092	38.70

Table 29: Cut-flow for the $e^+e^- \to f_0(980)\psi(2S)$ process at $\sqrt{s} = 4.946$ GeV.

Extraction of the $\sigma(f_0(980)\,\psi(2S))$

$f_0(980)$ contribution

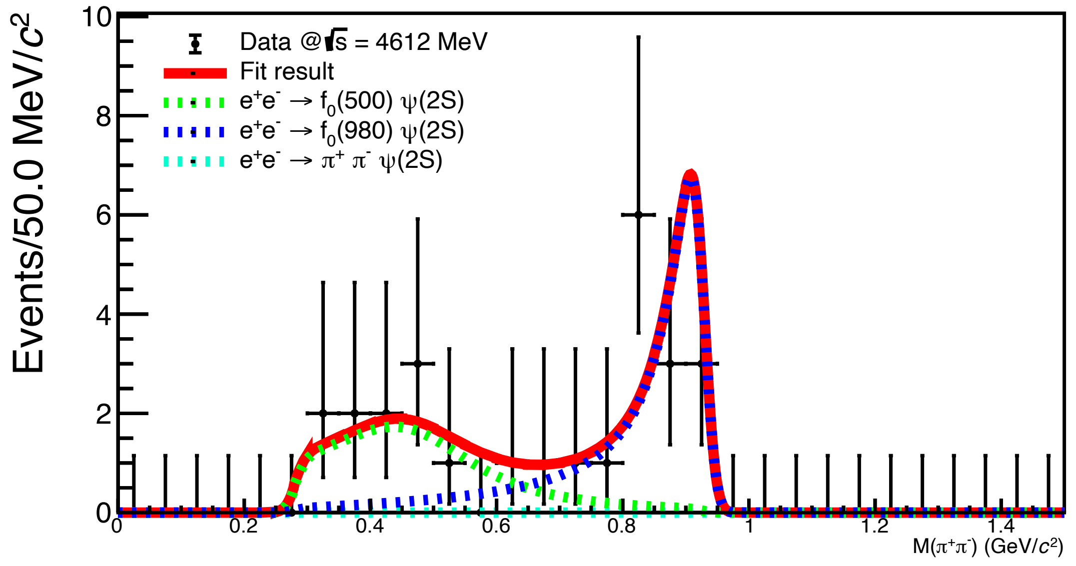

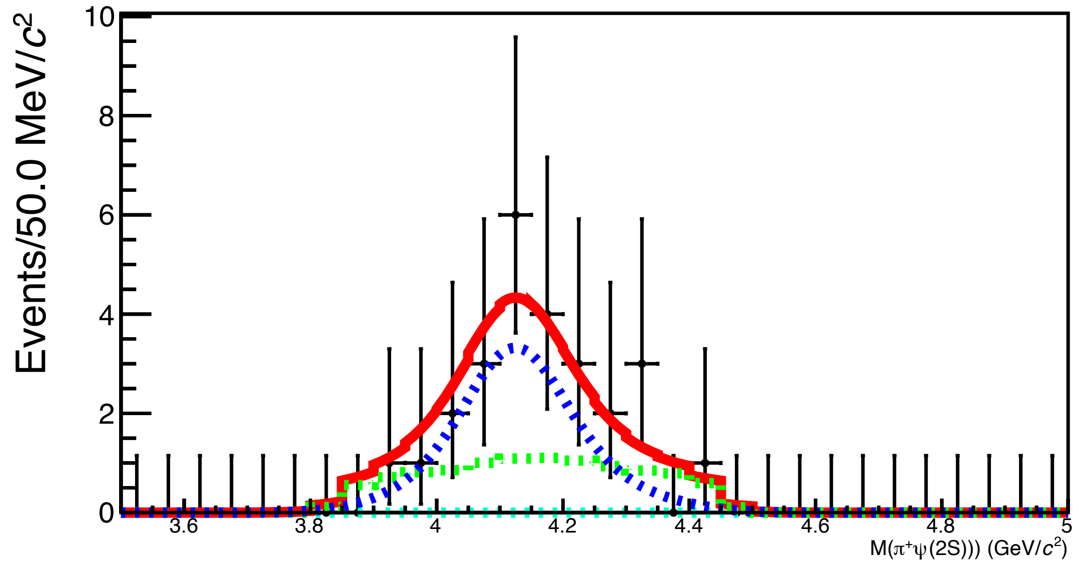

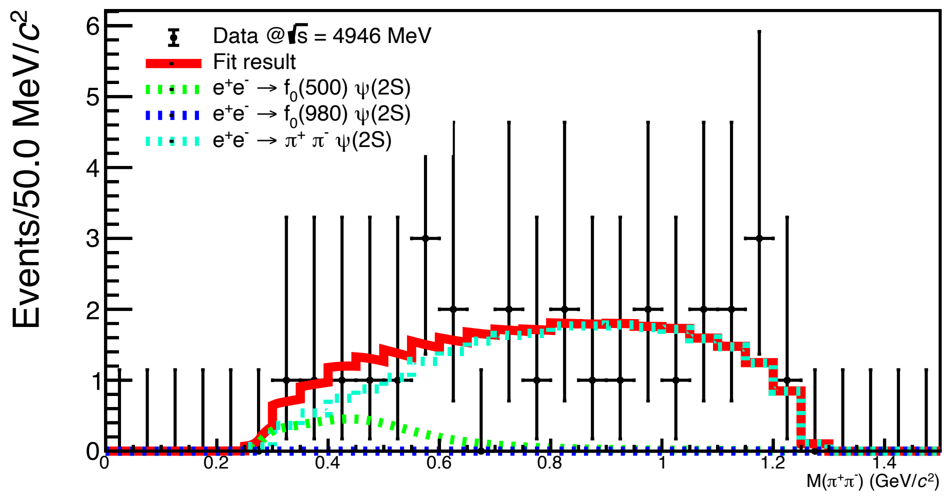

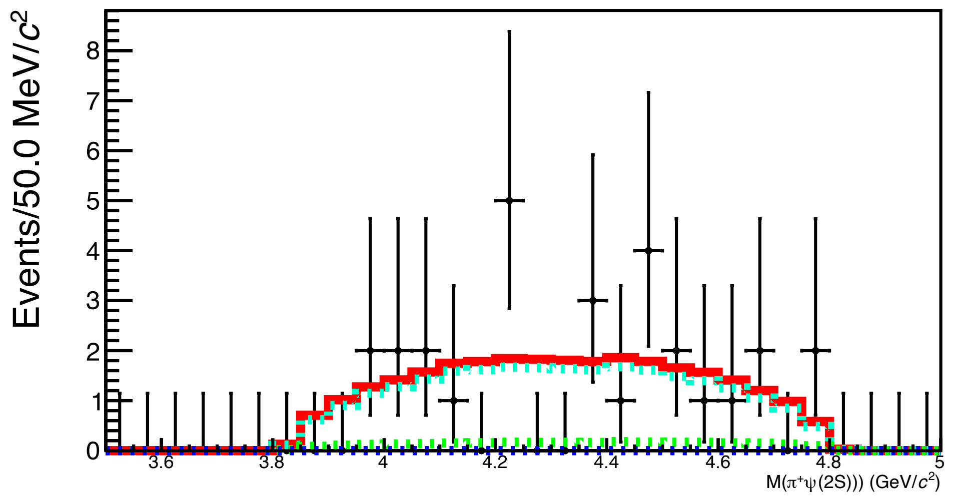

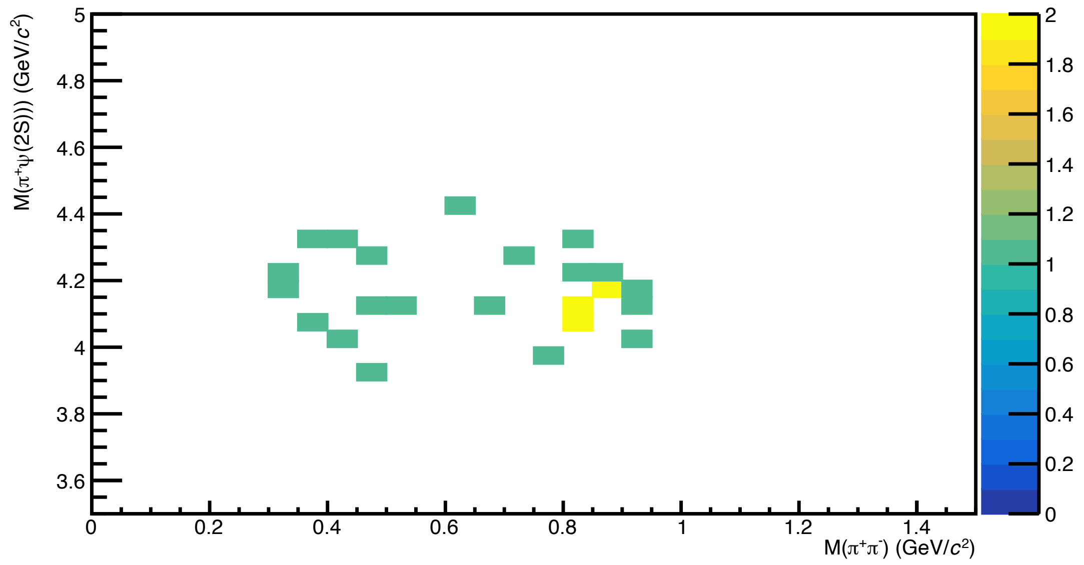

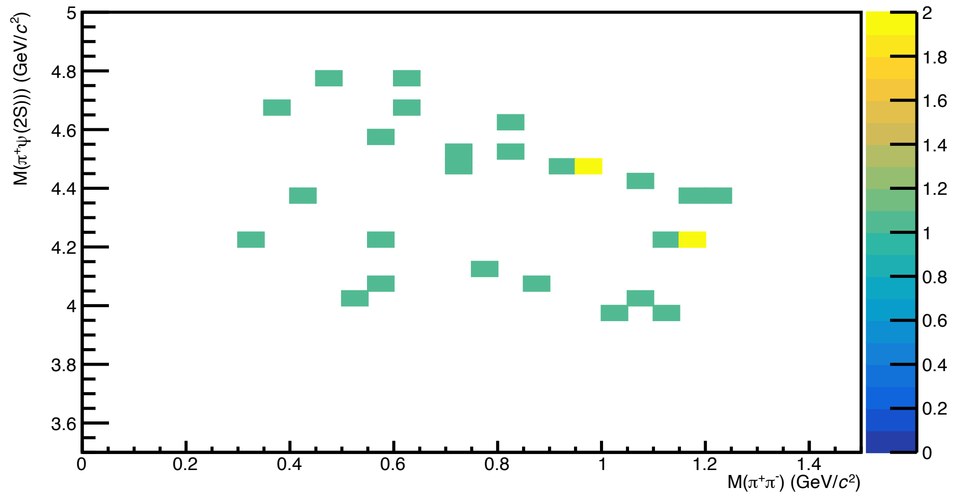

Extraction of the σ(f_0(980) ψ(2S))

f_0(980) contribution

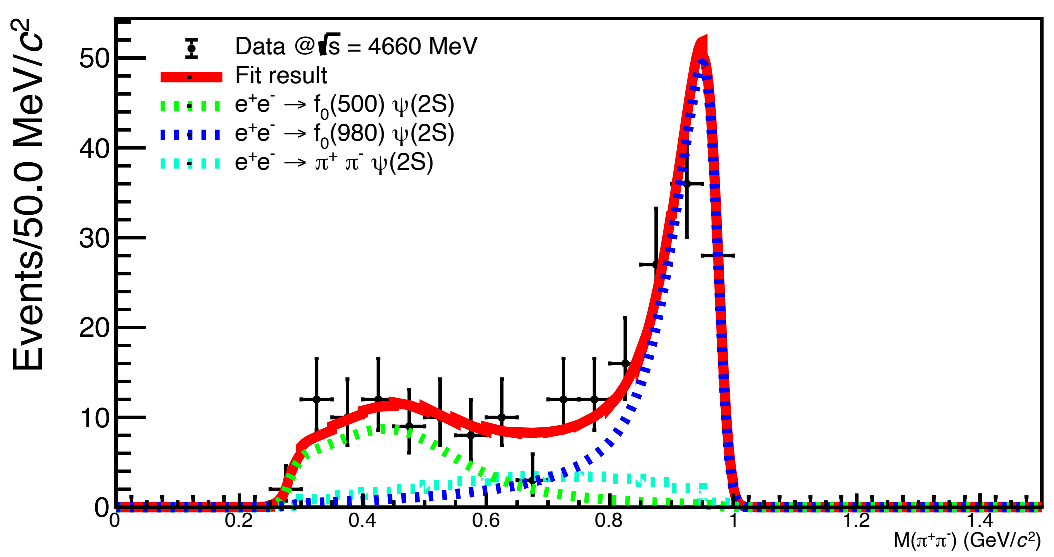

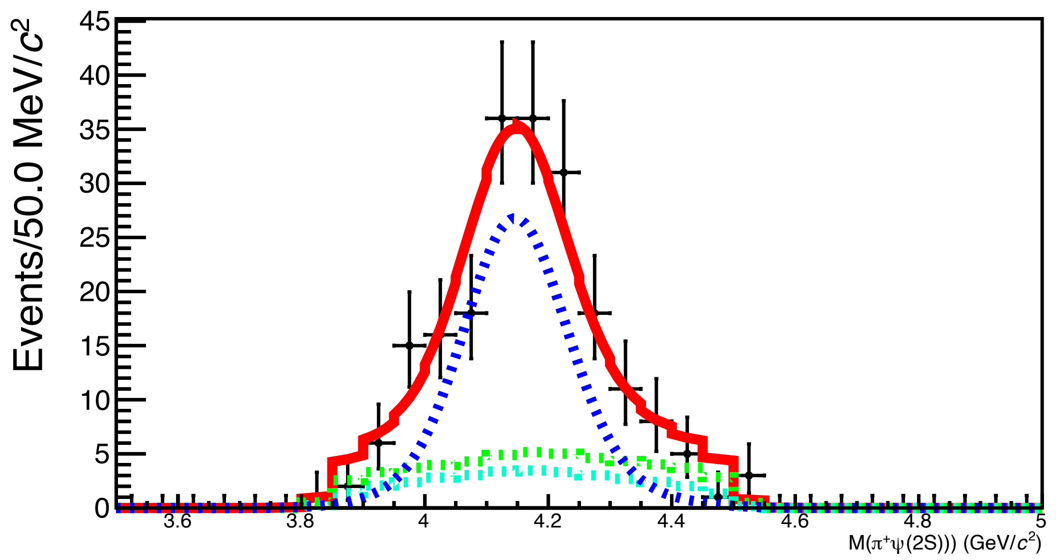

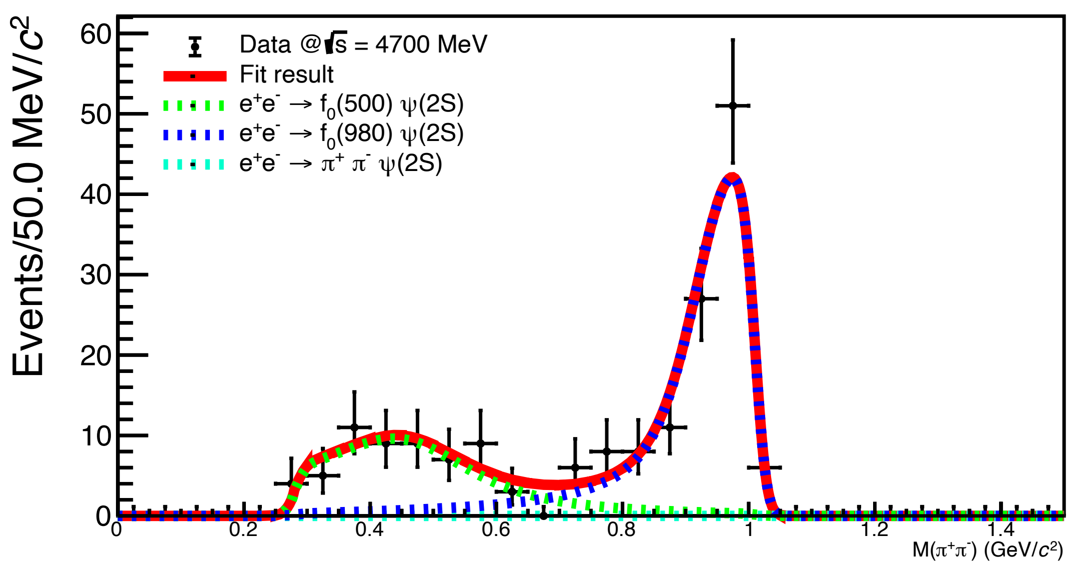

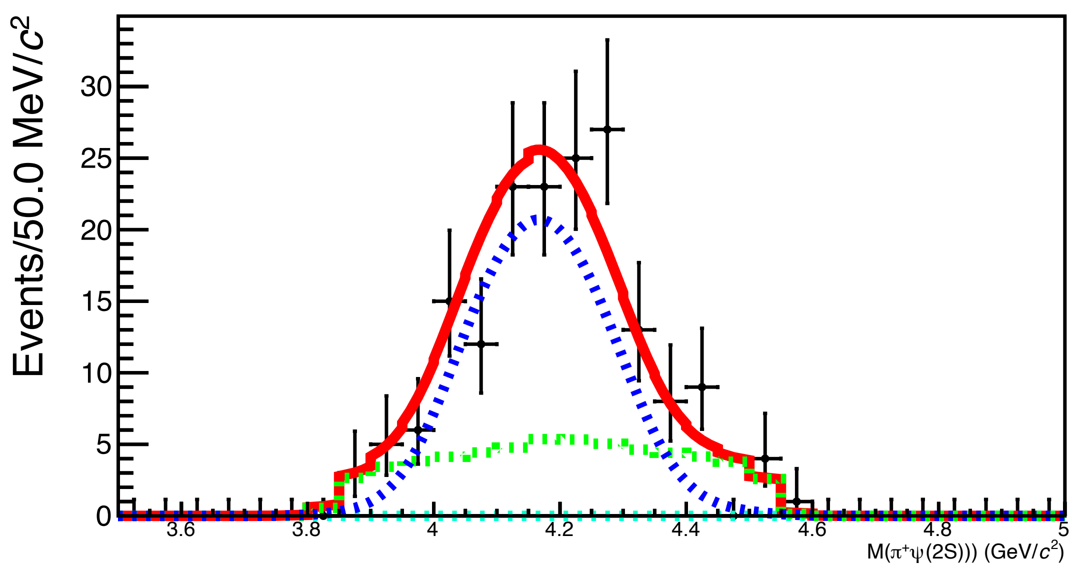

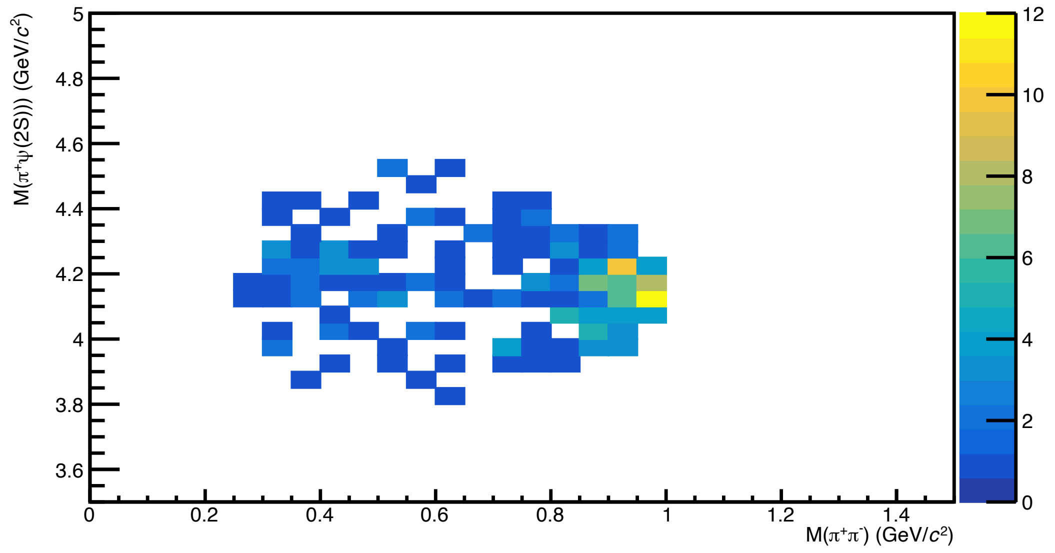

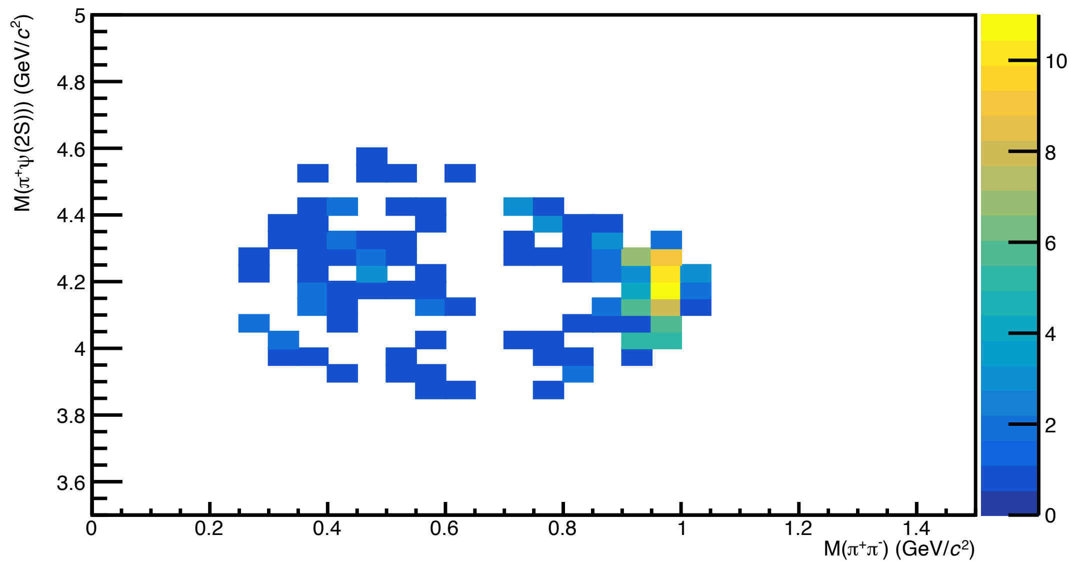

$\sigma(e^+e^- \longrightarrow \pi^+\pi^-\psi(2S))$ vs $\sigma(f_0(980)\,\psi(2S))$

Number of Events

E_{CoM} (MeV)	$N_{e^+e^-\to\pi^+\pi^-\psi(2S)}$	$N_{e^+e^-\to f_0(980)\psi(2S)}$
4.612	26 ± 5	16 ± 4
4.626	156^{+14}_{-13}	107 ± 10
4.640	203^{+16}_{-15}	155 ± 11
4.660	202 ± 15	120 ± 10
4.680	518^{+24}_{-23}	337 ± 15
4.700	173 ± 14	120 ± 9
4.740	37^{+7}_{-6}	34 ± 4
4.750	77^{+9}_{-8}	63 ± 5
4.780	84^{+10}_{-9}	43 ± 7
4.840	66^{+9}_{-8}	43 ± 8
4.914	19^{+5}_{-4}	0 ± 2
4.946	23^{+6}_{-5}	0 ± 6

Cut Flow of Event Selection

$Z_c(4430)$ Channel

Cuts [$\sqrt{s} = 4.612$ GeV]	Events	Efficiency [%]
Total Tracks	300000	100
Fiducial	245103	81.70
Kinetic PID	205613	68.54
5 Trks Events - Kalman Fit 1C	56606	18.87
6 Trks Events - Kalman Fit 6C	85113	28.37
5&6 Trks Events	141719	47.24

Table 31: Cut-flow for the $e^+e^- \to \pi^\mp Z_c(4430)^\pm \to \pi^+\pi^-\psi(2S)$ process at $\sqrt{s} = 4.612$ GeV.

Cuts [$\sqrt{s} = 4.626$ GeV]	Events	Efficiency [%]
Total Tracks	300000	100
Fiducial	246479	82.16
Kinetic PID	208387	69.46
5 Trks Events - Kalman Fit 1C	56918	18.97
6 Trks Events - Kalman Fit 6C	86811	28.94
5&6 Trks Events	143729	47.914

Table 32: Cut-flow for the $e^+e^- \to \pi^\mp Z_c(4430)^\pm \to \pi^+\pi^-\psi(2S)$ process at $\sqrt{s} = 4.626$ GeV.

Cuts [$\sqrt{s} = 4.640$ GeV]	Events	Efficiency [%]
Total Tracks	300000	100
Fiducial	247866	82.62
Kinetic PID	209294	69.76
5 Trks Events - Kalman Fit 1C	55614	18.54
6 Trks Events - Kalman Fit 6C	88441	29.48
5&6 Trks Events	144055	48.02

Table 33: Cut-flow for the $e^+e^- \to \pi^\mp Z_c(4430)^\pm \to \pi^+\pi^-\psi(2S)$ process at $\sqrt{s} = 4.640$ GeV.

Cuts [$\sqrt{s} = 4.660$ GeV]	Events	Efficiency [%]
Total Tracks	300000	100
Fiducial	249041	83.01
Kinetic PID	208637	69.55
5 Trks Events - Kalman Fit 1C	52654	17.55
6 Trks Events - Kalman Fit 1C	90043	30.01
5&6 Trks Events	142697	47.57

Table 34: Cut-flow for the $e^+e^- \to \pi^\mp Z_c(4430)^\pm \to \pi^+\pi^-\psi(2S)$ process at $\sqrt{s} = 4.660$ GeV.

Cut Flow of Event Selection

$Z_c(4430)$ Channel

Cuts [$\sqrt{s} = 4.780$ GeV]	Events	Efficiency [%]
Total Tracks	300000	100
Fiducial	256032	85.34
Kinetic PID	215601	71.87
5 Trks Events - Kalman Fit 1C	47160	15.72
6 Trks Events - Kalman Fit 1C	99346	33.12
5&6 Trks Events	146506	48.84

Table 39: Cut-flow for the $e^+e^- \to \pi^\mp Z_c(4430)^\pm \to \pi^+\pi^-\psi(2S)$ process at $\sqrt{s} = 4.780$ GeV.

Cuts [$\sqrt{s} = 4.840$ GeV]	Events	Efficiency [%]
Total Tracks	300000	100
Fiducial	257755	85.92
Kinetic PID	213379	71.13
5 Trks Events - Kalman Fit 1C	43005	14.34
6 Trks Events - Kalman Fit 1C	98092	32.70
5&6 Trks Events	141097	47.03

Table 40: Cut-flow for the $e^+e^- \to \pi^\mp Z_c(4430)^\pm \to \pi^+\pi^-\psi(2S)$ process at $\sqrt{s} = 4.840$ GeV.

Cuts [$\sqrt{s} = 4.914$ GeV]	Events	Efficiency [%]
Total Tracks	300000	100
Fiducial	259691	86.56
Kinetic PID	217161	72.39
5 Trks Events - Kalman Fit 1C	42435	14.15
6 Trks Events - Kalman Fit 1C	102950	34.32
5&6 Trks Events	145385	48.46

Table 41: Cut-flow for the $e^+e^- \to \pi^\mp Z_c(4430)^\pm \to \pi^+\pi^-\psi(2S)$ process at $\sqrt{s} = 4.914$ GeV.

Cuts [$\sqrt{s} = 4.946$ GeV]	Events	Efficiency [%]
Total Tracks	300000	100
Fiducial	260176	86.73
Kinetic PID	218211	72.74
5 Trks Events - Kalman Fit 1C	42208	14.07
6 Trks Events - Kalman Fit 6C	104045	34.68
5&6 Trks Events	146253	48.75

Table 42: Cut-flow for the $e^+e^- \to \pi^\mp Z_c(4430)^\pm \to \pi^+\pi^-\psi(2S)$ process at $\sqrt{s} = 4.946$ GeV.

M(π±ψ(2S)) Comparison